ANALYSIS OF FUNGAL DEGRADATION PRODUCTS OF AZO DYES

by

XUEHENG ZHAO

(Under the Direction of Ian R. Hardin)

ABSTRACT

Azo dyes, which represent about one- half of all dyes in common use, are also the most common synthetic colorants released into the environment. Bioremediation of azo dyes in textile waste effluents by fungi is an alternative to conventional methods for its relatively low expense involved and environmental friendly nature. However, knowledge of fungal degradation mechanisms of organic pollutants including dyes is still lacking. This study employed a comprehensive approach for investigating the degradation of carefully chosen model azo dyes by white rot fungi using a wide spectrum of analytical techniques. The metabolites of ionized and unionized azo dyes were identified and quantified. Possible pathways leading to formation of these products are discussed.

INDEX WORDS: Azo dyes, White rot fungi, Biodegradation, Mechanism, Identification, High performance liquid chromatography, Capillary electrophoresis, Electrospray-mass spectrometry, Gas chromatography- mass spectrometry, Thin layer chromatography

# ANALYSIS OF FUNGAL DEGRADATION PRODUCTS OF AZO DYES

by

XUEHENG ZHAO

B.E. Beijing Institute of Clothing Technology, China, 1994

M.E. Beijing Institute of Clothing Technology, China, 1997

A Dissertation Submitted to the Graduate Faculty of The University of Georgia in Partial Fulfillment of the Requirements for the Degree

DOCTOR OF PHILOSOPHY

ATHENS, GEORGIA

2004

# ANALYSIS OF FUNGAL DEGRADATION PRODUCTS OF AZO DYES

by

XUEHENG ZHAO

Major Professor: Ian R. Hardin

Committee: George L. Baughman
Dennis R. Phillips
Danny E. Akin

Electronic Version Approved:

Maureen Grasso
Dean of the Graduate School
The University of Georgia
August 2004

DEDICATION

To my parents, for their love and patience in me.

ACKNOWLEDGEMENTS

The past five years have been very enriching and have taught me many things. I would like to thank many people who made my study at Georgia successful.

I would like to thank Dr. Ian R. Hardin for his support, guidance and for letting me know the importance to communicate with people in different fields.

Without the support of Prof. George L. Baughman, I would not learn so much from my research. His love in chemistry inspired me and his encouragement and confidence in me motivated me to perform the best in the daily work. Special thanks to Dr. Dennis R. Phillips for his help and guidance in mass spectrometry setup and operation, without which a major part of my dissertation would not have been possible. I would also like to thank Dr. Danny E. Akin for serving on my committee.

I appreciate Yiping, Wang, Susan, Min and other TMI faulty, staff and graduate students, who have given me valuable help and friendship and contributed my success in my study.

Finally, my special gratitude goes to my parents and my sister for their forever love and support. I would like thank my wife, Yarong, without her tremendous help and patience, I would not be of success in my life.

TABLE OF CONTENTS

Page

LIST OF TABLES

Page

LIST OF FIGURES

Page

# CHAPTER 1

# INTRODUCTION AND REVIEW OF LITERATURE

Azo dyes, which represent about one-half of all dyes in common use, are employed as coloring agents in the food, pharmaceutical, and textile industries. The popularity and widespread use of azo dyes is due to several factors. As a group, they are color-fast and encompass the entire visible spectrum, and many are easily synthesized from inexpensive and easily obtained starting materials. Also azo dyes are typically amenable to structural modification, and can be made to bind to most synthetic and natural textile fibers.

It is estimated that about 15 percent of dyes is released into waste water during textile processing (Wesenberg et al., 2003), with azo dyes being the most common synthetic colorants released into the environment (Bumpus, 1995). Because they are highly colored, azo dyes are readily apparent and can create a significant environmental problem by affecting water transparency as well as aesthetic problems (Banat et al., 1996). Dyes in wastewater not only present aesthetic objections, but they can pose threats to public health. Some of the dyes, their precursors, or their biotransformation products such as aromatic amines, have been shown to be carcinogenic (Razo-Flores et al., 1997). Most textile effluents have to be treated to remove these dyes to meet increasingly stringent legislation or to meet local citizenry objections.

Dyes are designed to be resistant to light, water and oxidizing agents, so it is difficult to remove them once they are released into the environment. Dye-containing effluents are only slightly decolorized by conventional biological wastewater treatments (Wesenberg et al., 2003; Shaul et al., 1991). Generally, textile dyes in wastewater can be physically or chemically

removed by flocculation, adsorption, extraction, filtration or oxidation. Most physical methods simply accumulate and concentrate dyes and create solid waste, but a disposal problem still exists. Chemical oxidation with either peroxide or ozone can destroy dyestuffs effectively but this approach is very expensive.

It is necessary to clarify the concepts of decolorization, degradation, and mineralization of dyes in that these words often occur in the literature and sometimes were misused. Decolorization is simply the disappearance of the color in wastewater without the actual breaking apart of the dye molecules, which does not necessarily mean degradation of the complex dye molecules. Degradation is the destruction of the large dye molecule to smaller components, along with the breakdown of the chromophores. While chromophore groups of dyes may be destroyed, the intermediate produced may be more toxic than the original compounds and could present significant problems for receiving water bodies (Hao et al., 2000). Mineralization means organic compounds are converted to inorganic compounds, i.e., nitrate, carbon dioxide, and water. In this case, a complete detoxification is achieved and no secondary pollution will be introduced.

Bioremediation of azo dyes in textile waste effluents by bacteria or fungi is an alternative to conventional methods and a very promising area of study because of the relatively low expense involved. It has been shown that microorganisms are able to utilize a wide of variety of organic compounds as precursors for the synthesis of their own cell material or as sources of energy, even when such compounds are present at low concentrations in the environment (Egli, 1995). Bioremediation includes biodegradation and biotransformation, with a goal to mineralize hazardous contaminants in the environment. Thus, there is less potential for environmental

impact with bioremediation because this method is targeted to break down the dye molecules to non-toxic inorganic compounds.

A problem emerges when anaerobic bacteria are used in degradation of azo dyes. In most cases, bacterial anaerobic degradation is initiated by the reduction of the azo linkage to generate aromatic amines (Spadaro et al., 1992), which may be strongly carcinogenic and are themselves a disposal problem.

By far the single class of microorganisms most efficient in breaking down synthetic dyes is white rot fungi (Wesenberg et al., 2003). The nonspecific nature of the lignin-degrading systems of white rot fungi is a potential advantage for biotreatment of textile effluents, since a mixture of dyes, surfactants and other compounds exist in the wastewater. Another important advantage for degradation of azo dyes using white rot fungi is that ligninolytic enzymes degrade azo dyes by oxidation, in contrast to the reduction pathway in bacterial degradation.

Previous work in our laboratories demonstrated the feasibility of using white rot fungi to decolorize a range of commercial dyes of different structures (azo, disazo, anthraquinone) (Cao, 2000). Various white rot fungi, including *Phanerochaete chrysosporium, Pycnoporus cinnabarinus, Trametes versicolor, Ceriporiopsis subvermispora, Cyathus stercoreus, Pleurotus ostreatus, Phellinus tremellia, Phellinus oxysponum,* and *Phellinus pini*, were screened for their ability to decolorize commercially used dyes. Among them, *Pleurotus ostreatus* demonstrated a high potential for decolorizing various azo dyes (Cao, 2000).

For biotreatment applications, it is important to identify the final degradation products as well as intermediates of dyes by fungi because of concern that these compounds may increase the aquatic toxicity of the overall effluent. However, knowledge of fungal degradation mechanisms of organic pollutants including dyes is still lacking. Without insight into the

intermediates generated in biodegradation, the true technical potential of white rot fungi cannot be evaluated. The purpose of the study described in this dissertation is to set up analytical methods aiming at identification of products and understanding the processes that create such products. A comprehensive approach for investigating the degradation of dyes by white rot fungi using a wide spectrum of analytical techniques was established and used for examination of the degradation products of carefully selected model azo dyes. The metabolites of ionic and nonionic azo dyes were identified and quantified. With identification of these products, some fundamental insights into fungal degradation mechanisms and toxicity of wastewater containing azo dyes after decolorization by white rot fungi can be proposed.

### 1.1 Decolorization of azo dyes by white rot fungi

Azo dyes are considered recalcitrant xenobiotic compounds due to the presence of a nitrogen double bond (-N=N-) bond and other groups (i.e. sulfonic group) that are not easily biodegraded (Adosinda, et al., 2001). Wastewaters containing these azo dyes are usually resistant to normal biological waste treatment for color removal.

In recent years, extensive studies of microbial degradation of azo dyes have been conducted and the potential for using white rot fungi to degrade dyes has been demonstrated (Bumpus, 1995; Heinfling, et al., 1997). Decolorization of azo dyes by the ligninolytic fungus, *Phanerochaete chrysosporium,* was described for the first time by Cripps et al. (1990). Three azo dyes, Orange II (4-[(2-hydroxy-1-naphthalenyl)azo]-benzenesulfonic acid), Tropaeolin O (4-[(2,4-dihydroxyphenyl)azo]-benzenesulfonic acid), and Congo Red (3,3′- [1,1′- biphenyl]-4,4′-diylbis(azo)]bis[4-amino-1-naphthalenesulfonic acid]) were decolorized extensively (96-100 percent) during five days of incubation. Overall, *Phanerochaete chrysosporium* has been the

most intensively studied dye-decolorizing white rot fungus. A range of acid, reactive, and mordant azo dyes have been shown to be decolorized by this ligninolytic fungus (Knapp et al., 1995; Chagas and Durrant, 2001; Moreira et al., 2000).

The promising results obtained with *Phanerochaete chrysosporium* led to the study of the potential of other species of ligninolytic basidiomycetes (Adosinda et al., 2003). Novotny and co-workers (2001) screened 103 wood-rotting fungal strains for decolorization of azo and other types of textile dyes. *Irpex lacteus* and *Pleurotus ostreatus* degraded dyes from all groups. Work at the University of Georgia also demonstrated that *Pleurotus ostreatus* was an efficient degrader of azo dyes (Cao, 2000). Other white rot fungi, such as *Trametes versicolor, Bjerkandera adusta,* and *Thelephora sp*., have also been shown to be efficient in decolorizing of different azo dyes (Selvam et al., 2003; Heinfling et al., 1997).

### 1.2 Enzymes of white rot fungi involved in the degradation

Ligninolytic fungi are able to degrade numerous aromatic organic pollutants via oxidative mechanisms (Adosinda et al., 2001; Bogan and Lamar, 1995). A correlation between dye decolorization and the production of ligninolytic enzymes was implied by the work of Wesenberg and co-workers (Wesenberg et al., 2003). The ligninolytic enzymes are extracellularly excreted by the fungi to initiate the oxidation of substrates in the extracellular environment of the fungal cells (Mester and Tien, 2000). Essential extracellular enzymes involved into the degradation of lignin in wood and recalcitrant pollutants (i.e. azo dyes) in the environment are laccase, lignin peroxidase (LiP), and manganese peroxidase (MnP). All of these enzymes are generally believed to form during secondary metabolism of white rot fungi (Hou et al, 2003; Zapanta et al., 1997).

LiP is a classical hemeprotein peroxidase containing heme in the active site with molecular weight between 38 and 47 KDa (Wesenberg et al., 2003). Due to its high redox potential, LiP is able to directly oxidize non-phenolic lignin units (Sarkar et al., 1997). LiP reacts directly with aromatic substrates by abstracting single electrons from their aromatic rings, leading to the formation of a cation radical and subsequent cleavage reactions (Zheng and Obbard, 2002). A characteristic of LiP, which is also shared by non-ligninolytic peroxidases, is its relative unspecificity for substrates such as phenolic compounds and dyes (Martinez, 2002). Whereas phenoxy radicals are the first product of phenolic substrate oxidation by peroxidases, aromatic cations are formed after non-phenolic aromatic ring oxidation by LiP (Martinez, 2002; Kersten et al., 1985).

The catalytic cycle of peroxidases is shown in Figure 1. The ligninolytic peroxidases have a typical enzymatic cycle characteristic of other peroxidases (Mester and Tien, 2000; Tien and Kirk, 1984; Wariishi et al., 1988). The heme group of the native enzyme (ferric form) is oxidized by $H_2O_2$ with two electrons to compound I. One electron is removed from ferric (Fe(III)) iron to form ferryl (Fe(IV)) while the second electron is withdrawn from the porphyrin ring to form a porphyrin cation radical (Aust, 1995). During this reaction step, $H_2O_2$ is reduced to water. Compound I oxidizes substrates by one electron and is reduced to compound II. In this step, the porphyrin ring gains the electron. Thus, compound I is able to oxidize substrates with a higher redox potential than compound II (Mester and Tien, 2000). Compound II then reacts with reducing substrates by gaining one electron and changing back to resting enzyme. Substrates (RH) of compound I can also react with compound II and give rise to radical R•. Compound II can also react with $H_2O_2$ resulting in compound III (Cai and Tien, 1992), which leads to inactivation of the peroxidase (Torres et al., 2003).

To avoid inactivation of LiP, veratryl alcohol completes the catalytic cycle of LiP by reducing compound II to resting enzyme. Veratryl alcohol (3,4-dimethoxybenzyl alcohol) is a secondary metabolite synthesized from glucose by several fungi, but mainly the basidiomycetes (Suguimoto et al., 2001; Jong et al., 1994). It is oxidized via two separate one-electron oxidations to give veratraldehyde (Zapanta and Tien, 1997; Tien, 1987). Veratryl alcohol is thought to be produced at the same time as LiP (Fenn and Kirk, 1981). In liquid cultures, the addition of veratryl alcohol causes an increase in LiP activity (Faison and Kirk, 1985). Veratryl alcohol plays a role in the LiP action in three ways. Firstly, it acts as a cation radical redox mediator of remote substrates. Secondly, it acts to protect LiP from inactivation by $H_2O_2$. Finally, it acts to complete the catalytic cycle of LiP in the presence of substrates that cannot reduce compound II to native enzyme (Zapanta and Tien, 1997; Goodwin et al., 1995; Schoemaker et al., 1994).

Like LiP, MnP is a heme-containing peroxidase (Zapanta and Tien, 1997) and is the most common ligninolytic peroxidase produced by almost all white rot basidiomycetes (Wesenberg et al., 2003). MnP is a glycoprotein with a heme (ferric protoporphyrin) group and a molecular weight of 32 to 62.5 KDa (Hofrichter, 2002; Glenn and Gold, 1985). It shares mechanistic properties with LiP and forms the oxidized intermediates, compound I and compound II (Zapanta and Tien, 1997; Cai and Tien, 1993). It also requires the presence of $H_2O_2$ to oxidize lignin and lignin-related compounds (Mester and Tien, 2000).

MnP exhibits a dependence on Mn (II) as a substrate for compound II (Wariishi et al., 1988). Mn (II) is also a preferred substrate for compound I. In the degradation of lignin and other substrates, MnP oxidizes Mn (II) to Mn (III) in the presence of $H_2O_2$, and Mn (III) oxidizes a variety of compounds (Mester and Tien, 2000; Glenn et al., 1986). The chelation of Mn (II) and

Mn (III) by organic acids, such as oxalate, is necessary for MnP activity (Zapanta and Tien, 1997). Oxalate is an organic acid chelator produced by white rot fungi at the same time as MnP in the liquid cultures of *Phanerochaete chrysosporium* (Zapanta and Tien, 1997; Wariishi et al., 1992; Kuan and Tien, 1993).

Laccase belongs to a group of enzymes called blue copper oxidases with a molecular weight of 60 to 390 KDa (Call and Muke, 1997). Laccase also has broad substrate specificity and is capable of oxidizing phenols and aromatic amines by reducing molecular oxygen (instead of $H_2O_2$) to water by a multicopper system (Hublik and Schinner, 2000; Hou et al., 2003). In the reaction, the substrates are oxidized by one electron to generate the corresponding phenoxy radicals, which either polymerize to yield a phenolic polymer or are further oxidized by laccase to produce a quinone (Chivukula and Renganathan, 1995). In this procedure, oxygen gets the electron from the substrate and is reduced to water.

Like MnP, laccase acts primarily on phenolic units, but also on non-phenolic ones in the presence of primary co-substrates (Sarkar et al., 1997; Bourbonnais et al., 1996). It was found that a nitrogen limited culture is of benefit to laccase production, and that certain redox mediators, such as 2,2'-azino-bis-(3-ethylbenzothiazole-6-sulfonic acid) (ABTS) and 1-hydroxybenzotriazole (HOBT), can extend this specificity to non-phenolic compounds (Hou et al. 2003, Mester and Tien, 2000). It is still not clear, however, if a laccase mediator system exists in the lignin degradation system (Mester and Tien, 2000).

*Pleurotus ostreatus* also produces other extracellular enzymes, *Pleurotus ostreatus* peroxidase (Kang et al., 1993), Remazol Brilliant Blue R decolorizing enzyme (Shin et al., 1997), a new kind of enzyme called versatile peroxidase (Martinez, 2002), and glucose oxidase (Shin et al., 1993). *Pleurotus ostreatus* peroxidase and Remazol Brilliant Blue R decolorizing

enzyme are $H_2O_2$ dependent, catalyzing oxidation of phenolic compounds by one electron but having no affinity for nonphenolic compounds. Versatile peroxidase, however, is able to oxidize both LiP and MnP substrates (Martinez, 2002). It was shown that versatile peroxidase could efficiently oxidize some aromatic substrates, including dyes (Martinez, 2002; Heinfling et al., 1998).

All three major ligninolytic enzymes are produced in multiple isoforms and are affected by many external factors, such as nutrient level, mediator compounds and metal ions (Wesenberg et al., 2003). It has also been shown that both the composition of culture media and the fermentation time exert a considerable influence on the activity of peroxidases from white rot fungi (Morais et al., 2002).

### 1.3 Enzymatic reactions with azo dyes

Despite the fact that ligninolytic enzymes have been intensively studied for their role in degradation of lignin and some other organic pollutants, their mechanisms of biodegradation are not well understood. They include a complex process of oxidation, reduction, methylation, and hydroxylation. The reaction of the extracelluar ligninolytic enzymes also involves numerous low molecular weight cofactors that may serve as redox mediators (Mester and Tien, 2000).

LiP is considered to be the principal decolorizing enzyme in cultures of *Phanerochaete chrysosporium* and it is clear that ligninolytic enzymes play a significant role in biodegradation of dyes by white rot fungi (Podgornik et al., 1999; McMullan et al., 2001). Whether a compound can serve as a substrate for LiP appears to be determined by the size of the molecule and its redox potential (Mester and Tien, 2000). LiP has a higher redox potential than other

peroxidases. The role of purified lignin peroxidase in the decolorization of several azo dyes has been investigated (Rodriguez et al., 1999; Paszczynski et al., 1991).

Spadaro and Renganathan (1994) described the mechanism for the peroxidase-catalyzed degradation of an azo dye, Disperse Yellow 3. The naphthol analog of Disperse Yellow 3 [1-(4'-acetamidophenylazo)-2-naphthol] was also used as a model compound in their study. Three peroxidases, lignin peroxidase (LiP), manganese peroxidase (MnP), and horseradish peroxidase (HRP), were investigated in the degradation of azo dyes and the products from each system were identified. The peroxidases were indicated to be responsible for the degradation of azo dyes. Asymmetric cleavage of nitrogen-nitrogen double bond (-N=N-) occurred in the degradation. The intermediate compounds generated were suggested to be 4-acetamidophenyldiazene and 4-methyl-1,2-benzoquinone. Phenyldiazene is unstable and is readily oxidized by oxygen. The azo linkage is released as molecular nitrogen and acetanilide, one of the major products from Disperse Yellow 3 and its naphthol analog, is proposed to form through phenyl radical abstracting a hydrogen radical from the surrounding.

Goszczynski and co-workers (1994) studied the mechanism of sulfonated azo dyes degradation by peroxidases of *Phanerochaete chrysosporium* and proposed a cationic radical pathway that was similar to that by Spadaro and Renganathan (1994). However, Goszczynski and co-workers indicated symmetrical splitting of azo linkage as another possibility for initial attack on azo dyes.

A mechanism for the peroxidase-catalyzed oxidation of phenolic azo dyes has been proposed by Torres and co-workers (2003). In their scheme, two successive one-electron oxidations of the phenolic ring by peroxidase produce a carbonium ion. Then water reacts with the phenolic carbon bearing the azo bond to produce an unstable intermediate. Subsequent

reactions of the intermediate produce a quinone and an amidophenyldiazine. The latter could react with oxygen to give rise to a phenyl radical via the unstable intermediate phenyldiazene radical. It was also suggested that detoxification of azo dyes is achieved because of the absence of aromatic amines in the final products. Laccase-catalyzed oxidation of azo dyes apparently follows a similar mechanism.

Pasti-Grigsby and co-workers (1992) also found that various sulfonated azo dyes were not equally susceptible to microbial attack. Twenty-two azo dyes were studied to determine the influence of aromatic substitution on azo dye degradation by *Phanerochaete chrysosporium*. They found that dyes with hydroxyl and azo groups in the 1,2-positions were degraded fastest among test dyes. Spadaro and Renganathan (1992) indicated that aromatic rings with substituents such as hydroxyl, amino, acetamido, or nitro groups were degraded to a greater extent than unsubstituted rings.

### 1.4 Mineralization of azo dyes by white rot fungi

Ligninolytic enzymes mineralize lignin by combining with other additional enzymes (Wesenberg et al., 2003). It has been demonstrated that some azo dyes can also be mineralized to carbon dioxide by white rot fungus *Phanerochaete chrysosporium* (Paszczynski et al., 1992; Spadaro et al., 1992).

Spadaro and co-workers (1992) showed that *Phanerochaete chrysosporium* could mineralize the radio-labeled azo compounds 4-phenylazophenol, 4-phenylazo-2-methoxyphenol, Disperse Yellow 3 (N-[4-[(2-hydroxy-5-methylphenyl)azo]phenyl]-acetamide), 4-phenylazoaniline, N,N-dimethyl-4-phenylazoaniline, Disperse Orange 3 (4-[(4-nitrophenyl)azo]-benzeneamine) and Solvent Yellow 14 (1-(phenylazo)-2-naphthalenol) to the extent of 23.1 percent to 48.1 percent.

Paszczynski and co-workers (1992) used $^{14}C$-labeled azo dyes, such as Orange I (4-[(4-hydroxy-1-naphthalenyl)azo]-benzenesulfonic acid), Orange II (4-[(2-hydroxy-1-naphthalenyl)azo]-benzenesulfonic acid), Acid Yellow 9 (2-amino-5-[(4-sulfophenyl)azo]-benzenesulfonic acid), 4-(3-methoxy-4- hydroxyphenylazo) benzenesulfonic acid, and 4-(2-sulfo-3'-methoxy-4-hydroxyazobenzene-4-azo) benzenesulfonic acid mono sodium salt, to determine that the mineralization of these dyes by *Phanerochaete chrysosporium* was in the range of 17.2 percent to 34.8 percent.

Nevertheless, it is clear that dye decolorization is not equivalent to dye mineralization. There is a gap in current knowledge between decolorization and degradation mechanisms, with a lack of knowledge concerning potentially toxic colorless intermediates (Wesenberg et al., 2003). The nature of metabolites of azo dyes and their biodegradability are not clear yet and need further investigation, since complete mineralization of azo dyes by white rot fungi cannot be expected (Heinfling et al., 1997). It is generally agreed that practical application of biodegradation systems using white rot fungi must be preceded by a better understanding of the biodegradation mechanisms involved.

### 1.5 Analytical techniques

Due to the different properties of azo dyes and their metabolites, such as solubility, volatility, and structure, state-of-the-art analytical methodologies are needed. Therefore, a wide range of advanced analytical techniques, including spectrophotometry, chromatography, mass spectrometry, and capillary electrophoresis, have been employed in this study. The inherent complexity of dye structures and the not well-understood biotransformation mechanisms make

the identification of unknown metabolites a difficult task and the forte of each technique had to been used to tackle problems.

*1.5.1 Chromatography*

The chromatographic technique was first developed by Tswett in 1906 to separate colored compounds (Reichstein, 1992) and became an indispensable tool for chemical analysis. In the present work, three chromatographic techniques were used in the identification and quantification of degradation products of azo dyes: thin layer chromatography, gas chromatography and high performance liquid chromatography.

Thin layer chromatography (TLC) has a unique advantage in analysis of dyes because the colored spots can be easily seen in the plates. As an off-line analytical technique, TLC is broadly used in analysis of dyes and intermediates because of its simple and inexpensive properties (Ansari and Thakur, 2000; Milojkovic-Opsenica et al., 2003; Sherma, 2000). TLC has been used before in the analysis of metabolites from biodegradation of dyes (Bras et al., 2001).

Gas chromatography is a principal tool for analysis of thermally stable, volatile and semivolatile organic compounds in mixtures with a wide range of complexity. As a powerful detector, mass spectrometry supplies unambiguous mass information for the unknown compounds when coupled on-line with gas chromatography (GC-MS) and is particularly suitable for analysis of unknown metabolites from hydrophobic azo dyes with low molecular weight. GC-MS is particularly useful for identification of products from disperse azo dyes, which are relatively small molecules that lack sulfonic acid groups. GC-MS has been widely used to identify products of dyes degraded with enzymes or fungi (Adosinda et al., 2003; Chivukula and Renganathan, 1995a; Chivukula et al., 1995b; Spadaro and Renganathan, 1994). The major

limitation of this technique is that the sample must be volatile and thermally stable at the temperature of analysis (Poole and Poole, 1992).

High performance liquid chromatography (HPLC) has been used for analysis of various dyes in wastewater and metabolites from various degradation procedures (Baiocchi et al., 2002; Conneely et al., 1999; Nachiyar and Rajkumar, 2003; Pielesz et al., 2002; Plum et al., 2003; Vinodgopal and Peller, 2003; Wang and Tsai, 2003). HPLC is advantageous over GC because it does not need the sample to be volatile or stable to elevated temperatures.

Reversed phase liquid chromatography (RPLC) is the most commonly used mode in HPLC and was employed in this study. Reversed phase means that the stationary phase is less polar than the mobile phase. Solute retention in RPLC is mainly driven by the hydrophobic interaction between the solute and the non-polar stationary phase. Thus, compounds with different polarity elute at different retention times. Resolution is governed by three parameters: retention, column efficiency and selectivity. The most popular detector used for HPLC is the UV-VIS. Under adequate peak resolution, UV-VIS systems can detect components in a complex mixture to ppb levels and quantitate them to ppm levels.

*1.5.2 Capillary electrophoresis (CE)*

Capillary electrophoresis (CE) has been used for analysis of dyes recently and can be more suitable than HPLC for the analysis of charged dyes because of its separation principle, higher separation efficiency and simpler method development (Takeda et al., 1999). Other advantages of CE also include low sample quantities (usually nanoliters) and low consumption of organic solvents. CE employs the powerful separation mechanisms of electrophoresis and the instrumentation and automation techniques of chromatography. Electrophoresis is based on "differential migration of electrically charged particles in an electric field" (Righetti, 1992).

Capillary zone electrophoresis (CZE) is a versatile CE mode and employed in this study. CZE performs electrophoresis in a capillary (usually 50-100 μm I.D.) and separation is based on differences in the speed of migration (migration velocity) of ions when a strong electric field is applied across the capillary.

Both physical and chemical parameters that are crucial to an optimum separation have been summarized by Benedek and Guttman (2001). Physical parameters include the field strength, temperature, column length and diameter, and injection mode and size. The chemical parameters are the type and composition of electrolyte (including pH, concentration, viscosity, and additives), sample composition, and the capillary coating.

*1.5.3 Mass spectrometry (MS)*

Mass spectrometers analyze mass/charge (m/z) ratios and the relative abundance of positive or negative gas phase ions formed from a sample. These data, in turn, can provide structural information and molecular weight of analytes, with the ability for quantitative assays. The mass spectrometers coupled with CE include magnetic sector, ion trap, time of flight (TOF), and Fourier transform ion cyclotron (FTICR) (Perkins and Tomer, 1994; Wey and Thormann, 2002; Verhaert et al., 2001; Marshall, 2000; Severs et al., 1996).

The ion trap mass spectrometer has been shown to be very useful for the structural elucidation and is used in this study. Because the ion trap performs functions through mass accumulation and selective mass isolation, it can supply highly sensitive and selective mass measurements. Its unique $MS^n$ capability provides valuable information on compound structure. CE-$MS^n$ is suited for the analysis of compounds at low concentrations in small amount of complex samples.

*1.5.4 CE-MS interface*

Since its first introduction in 1987 (Olivares et al., 1987), capillary electrophoresis- mass spectrometry (CE-MS) has been applied to the fields of environmental science, forensics, pharmaceutics and life science. CE-MS combines the capillary electrophoretic concepts introduced by Mikkers and Jorgenson in the early 1980s with MS using electrospray ionization (ESI) developed concurrently by Dole and Fenn (Schmitt-Kopplin and Frommberger, 2003). Compared to ultraviolet (UV) detection, which offers little information on the structure of unknown compounds, mass spectrometric (MS) detections reveal unambiguous information on the solute's molecular weight and possibly its structure. Although CE-MS has been used in the determination of dyes in wastewater (Riu et al., 1997), this study is the first one to use this technique to identify and quantify metabolites of dyes in fungal decolorization.

The interface of CE-MS is a critical part in the connection of these two instruments. In contrast to the widely used HPLC-MS, the amount of sample injection for CE-MS is usually in a range of nanoliters instead of the microliter range used in LC-MS. Another major difference compared to LC-MS is the flow rate, which is driven by the electroosmotic flow and is in the range of sub-microliters. Both of these characteristics have to been considered in the development of the CE-MS interface.

Smith and co-workers first developed an interface using an electrospray ionization technique combined with a sheath liquid (Smith et al., 1988). This technique is commonly used in the CE-MS instruments for its ease of implementation and versatility (Kirby et al., 1996). The interface uses coaxial sheath-flow design. The CE capillary is in the center of the triple tubes, surrounded by the sheath liquid tube and the nebulizing gas tube. The sheath liquid electrically connects the CE outlet to the sprayer and produces the necessary flow for a stable electrospray. A gas-

assisted nebulizer generates gas phase ions from the CE effluent under application of a high voltage (HV) field. The function of nebulizing gas is to combine with the applied HV and drying gas to supply efficient droplet generation (Figure 1.3).

Electrospray ionization (ESI) is conducted at atmospheric pressure and consists of four steps: formations of ions, nebulization, desolvation, and ion evaporation. Nebulizing gas and the strong electrostatic field (2-6V) in the spray chamber draw out the sample solution and break it into droplets. An electrical charge will be created on the surface of droplets by the electrostatic field and finally dispersed into a fine spray of charged droplets. The solvent in droplets along with analyte ions is evaporated by a counter flow of heated dry nitrogen. Large droplets will break into small ones with high surface-charge density through the decrease of diameter and increase of Coulomb repulsion. This disintegration will continue until charge density reaches approximately $10^8$ V/cm$^3$, and then ion evaporation will occur. Single ions are emitted directly from the charged droplets into the gas phase (Fenn et al., 1989).

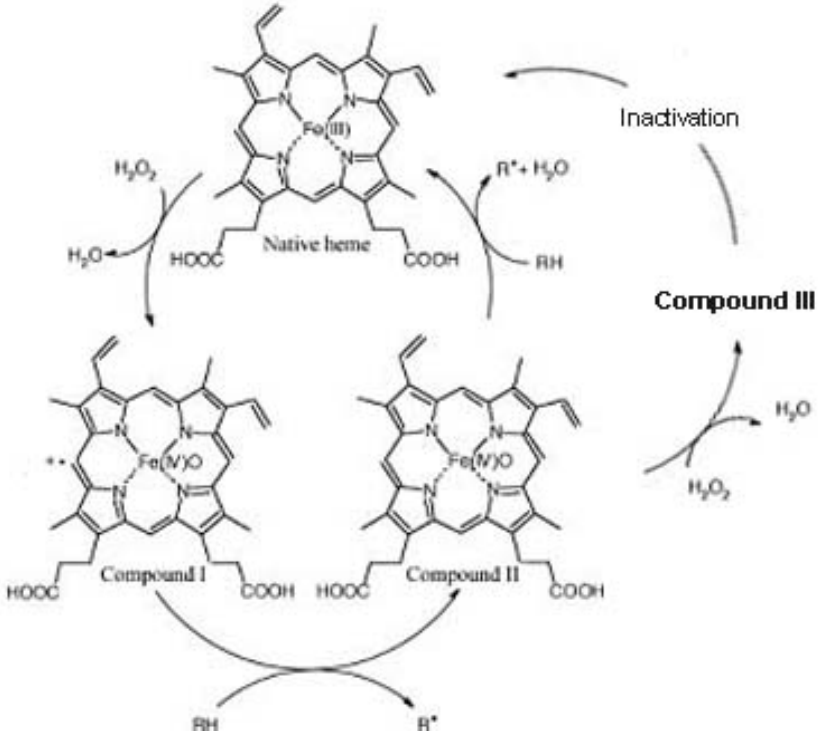


**Figure 1**.**1** Catalytic cycle of heme-containing peroxidases.
(Modified based on Torres et al., 2003)

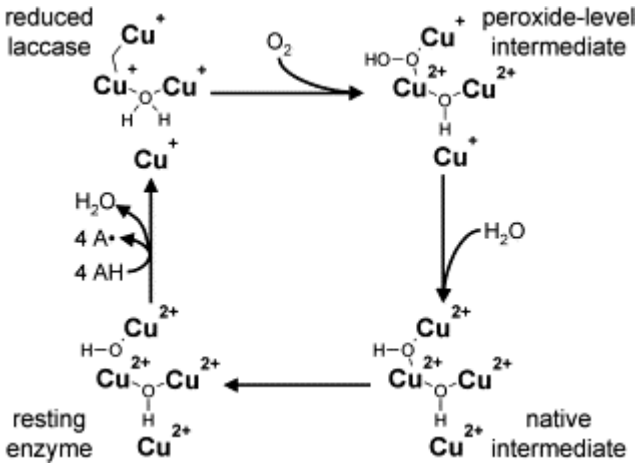


**Figure 1**.**2** Illustration of the catalytic cycle of laccases (Wesenberg et al., 2003).

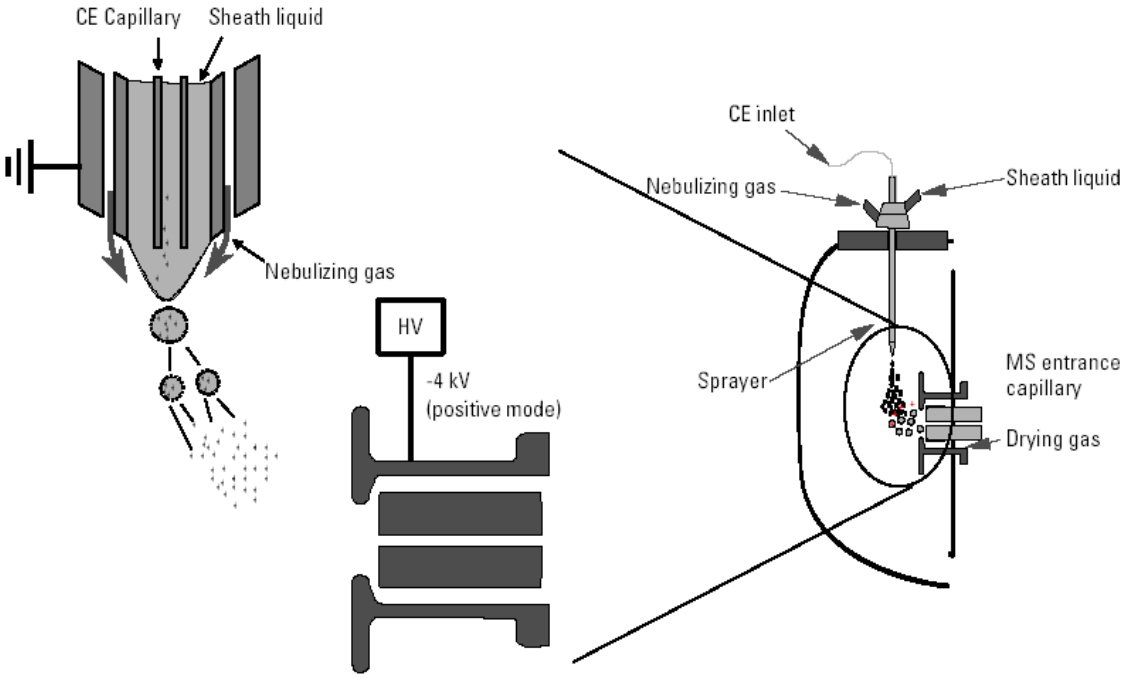


**Figure 1.3** Interface of CE-MS (Agilent® Technologies)

# CHAPTER 2

# MATERIALS AND METHODS

## 2.1 Materials

### *2.1.1 Chemicals*

Two model non-ionic dyes, Disperse Orange 3 (4-[(4-nitrophenyl)azo]-benzeneamine, Color Index No. 11005, 90% colorant content), Disperse Orange 3 (Color Index No. 11005, 20% colorant content), and Disperse Yellow 3 ((N-[4-[(2-hydroxy-5-methylphenyl)azo]phenyl]-acetamide, Color Index No. 11855, 30% colorant content) (Table 2.1), was purchased from Aldrich Chemical Co. (Milwaukee, Wis.). The commercial forms of these dyes contain dispersing agents and surfactants. The structures of disperse dyes are shown in Figure 2.1. Compounds used as standards were analytical grade reagents and were obtained from Aldrich Chemical Co.. They are: 4-nitroaniline, 4-nitrophenol, 4-nitroanisole, nitrobenzene, veratryl alcohol, veratryl aldehyde, 1,4-phenylenediamine, 1,4-dinitrobenzene, 4-nitrocatechol, 2-amino-5-nitrophenol, aniline, 2-nitroaniline, 3-nitroaniline, acetanilide, 4'-aminoacetanilide, 4-acetamidophenol, 4'-nitroacetanilide, and 6-amino-m-cresol.

Two model ionic azo compounds, 4-[(4-hydroxyphenyl)azo]-benzenesulfonic acid and 4-[(2-hydroxy-1-naphthalenyl)azo]-benzenesulfonic acid (Orange II, Color Index No. 15510) (Table 2.1, Figure 2.1), were purchased from Aldrich Chemical Co. (Milwaukee, Wis.). Compounds used as standards, benzenesulfonic acid, 4-hydroxy-benzenesulfonic acid, veratryl

alcohol, veratryl aldehyde, and other possible products, sulfanilic acid, 1,2-naphthoquinone, benzenequinone, were analytical grade reagents and were obtained from Aldrich.

Acetonitrile (Aldrich) and methanol (EMD Chemicals, Gibbstown, NJ) used in analysis and sample preparation were of HPLC grade. Phosphoric acid (85%), potassium dihydrogen phosphate and sodium hydroxide pellets were analytical grade (J. T. Baker, Phillipsburg, NJ). Ammonium acetate was obtained from Aldrich and ammonium hydroxide (28%) was purchased from J. T. Baker (Phillipsburg NJ). All other chemicals used throughout this study were reagent-grade chemicals. Purified water was obtained from an ion exchange and membrane filtration system from U.S. Filter (Warrendale, PA).

*2.1.2 Microorganism*

Previous workers in our lab had screened a number of white rot fungi for their ability to decolorize a variety of dyes (Cao, 2000). One of the most effective organisms, *Pleurotus ostreatus* (strain Florida), was used in this work. This fungus was obtained from the laboratory of Dr. Karl-Erik Eriksson at the University of Georgia. The culture was maintained on malt agar plates (malt extract 20 g/L, agar 15 g/L) at 30°C, with subcultures routinely made every month.

*2.1.3 Culture conditions of white rot fungus*

Nitrogen-limited cultures of *Pleurotus ostreatus* grown in Kirk's medium (Table 2.1) were incubated at 30 ºC in 250 ml Erlenmeyer flasks at pH 5.0. Cultures were established in the incubator, shaken at 200 rpm, and allowed to grow for three days.

## 2.2 Methods

### *2.2.1 Purification of disperse azo dyes*

Disperse Orange 3 (DO3) was further purified by recrystallization from acetonitrile. The purity of DO3 was examined by high performance liquid chromatography (HPLC) using UV-Visible detection, and observable impurities were not found. Disperse Yellow 3 (DY3) was also purified by recrystallization with ethyl alcohol and the purity was checked by HPLC. The purified DY3 was used in the degradation product analysis with thin layer chromatography.

### *2.2.2 Degradation of disperse azo dye*

On day three, DO3, which had been finely ground, was added to flasks containing the fungal system to give an initial solid to liquid ratio (wt/v) of 80 ppm of the dye. The shaking rate in the biodegradation was reduced to 150 rpm and samples were taken daily over a period of 9 days. Controls were carried out under the same conditions but without dyes and /or inoculum. All results reported are based on at least three replicated experiments.

Commercial disperse dyes contain formulating agents and exist in the dispersion forms when put in water. A concentration of 200 ppm of commercial dye in dispersion was added to each flask. Controls were carried out under the identical conditions with fungal degradation but without dyes and /or inoculum.

### *2.2.3 Biodegradation of ionic acid azo dyes*

The concentration of each dye was 100 ppm in the flask and samples were taken daily everyday for 7 days. Controls were carried out under the identical conditions with fungal degradation but without dyes and /or inoculum.

*2.2.4 Thin Layer Chromatography (TLC)*

The supernatant liquid (around 125 ml) from the fungal culture was filtered, and then extracted three times with methylene chloride (totally 60 ml). The organic phases were combined and concentrated to about 10 ml. The samples were kept at low temperature for further analysis. A salting out procedure in sample solution was used to facilitate the extraction.

The analysis was performed on a 5 × 20 cm Selecto Silica Gel 60, F-254 plates from Selecto Scientific (Suwanee, GA). The specimens with a volume of 4-5 microliters were applied to the starting line. The mobile phases were ethyl acetate - hexane (2:1) for products from DO3 and ethyl acetate - hexane (4:1) for products from DY3. The chromatograms were run until the solvent front traveled 80 mm. Spots of original dyes were easily to be detected on the plate because of their color. Non-colored products were detected under UV light (254 nm). The $R_f$ value of each product was compared to the standard to determine the identification of the structure. To prevent errors from a single run, all the samples were run on three different plates and the average $R_f$ values of spots for the three runs were used in identification. For the purpose of double-checking, the standard compounds were run on the same plate again with the degradation solutions.

*2.2.5 Gas chromatography-mass spectrometry (GC-MS)*

Cultures were gravity filtered with P8 filter paper from Fisher Scientific (Hampton, NH). The filtrate from each flask (around 120 ml) was extracted with methylene chloride three times. The combined organic layers, approximately 30 ml, were concentrated to about 1 ml under reduced pressure after drying with sodium sulfate.

GC-MS was performed using a QP5000 mass spectrometer from Shimadzu (Kyoto, Japan) fitted with a GC-17A gas chromatograph (Shimadzu; Kyoto, Japan). The ionization voltage was

70 eV. Gas chromatography was conducted in the temperature-programming mode with a XTI-5 column (0.25 mm by 30 m) from Restek (Bellefonte, PA). The initial column temperature was held at 40 °C for 4 min, then increased linearly to 270°C at 10 °C/min, and held for 4 min at 270°C. The temperature of the injection port was 275 °C and the GC/MS interface was maintained at 300°C. Helium was used as carrier gas with a flow rate of 1.0 ml/min. Injection was splitless to increase sensitivity. Identification of degradation products was made by comparison of retention time and fragmentation pattern with known reference compounds as well as with mass spectra in the NIST spectral library stored in the computer software (version 1.10 beta, Shimadzu) of the GC-MS.

*2.2.6 UV-Visible spectrophotographic analysis*

Aliquots of 1-2 ml volume of supernant were taken from the each reaction flask at regular time intervals and their absorbance was measured immediately using a UV-Visible recording double beam spectrophotometer (Shimadzu, Kyoto, Japan). All samples had to be diluted before measurement to keep recorded absorbance below 2.5 absorbance units. Because of the low water solubility of non-ionic disperse dyes, an equal volume of methanol was mixed with the sample solution to ensure complete solubilization prior to measurement. Degradation of original dyes was determined spectrophotometrically by monitoring the absorbance at the wavelength maximum for each dye.

It was observed that some dyes were absorbed by the fungal biomass without degradation. In that case, the actual biodegradation was not equal to the measured decolorization and should be adjusted by subtraction of the absorbed dye. Aliquots of clear dye solution were taken from each reaction flask daily and measured immediately using a UV-Vis recording double beam spectrophotometer (Shimadzu, Kyoto, Japan). The same amount of dye solution was replenished

into the fungal medium to keep a constant volume in the degradation system. The adsorption of dye by fungal biomass was specifically measured with UV-Visible spectrophotometer. Adsorption of the dye was determined by experimentation with dead cells. Fungal pellets were collected after 3 days incubation and were autoclaved to kill living cells. Then they were put back into the liquid medium with a dye concentration of 100 ppm and were incubated for six hours at conditions identical to those for the biodegradation. The percent of adsorption was determined by measuring the decrease at the wavelength maximum for the specific dye.

*2.2.7 High performance liquid chromatography (HPLC)*

Three milliliters of supernatant were taken from the fungal culture by pre-autoclaved pipette each day for 9 days. The same amount of liquid medium containing 200 ppm disperse dye was added after each sampling to keep a constant volume in the culture flask. Four replicate flasks with the same dye concentration were used for the study and results were reported as an average of the four samples. It was observed that no significant variation of dye concentration was induced by photo-degradation and no degradation products were detected in control samples (that is, samples with no fungal culture included). The samples were filtered through a 0.45 μm membrane filter prior to HPLC analysis.

A Hewlett-Packard 1100 series HPLC system (Hewlett-Packard GmbH, Germany), consisting of a model G1311A quaternary pump, G1322A degasser, and a diode array detector (Model G1315A), was used to perform the analysis. HP ChemStation software (version 3.1) was used for data processing and reporting. A volume of 100 μl was added by an automatic injector (Model 1313A). The flow rate was held at 1 ml/min during the run.

Standards were created by dilution of stock solutions, which were prepared in methanol or water (1.00 mg/ml) and were stored at 4°C, to give concentrations of 0.05, 0.10, 0.25, 0.50, and

1.25 μg/ml. Calibration equations were obtained by linear regression of peak areas against concentrations of the standard solutions. Concentration of products in the samples was calculated using the linear regression equations. Because most of the disperse dye exists in the form of particles in the liquid, and was retained by the membrane filter, quantitation of the dye was not conducted in the study. Peak areas were always based on $\lambda_{max}$ of each compound . All calibration curves were linear ($r^2 > 0.999$) over the investigated concentration range.

*2.2.8 Capillary electrophoresis – mass spectrometry (CE-MS)*

The CE equipment used was Hewlett Packard$^{3D}$ CE (Palo Alto, CA). The capillaries for CE separation (50 μm I. D., 360 μm O. D.) were preconditioned with acetonitrile, 1 N NaOH, 0.1 M HCl, and water for 10 min each, and conditioned with running buffer for 20 min before the first run and for 3 min between runs. Sheath liquid was delivered by a syringe pump (Cole-Parmer Instrument Co. Vernon Hills, IL) using a 1000 mL syringe (Hamilton Co. Reno, NE). Hydrodynamic injection was performed with a pressure of 50 mbar (1 mbar = 100 Pa). The voltage applied in separation was +30 kV. The mass spectrometer used was an Esquire 3000 plus ion trap equipped with an electrospray ionization (ESI) interface (Bruker Daltonics, Billerica, MA), which was operated in negative ionization mode. ESI voltage was 4.0 kV. CE and MS are connected through a commercial interface based on coaxial sheath flow. The length of the CE capillary was 100 cm. The position of the CE capillary with ESI needle was adjusted during optimization. Mass spectrometric parameters used in the analysis were listed as follows: maximum accumulation time 50 ms; scan 60-400 m/z; average 8; compound stability 100%; scan range normal; trap drive level 100%; ion charge control activated; mass resolution 0.45 u. The standard solutions and buffers were filtered with 0.20 μm Spartan-13 NY membrane (Schleicher & Schuell MicroScience, Dassel, Germany).

Quantification of major degradation products from the model azo dyes was carried out with a Hewlett Packard$^{3D}$ CE coupled with an Esquire 3000 plus ion trap mass spectrometer. The configuration of the ESI interface and the running conditions of CE-MS were described in detail in Chapter 5. Hydrodynamic injection was performed with a pressure of 50 mbar (1 mbar = 100 Pa). The length of CE capillary (50 μm I. D., 360 μm O. D.) was 100 cm and pretreatment of the new capillary followed that described in Chapter 5. Establishment of the calibration curve and quantification calculation were conducted with *QuantAnalysis*™ software of Bruker Daltonics.

### 2.3 Strategy for this research

Despite the fact that decolorization of dyes by white rot fungi has been extensively studied, the details of how this biodecolorization of azo dyes occurs is still lacking. There have been few attempts to comprehensively examine dye effluent systems after biotreatment by white rot fungi. Decolorization, by itself, demonstrates only the transformation of the chromophoric group of a dye. It does not reveal much about the degradation of the dye molecules or the potential for production of toxic by-products. The objectives of this study are to use state-of-the-art analytical techniques to investigate the degradation products of dyes by white rot fungi, to examine the decolorization of two widely used nonionic disperse azo dyes and two ionic dyes with different structures (Table 2.1) in white rot fungal cultures, to analyze biodegradation products generated in the biotreatment system, and to elucidate possible degradation mechanism. The dissertation consists of study of biodegradation of model nonionic azo dyes, which includes Chapter 3, and Chapter 4, and study of biodegradation of model ionic azo compounds, which is described in Chapter 5.

**Table 2.1** Model azo dyes used in this study

| DESIGNATION | DYE NAME | CHEMICAL NAME | CAS NO. | COLOR. INDEX NO. |
|---|---|---|---|---|
| DO3 | Disperse Orange 3 | 4-[(4-nitrophenyl)azo]-benzeneamine | 730-40-5 | 11005 |
| DY3 | Disperse Yellow 3 | N-[4-[(2-hydroxy-5-methylphenyl)azo]phenyl]-acetamide | 2832-40-8 | 11855 |
| 4HABA | | 4-[(4-hydroxyphenyl)azo]-benzenesulfonic acid, sodium salt | 2918-83-4 | |
| Orange II | Acid Orange 7 | 4-[(2-hydroxy-1-naphthalenyl)azo]-benzenesulfonic acid, sodium salt | 633-96-5 | 15510 |

**Table 2.2** Composition of Kirk's medium (Kirk et al. 1978)

| CHEMICALS | CONCENTRATION (G/L) |
|---|---|
| Potassium dihydrogenphosphate | 0.2 |
| Magnesium sulfate | 0.05 |
| Calcium chloride | 0.01 |
| Ammonium tartrate | 0.22 |
| Glucose | 10 |
| Nitrilotriacetate | 1.5e-3 |
| $MgSO_4 \bullet 7H_2O$ | 3.0e-3 |
| $MgSO_4 \bullet H_2O$ | 5.0e-4 |
| NaCl | 1.0e-3 |
| $FeSO_4 \bullet 7H_2O$ | 1.0e-4 |
| $CoSO_4$ | 1.0e-4 |
| $ZnSO_4$ | 1.0e-4 |
| $CuSO_4 \bullet 5H_2O$ | 1.0e-5 |
| $AlK(SO_4)_2$ | 1.0e-5 |
| $H_3BO_3$ | 1.0e-5 |
| $NaMoO_4$ | 1.0e-5 |
| Biotin | 1.0e-3 |
| Folic acid | 2.5e-3 |
| Thiamine• HCl | 2.5e-3 |
| Riboflavin | 2.5e-3 |
| Pyridoxine• HCl | 5.0e-3 |
| Cyanocobalamine | 5.0e-5 |
| Nicotinic acid | 2.5e-3 |
| DL-calcium pantothenate | 2.5e-3 |
| p-Aminobenzoic acid | 2.5e-3 |
| Thioctic acid | 2.5e-3 |

A quantity of 1.2 ml glacial acetic acid was added to 1 liter of the above solution and the pH was adjusted to 5.0 by 6 N sodium hydroxide solution.

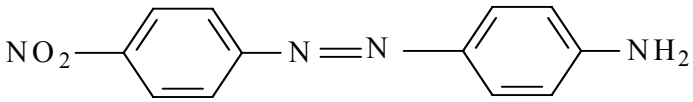

Disperse Orange 3 (DO3)

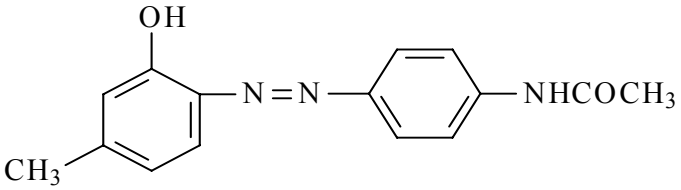

Disperse Yellow 3 (DY3)

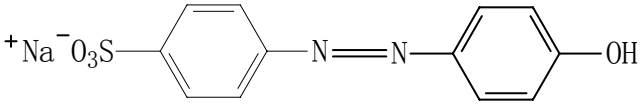

4-[(4-hydroxyphenyl)azo]-benzenesulfonic acid, sodium salt (4HABA)

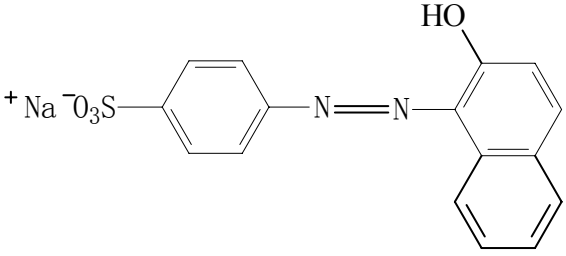

Acid Orange 7 (Orange II)

**Figure 2.1** Structures of model azo dyes

# CHAPTER 3

# IDENTIFICATION AND QUANTIFICATION OF DEGRADATION PRODUCTS OF DISPERSE ORANGE 3

## 3.1 Identification of products

### *3.1.1 Thin layer chromatography (TLC)*

Thin layer chromatography was used to primarily identify the degradation products from DO3. In the course of developing the optimal mobile phase for TLC, the following components were tested - benzene, methanol, acetone, chloroform, tetrahydrofuran, toluene, n-hexane, and ethyl acetate. The combination of n-hexane and ethyl acetate proved to be the best chromatographic system. Ethyl acetate and n-hexane were tried at different ratios and satisfactory separation of the degradation products was achieved at a 2:1 ratio.

The results indicated that two spots other than the dye itself could be detected on TLC. Six standard compounds, 4-aminophenol, 4-nitrophenol, 1,2-benzoquinone, 4-nitroaniline, aniline, and 1,4-phenylenediamine, were run on the same plate with the sample for qualitative identification of the separated spots. Among these compounds, 4-nitroaniline was a possible product. By running both samples and standard on the same plate several times, 4-nitroaniline and the product from DO3 showed identical $R_f$ value (Table 3.1). The filtered fungal spores were also extracted with methylene chloride and the organic layer was analyzed by the same TLC method. No additional degradation product was found.

Detection of 4-nitroaniline and another possible product from DO3 by TLC showed that this non-phenolic azo dye could be degraded in *Pleurotus ostreatus* culture. Since various extracellular enzymes are known to be present in *Pleurotus ostreatus*, some other degradation products were expected by the interaction of dye with these enzymes. The extracellular enzymes have been shown to use a cationic radical pathway to degrade azo dyes *in vitro* (Spadaro and Renganathan, 1994, Goszczynski et al. 1994). Despite these researches on the degradation of azo dyes by the free enzymes, mainly peroxidases, knowledge of expected degradation products from dyes in cell culture of white rot fungi is still lacking.

DO3 has no phenolic substituent, a type of azo dye whose degradation by white rot fungi has not been explored in depth before. Because of its structure, DO3 may display different characteristics in degradation by white rot fungi compared to phenolic compounds.

*3.1.2 Gas chromatography – mass spectrometry (GC-MS)*

The identification of several degradation products from purified DO3 by *Pleurotus ostreatus* was achieved with GC-MS (Figure 3.1). The results showed four compounds, nitrobenzene, 4-nitrophenol, 4-nitroaniline, and 4-nitroanisole, as degradation products (Figure 3.2a, 3.2b, 3.2e, 3.2f). One of these products, 4-nitroaniline, had also been detected by thin layer chromatography. None of these compounds was detected in the control samples. Veratryl alcohol (Figure 3.2d) and its oxidation product, veratraldehyde (Figure 3.2c), were also found in the *Pleurotus ostreatus* supernatant after incubation with azo dyes. Most of the other major peaks in the mass chromatogram (Figure 3.1) were impurities or compounds generated in fungal metabolism, which also appeared in the control samples.

## 3.2 Quantification of products

### *3.2.1 Determination of decolorization*

The absorptivities are intrinsic properties of a colorant and the spectral curves of dyes during biodegradation provided a means to determine the reaction rate and gave evidence of the structural change of dyes during biodegradation. Thus, decolorization of DO3 was determined using the decrease of absorbance maximum of dye.

DO3 (Figure 2.1) contains two substituted aromatic rings, one with an amino substituent and the other with a nitro substituent, typical of many monoazo disperse dyes. The visible spectrum of DO3 has its maximum at 415 nm (Figure 3.3). The decrease in absorbance at the maximum wavelength of this disperse dye occurred primarily in the first few days of treatment, with little further decrease in absorbance as the treatment time was increased. After ten days of biotreatment, $\lambda_{max}$ shifted to 388 nm and decreased by 57 percent. This change indicated that some products absorbed in the lower wavelength and color became yellow.

Bioaccumulation and sorption of hydrophobic organic compounds in biomass has been well reviewed by Baughman and Paris (1981), who suggested an octanol-water partition coefficient ($K_{ow}$) could be used in estimation of sorption. The $K_{ow}$ of DO3 is $10^{3.5}$, which indicates DO3 is very hydrophobic and its sorption by fungal cells is not insignificant. The sorption of disperse dyes by biomass contributed to the high decolorization of disperse dye. Sorption was determined by experimentation with dead cells. The fungal pellets were collected and autoclaved to kill living cells. Then they were put back in liquid medium with 200 ppm dye in shaker and operated for six hours at the identical conditions of biodegradation. The dead fungal cells adsorbed 10 percent of dye as determined using UV-Vis spectrophotometric analysis. Thus, degradation of dye accounted for four-fifths of the total decolorization.

*3.2.2 Optimization of the HPLC method for quantification*

HPLC was chosen to quantify products of the commercial azo dye in this study because of its accuracy, high separation efficiency and relatively simple sample preparation. The supernatant culture liquid sample contained background interferences such as nutrients and fungal cells but did not greatly complicate HPLC chromatography after filtration. The sample employed in the quantification needs not further purification except filtration. This method is more accurate and saves tedious work in sample preparation compared to the GC-MS analysis. The culture supernatant used in the HPLC analysis contains various organic compounds with different polarities. To separate the degradation products with the best resolution and highest sensitivity, two columns were tested in analysis and composition of mobile phase, pH value, and running temperature were optimized.

*3.2.2.1. Analytical column selection*

Two different analytical columns from Phenomenex (Torrance, CA) were tested for their effectiveness in analysis of biodegradation products. A Luna$^{TM}$ cyano column (150 × 4.6 mm I. D., 5 μm, Phenomenex) was first tested because of its ability to retain polar compounds (degradation products) without extensively retaining hydrophobic compounds (azo dyes with relatively larger molecules and low polarity).

Four key products, 4-nitrophenol, 4-nitroaniline, nitrobenzene, 4-nitroanisole, as well as veratryl alcohol, a secondary metabolite from white rot fungi and a mediator for lignin peroxidase, and its oxidation product, veratryl aldehyde, were the target analytes for HPLC analysis. Thus, HPLC was developed to separate these compounds first.

When the cyano column was used in HPLC analysis, the retention times for most degradation products and azo dyes were satisfactory. However, two products, 4-nitroaniline and

4-nitrophenol, could not be completely separated regardless of how other variables were changed. Although it took a longer time to separate all the target analytes with a gradient method on an Ultracarb$^{TM}$ ODS column (150 × 4.6 mm I. D., 5 μm, Phenomenex), the base-line resolution was achieved for all compounds of interest with little compromise in sensitivity. Thus, a stainless steel Ultracarb ODS column with 5 μm packing from Phenomenex (150 × 4.6 mm I. D.) was chosen as the analytical column and a RP-C18 guard pre-column was used to protect the analytical column.

*3.2.2.2 Composition of mobile phase*

The organic component in the mobile phase has an important influence in the selective separation of analytes. Both methanol and acetonitrile were tested as organic modifier in the mobile phase optimization. The chromatographic peaks of 4-nitrophenol and veratryl aldehyde broadened when methanol was used in the mobile phase. Adjusting the buffer pH to 2.5 did not sharpen those peaks to a satisfactory shape. The use of acetonitrile in the mobile phase not only gave a narrower peak but less baseline drift in the analysis. Thus, acetonitrile was used as organic modifier for the mobile phase throughout the analysis.

*3.2.2.3 pH value and concentration of buffer*

The effects of pH values of the buffer were investigated to obtain the best separation. Buffers with different pH values ranging from 3.0 to 7.0 were tried in the analysis. The separation performance declined as the pH value of the buffer increased. The pH 3.0 phosphate buffer provided the best separation efficiency among the buffers tested. Since further adjusting the pH values of the buffer to 2.5 and 3.5 did not improve the separation efficiency and resolution, the mobile phase consisting of buffer with pH 3.0 was chosen for subsequent experiments. Increasing the concentration of phosphate from 0.010 M to 0.025 M improved the

symmetry of the chromatographic peaks. The gradient method with the 0.025 M phosphate buffer (pH=3.0)- acetonitrile mobile phase was selected (Table 3.3). The chromatogram of the six standards is shown in Figure 3.4.

*3.2.2.4 Temperature*

Generally, increasing the temperature of the column will decrease the retention time for all analytes. However, increasing temperature does not necessarily improve column performance. A range of 20-40°C was tested in the study. At 20 °C, the separation was adequate but the running time was too long. Above 25 °C, the peaks of 4-nitrophenol and veratryl aldehyde began to overlap (Figure 3.5). Thus, 25 °C was chosen for the best resolution and an acceptable retention time.

*3.2.2.5 Selectivity*

To determine the selectivity and accuracy of the developed method, a known weight of each standard was spiked into the fungal culture system containing azo dye with a concentration of 200 ppm. All the products were well separated from each other and interferences from culture fluid constituents (Figure 3.6). Recovery of the spiked standards was reported based on average of four replicates. The recovery test showed that all the degradation products had instant recovery of more than 80 percent and more than 70 percent for recovery after 24 hours of treatment under the same biodegradation procedure.

*3.2.3 Quantification of products by HPLC*

Kinetic profiles of the degradation products are shown in Figure 3.7. One of the products, 4-nitroaniline, reached maximum on day 2 and then decreased, indicating that 4-nitroaniline was further degraded in the culture. Nitrobenzene increased markedly after three days and for the remaining nine days of biodegradation. Another product, 4-nitrophenol, was detected after 4

days along with its methylated product, 4-nitroanisole. The curves indicate a possible relationship between 4-nitroanisole and 4-nitrophenol.

### 3.3 Mechanism study of fungal degradation of DO3

The biodegradation of aromatic pollutants is a complex process of oxidation, reduction, methylation and hydroxylation (Mester and Tien, 2000). Thus, the biodegradation of azo dyes is complicated and consists of a mixture of these reactions.

*Pleurotus ostreatus* is known to produce three main liginolytic enzymes, including LiP in Kirk's media (Robinson et al. 2001). Veratryl alcohol is crucial in the lignin peroxidase cycle during oxidations of azo dyes. Helping to complete the catalytic cycle of LiP, veratryl alcohol acts as a third substrate (with hydrogen peroxide and azo dyes) in the reaction (Paszcznski and Crawford, 1991). Veratryl alcohol can be oxidized to veratraldehyde by LiP. Thus, identification of veratryl alcohol and veratraldehye in the degradation system implies that lignin peroxidase is involved in the degradation of this dye. Laccase degrades the azo dyes in a way that is similar to the mechanism for LiP, and both enzymatic reactions follow a radical-initiated oxidation (Chivukula and Renganathan, 1995).

Formation of nitrobenzene (III) occurs in accordance with this peroxidase reaction mechanism (Figure 3.8). It can be generated from the unstable intermediate, 4-nitrophenyldiazene (I), by homolytic bond cleavage to produce nitrobenzene and molecular nitrogen. Hydroxylization of the diazonium salt generated in the azo linkage asymmetric cleavage would yield 4-nitrophenol (IV).

The product 4-nitroanisole (V) is a result of multiple step degradation of DO3. Based on the quantification results, it was probable that 4-nitroanisole came from 4-nitrophenol (IV). To

further examine this possibility, 4- nitrophenol (IV) was added to fungal cultures and its degradation was examined by GC-MS in a separate experiment. Over a period of 4 days, the 4-nitrophenol (IV) was obviously degraded to 4-nitroanisole (Figure 3.9). 4-Nitroanisole was not detected in the control culture sample concurrently ran. Methylation of phenolic compounds by another fungus *Phanerochaete chrysosporium* has been reported (Valli and Gold, 1991; Valli et al., 1992). These results demonstrated that methylation also occurs with degradation by *Pleurotus ostreatus*. The oxidative coupling to form dimers or polymers from 4-nitrophenol, which is related to laccase oxidation (Hublik and Schinner, 2000), was not found in this study. This result may have occurred because these dimers or polymers are nonvolatile and not detectable in GC-MS analysis.

In the decolorization study using *Pleurotus ostreatus*, Rodriguez and co-workers (1999) found that an enzymatic mechanism other than extracellular enzymes could be involved in the decolorization. Formation of 4-nitroaniline (II) suggested a reduction system might be involved in the biodegradation. Although azo dyes resist biodegradation in aerobic conditions, the azo bond is vulnerable to reductive cleavage (Pinheiro et al., 2004). The ability of *Pleurotus ostreatus* to reduce 1,4-dinitrobenzene to 4-nitroaniline (II) has been observed when the possibility of 1,4-dinitrobenzene as a product was tested in the experiment. It is still unclear if reduction is the only pathway for the production of 4-nitroaniline (II), or if other reactions are involved. Another potential reduction product, 4-phenylenediamine, was not be detected in the culture supernatant by HPLC or GC-MS.

Our results demonstrate that three dominant degradation products, nitrobenzene, 4-nitrophenol, and 4-nitroaniline, and one minor product, 4-nitroanisole, were generated in the biodegradation of DO3 by whole cultures of *Pleurotus ostreatus.*

This study and others (Pasti-Grigsby et al., 1992) have found that the aromatic substitution pattern of azo dyes affects their degradation by white rot fungi. Because each phenyl ring in DO3 contains either an amino or a nitro group, the cation radical is more difficult to form for peroxidase-catalyzed oxidation than in phenolic azo dyes. We believe that this is the major factor in the production of 4-nitroaniline (II).

**Table 3.1** TLC analysis of DO3 degradation samples

| SAMPLES | SAMPLE INFORMATION | $R_F$ VALUES OF SPOTS | COLOR OF SPOTS |
|---|---|---|---|
| Disperse Orange 3 | Purified dye | 0.62 | Orange |
| Disperse Orange 3 | Control | 0.63 | Orange |
| Degradation sample | 3 days degradation | 0.63<br>0.54<br>0.44 | Orange<br>Yellow<br>Yellow |
| 4-Nitroaniline | Standard | 0.56 | Yellow |

Mobile phase: ethyl acetate-n-hexane (2:1)
Plates were detected under daylight and UV 254 nm light after drying in air.

**Table 3.2** UV-Vis spectrophotometric analysis of DO3 in degradation

| DAY | ABSORBANCE DECREASE (@ $\lambda_{MAX}$) (%) |
|---|---|
| 0 | 0 |
| 2 | 36 |
| 4 | 39 |
| 6 | 53 |
| 8 | 59 |
| 10 | 57 |

**Table 3.3** Mobile phase program for the HPLC gradient

| TIME (MIN) | FLOW (ML/MIN) | %A | %B | CURVE |
|---|---|---|---|---|
| 0.0 | 1.0 | 5.0 | 95.0 | Linear |
| 20.0 | 1.0 | 25.0 | 75.0 | Linear |
| 30.0 | 1.0 | 40.0 | 60.0 | Linear |
| 40.0 | 1.0 | 40.0 | 60.0 | |
| 45.0 | 1.0 | 5.0 | 95.0 | Linear |

A: Acetonitrile
B: 0.025 M phosphate buffer with pH 3.0

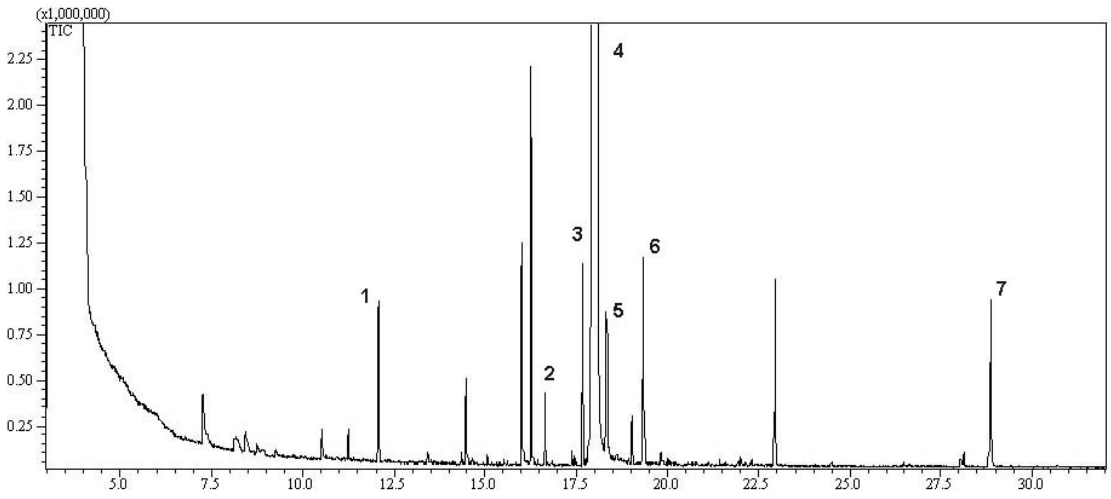


**Figure 3.1** Identification of products from DO3 and metabolites of *Pleurotus ostreatus* using GC-MS. Peak 1, nitrobenzene; Peak 2, 4-nitroanisole; Peak 3, veratraldehyde; Peak 4, veratryl alcohol; Peak 5, 4-nitrophenol; Peak 6, 4-nitroaniline; Peak 7, Disperse Orange 3. Unlabeled peaks belong to impurities or fungal contaminants, which also appealed in controls.

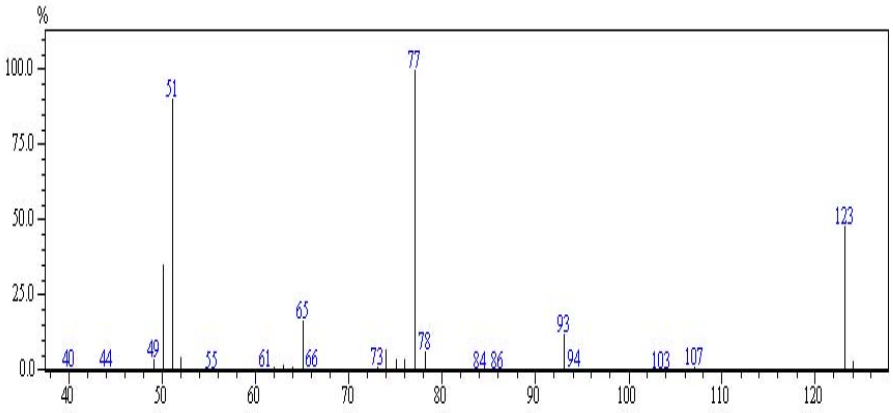


Mass spectrum of standard nitrobenzene (MW=123)

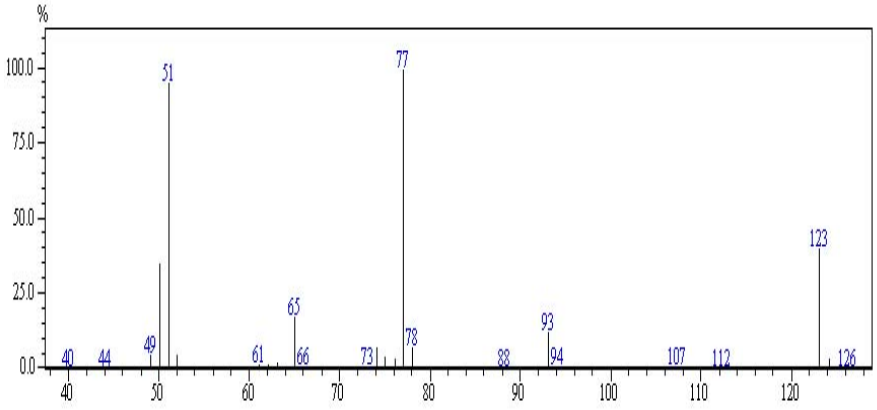


Mass spectrum of Compound 1

**Figure 3.2a** Mass spectra of standard and Compound 1 (nitrobenzene)

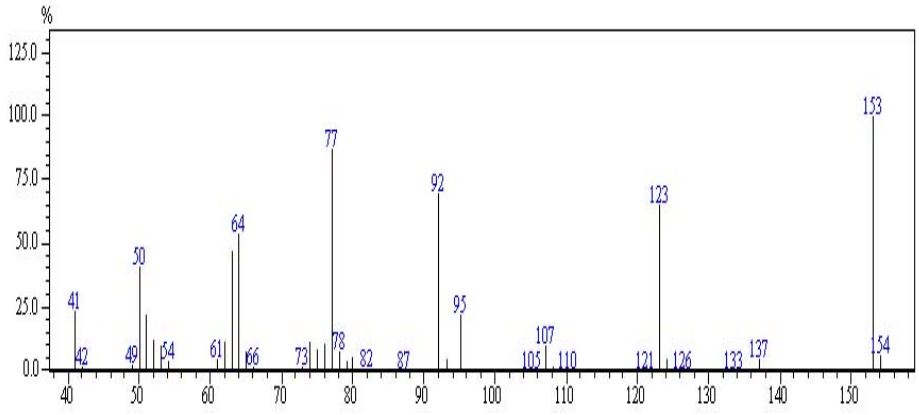


Mass spectrum of standard 4-nitroanisole (MW=153)

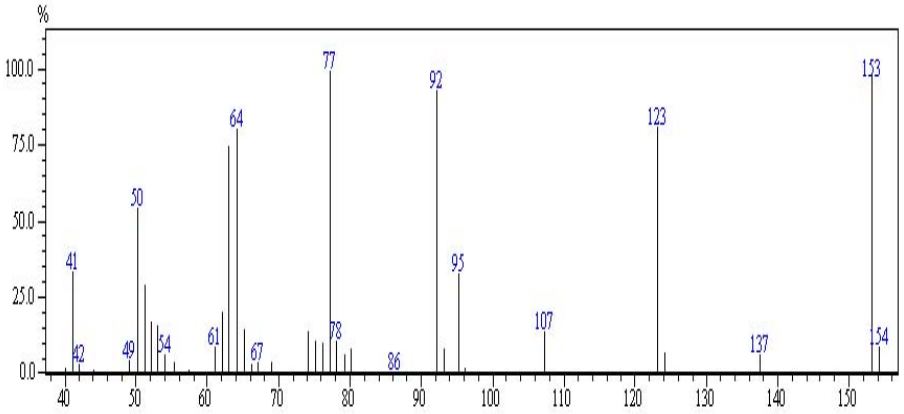


Mass spectrum of Compound 2

**Figure 3.2b** Mass spectra of standard and Compound 2 (4-nitroanisole)

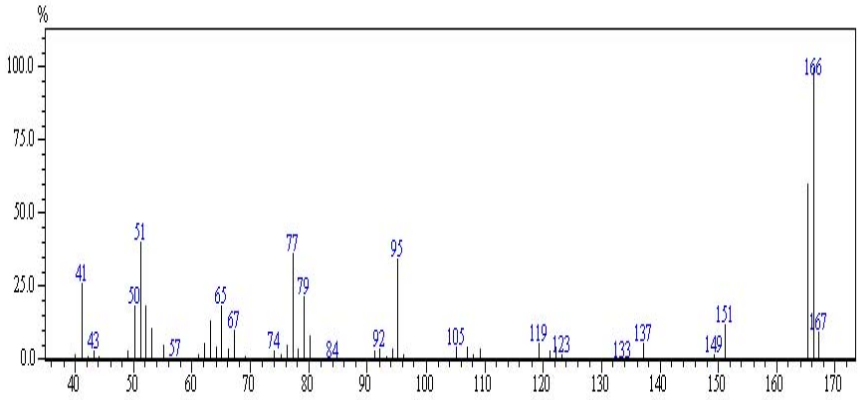


Mass spectrum of standard veratraldehyde (MW=166)

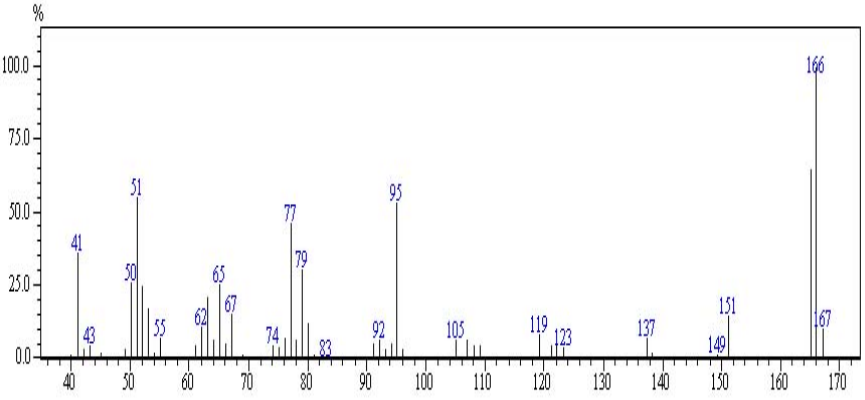


Mass spectrum of Compound 3

**Figure 3.2c** Mass spectra of standard and Compound 3 (veratraldehyde)

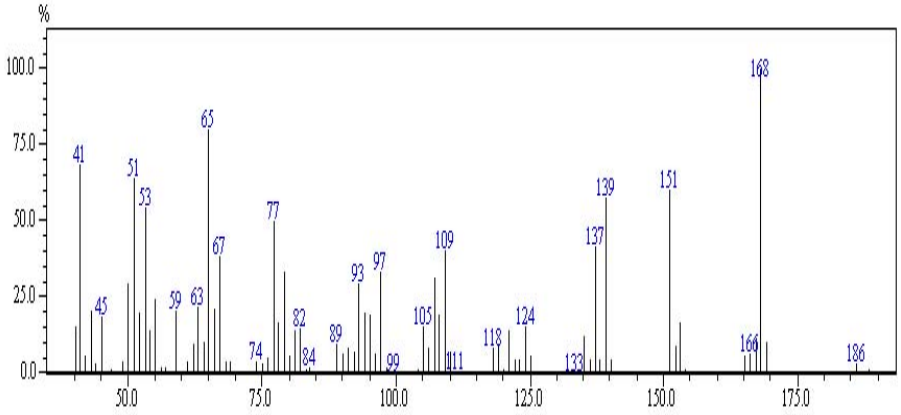


Mass spectrum of standard veratryl alcohol (MW=168)

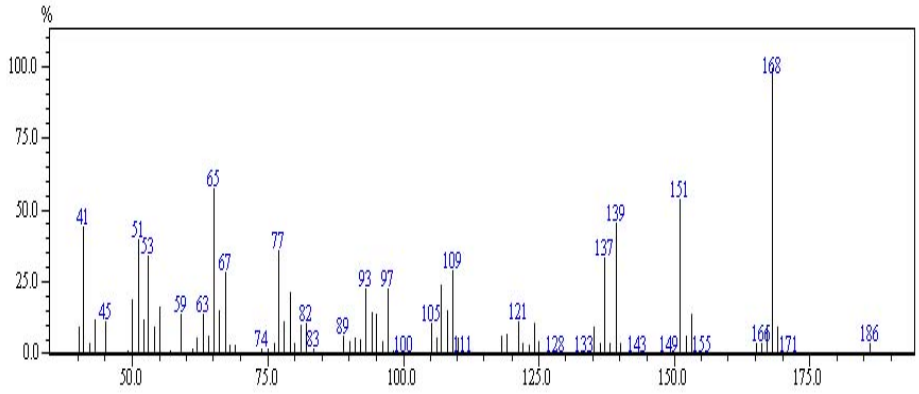


Mass spectrum of Compound 4

**Figure 3.2d** Mass spectra of standard and Compound 4 (veratryl alcohol)

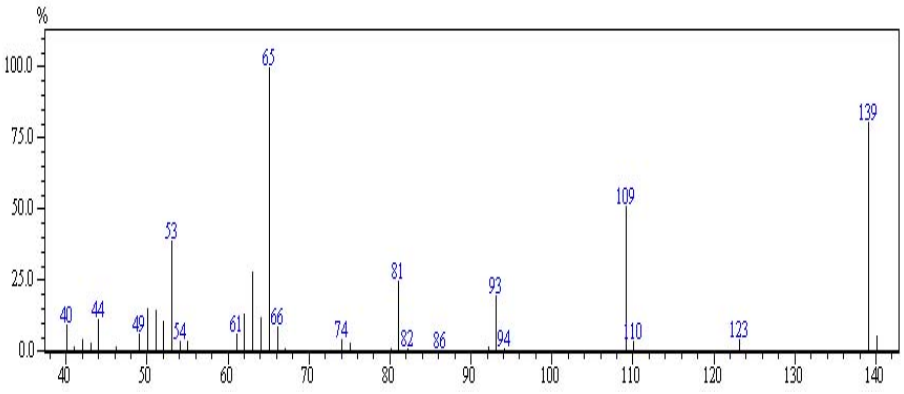


Mass spectrum of standard 4-nitrophenol (MW=139)

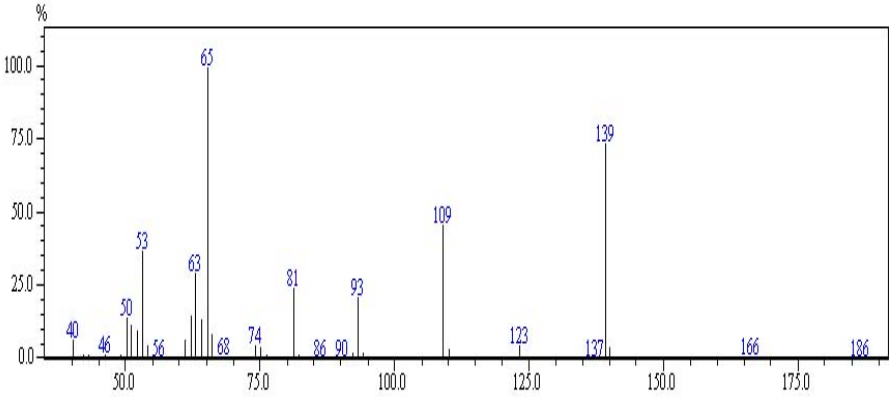


Mass spectrum of Compound 5

**Figure 3.2e** Mass spectra of standard and Compound 5 (4-nitrophenol)

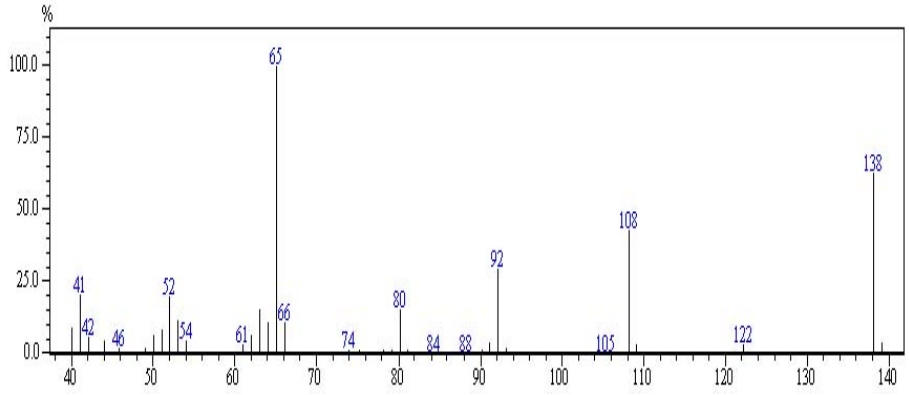


Mass spectrum of standard 4-nitroaniline (MW=138)

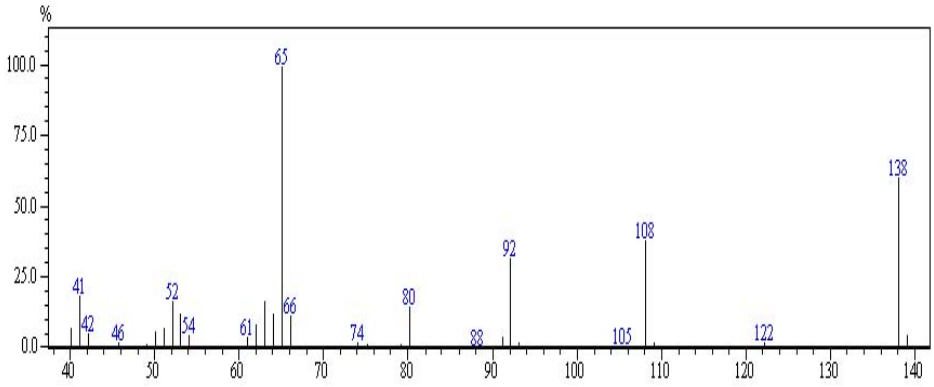


Mass spectrum of Compound 6

**Figure 3.2f** Mass spectra of standard and Compound 6 (4-nitroaniline)

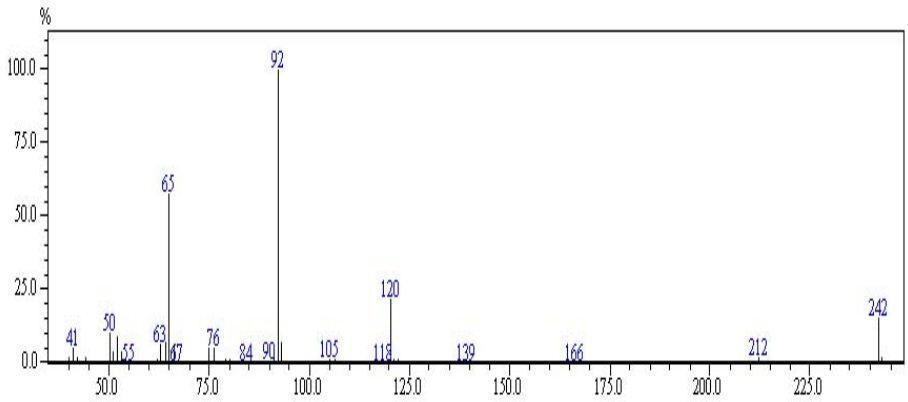


Mass spectrum of standard Disperse Orange 3 (MW=242)

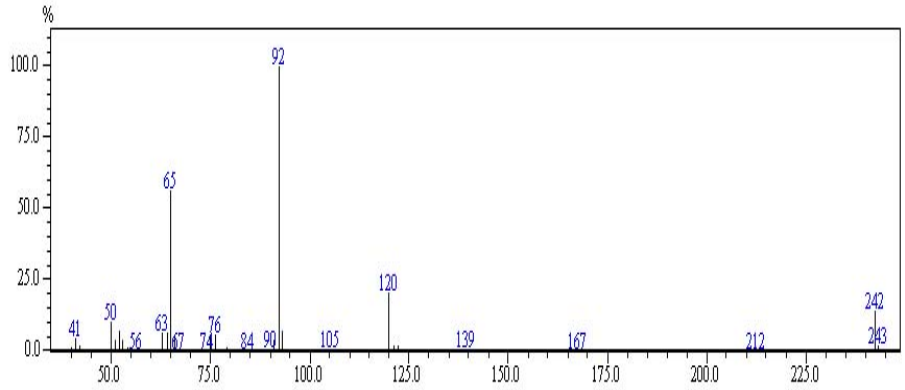


Mass spectrum of Compound 7

**Figure 3.2g** Mass spectra of standard and Compound 7 (DO3)

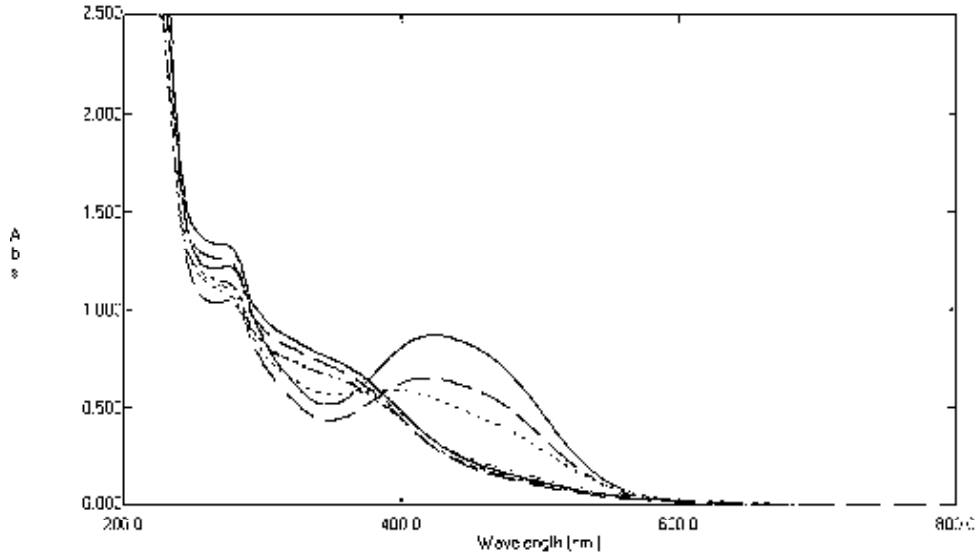


**Figure 3.3** UV-Vis spectra of DO3 during biodegradation by *P. ostreatus.* The curves represent 2 day intervals and absorbance at $\lambda_{max}$ (415 nm) decrease continuously in the degradation.

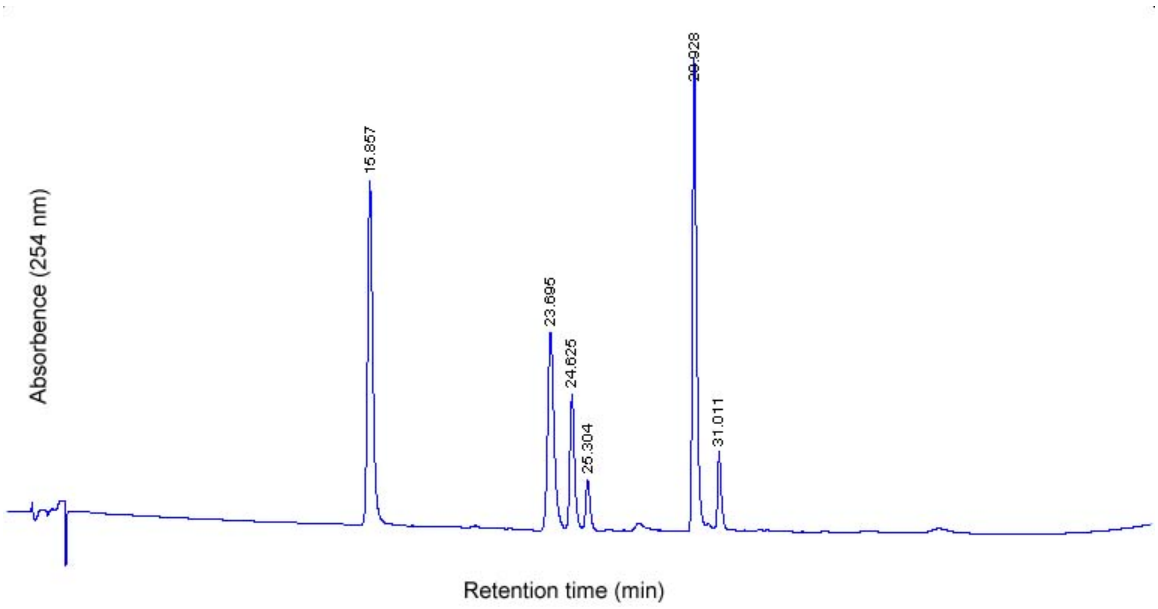


**Figure 3.4** Separation of veratryl alcohol ($t_R$=15.857 min), 4-nitroaniline ($t_R$=23.695 min), veratryl aldehyde ($t_R$=24.625 min), 4-nitrophenol ($t_R$=25.304 min), nitrobenzene ($t_R$=29.928 min), and 4-nitroanisole ($t_R$=31.011 min) standards by HPLC.

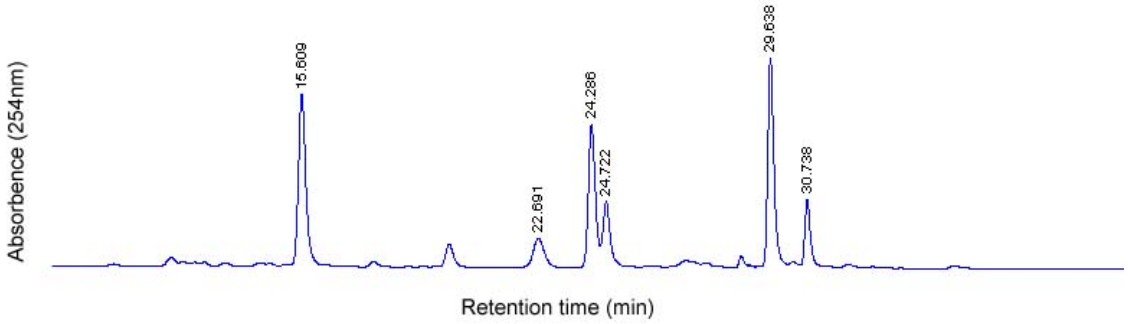


**Figure 3.5** Effect of temperature on HPLC (30°C): veratryl alcohol ($t_R$=15.509 min), 4-nitroaniline ($t_R$=22.691 min), veratryl aldehyde ($t_R$=24.286 min), 4-nitrophenol ($t_R$=24.722 min), nitrobenzene ($t_R$=29.538 min), and 4-nitroanisole ($t_R$=30.738 min).

**(A)**

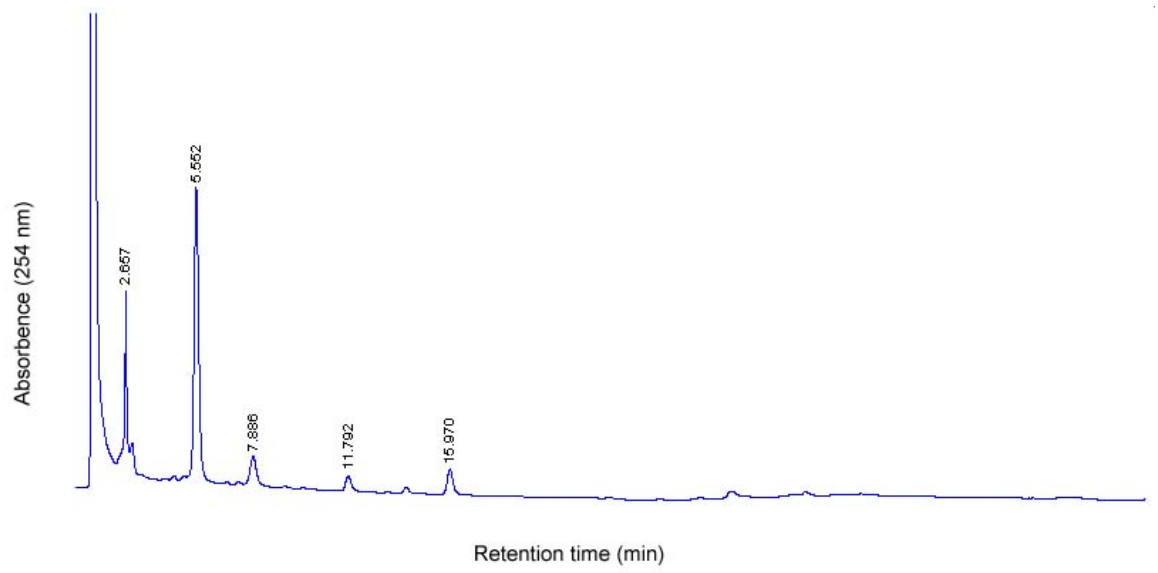


**(B)**

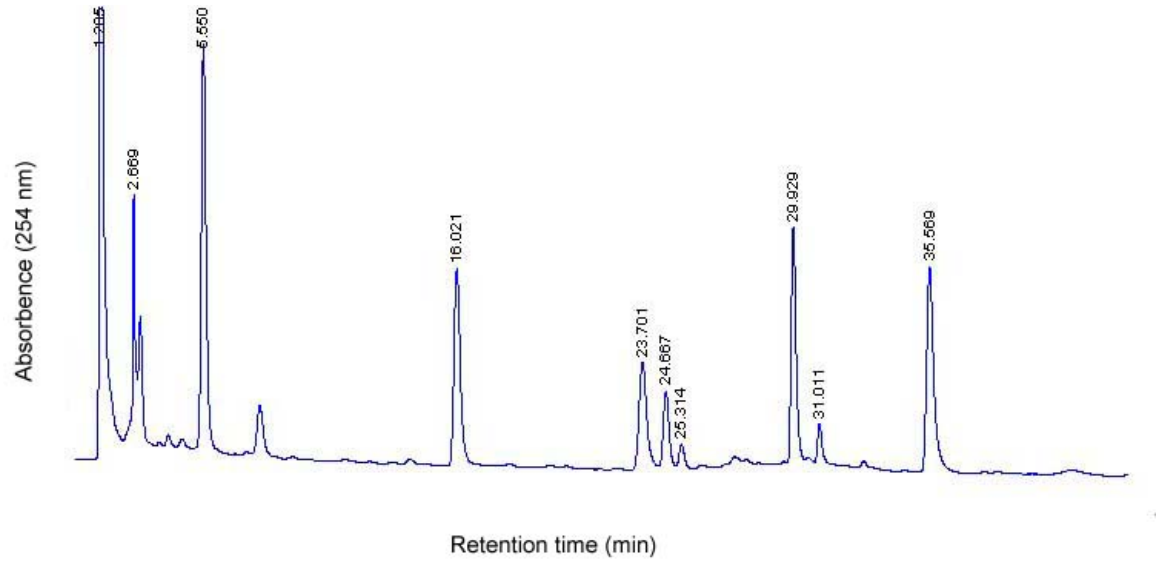


**Figure 3.6** Blank culture medium and culture medium spiked with standards

(A) Blank culture sample from 7 days fungal system. Veratryl alcohol ($t_R$=15.970 min)

(B) Sample with spiked standards: veratryl alcohol ($t_R$=16.021 min), 4-nitroaniline ($t_R$=23.701 min), veratryl aldehyde ($t_R$=24.667 min), 4-nitrophenol ($t_R$=25.314 min), nitrobenzene ($t_R$=29.929 min), 4-nitroanisole ($t_R$=31.011 min), Disperse Orange 3 ($t_R$=35.569 min).

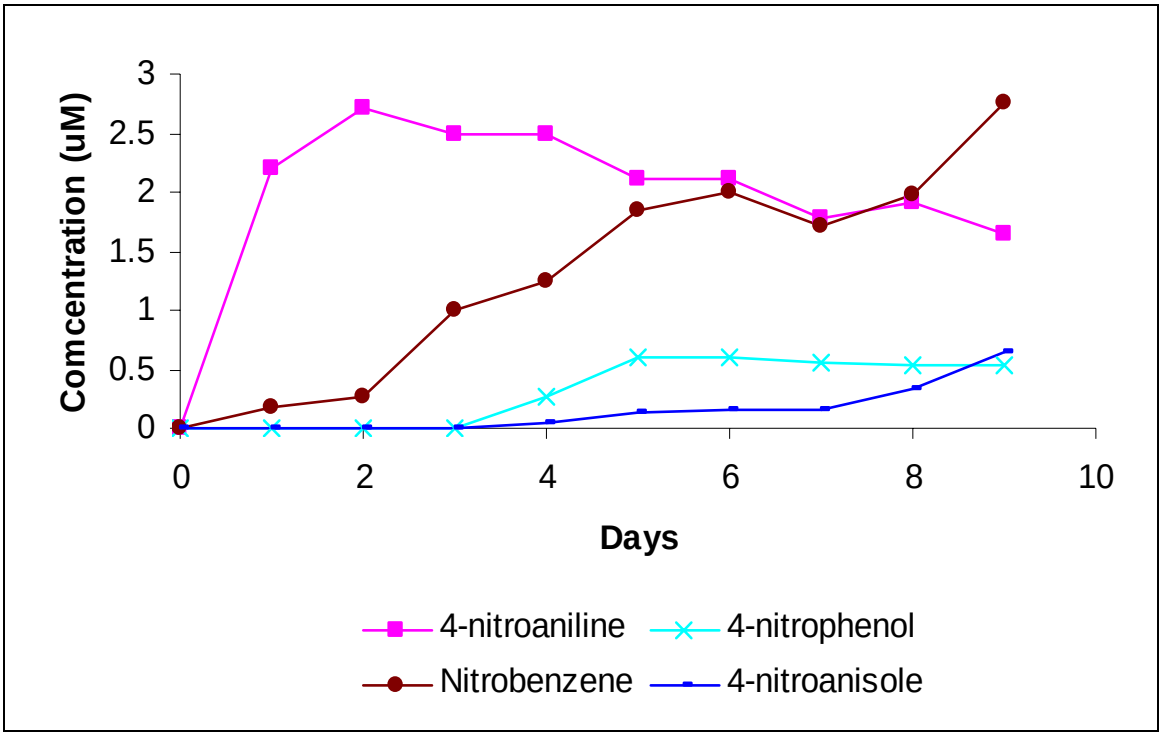


**Figure 3.7** Kinetic profiles of degradation products from DO3 by *Pleurotus ostreatus*

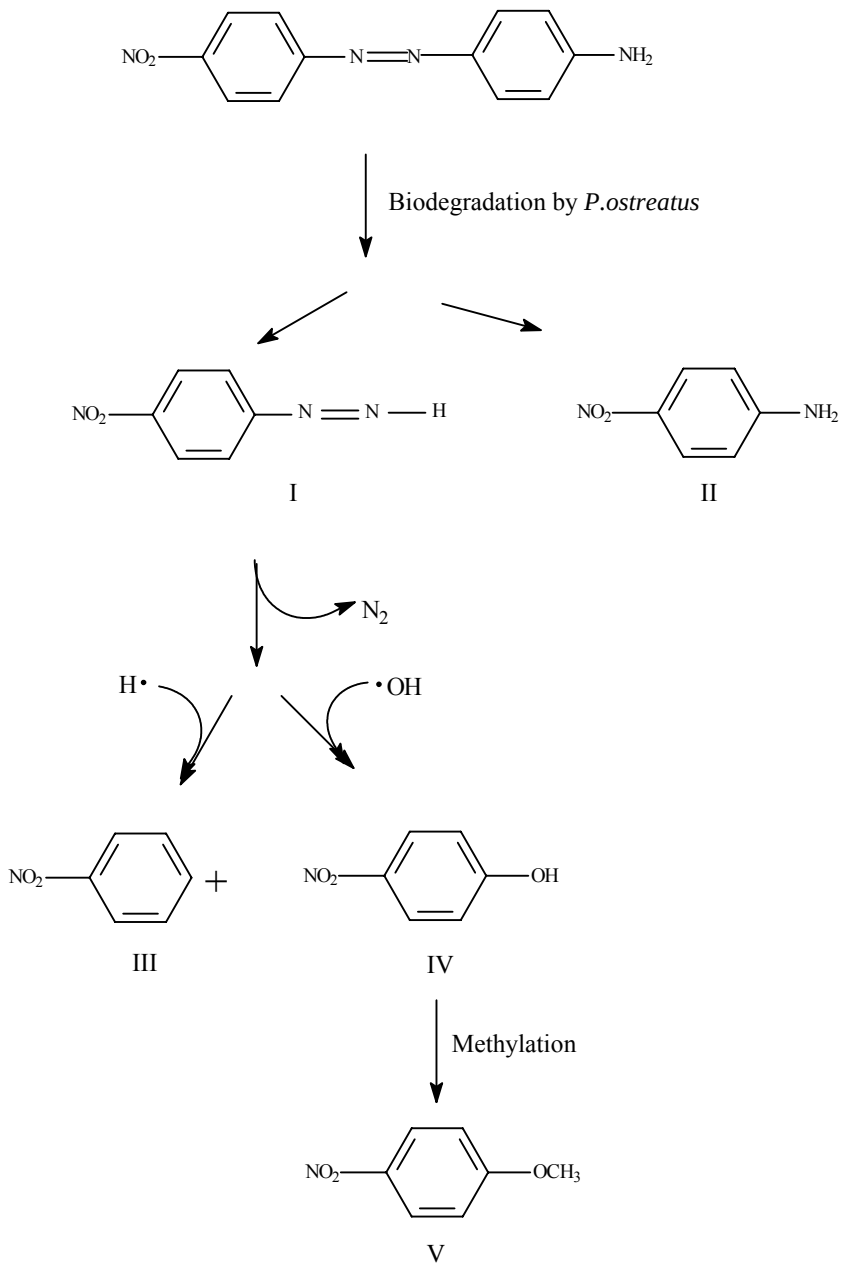


**Figure 3.8** Diagram of biodegradation pathway of DO3 by *Pleurotus ostreatus*.

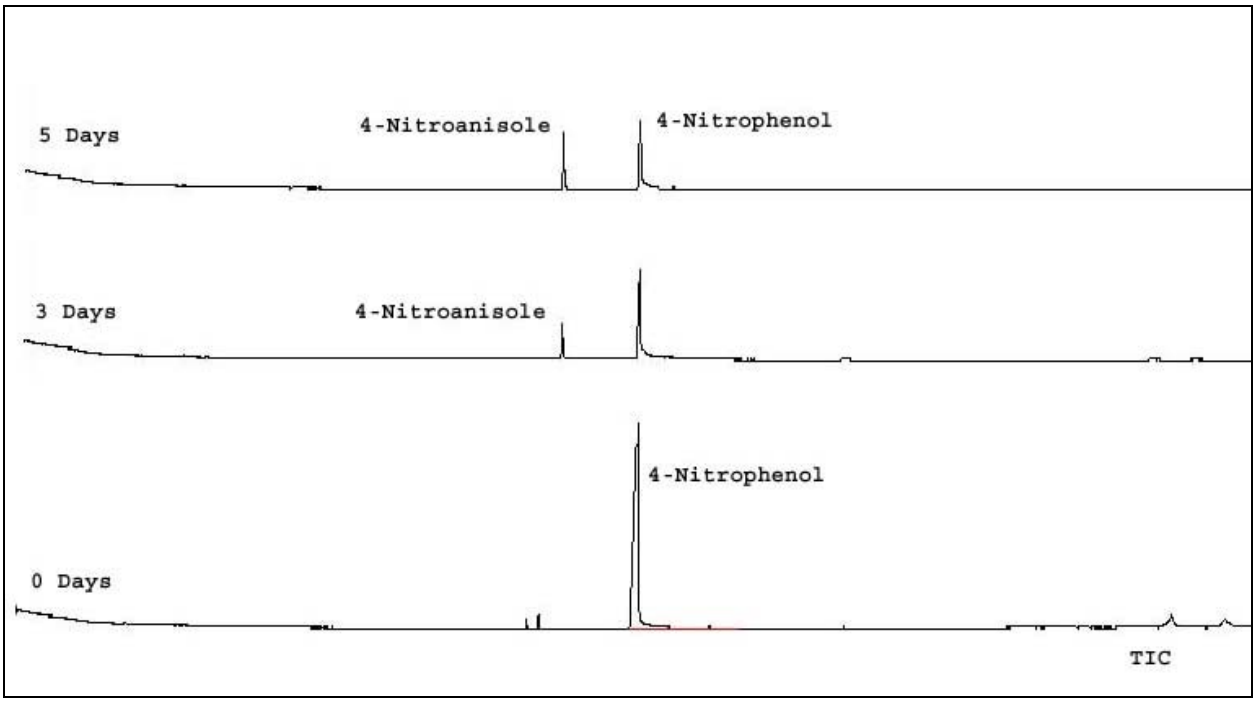


**Figure 3.9** Detection of 4-nitroanisole as the major degradation product from 4-nitrophenol by *Pleurotus ostreatus* using GC-MS

# CHAPTER 4

# IDENTIFICATION AND QUANTIFICATION OF DEGRADATION PRODUCTS FROM DISPERSE YELLOW 3

## 4.1 Identification of products

The second disperse dye examined was Disperse Yellow 3 (DY3), which is a phenolic azo compound (Figure 2.1) and a widely used yellow dye in the United States. It is also a potential carcinogen (Spadaro et al., 1992). TLC was used preliminarily to look for possible products. The mobile phase used in TLC was optimized based on the migration of dye and possible products. Ethyl acetate: n-hexane (4:1) was chosen and used for the TLC analysis. One possible degradation product from DY3 was detected by TLC at UV 254nm (Table 4.1). Acetanilide, 4'-aminoacetanilide, 4-acetamidophenol, 4'-nitroacetanilide, and 6-amino-m-cresol were run on TLC to identify this spot, but none of them was a match.

To identify the possible products, the supernatant of the degradation culture was extracted by methylene chloride three times, and the organic layer was concentrated before being analyzed with GC-MS. Figure 4.1 shows the GC-MS chromatograms for the first four days of degradation. The GC-MS method was adopted from that used with DO3. The presence of acetanilide in the decolorization sample was indicated by comparison of the mass spectrum and retention times of standard (Figure 4.2). Another major peak in the chromatogram was identified as veratryl alcohol, the mediator for LiP. All the other peaks in GC-MS could not be assigned to products, and control runs indicated that those peaks resulted from background and/or solvent.

HPLC was used to look for other possible products from biodegradation. This analysis resulted in a chromatogram with three peaks having polarity close to that of DY3 and had absorbance at 254 nm (Figure 4.3). These unknown peaks did not correspond to 4'-aminoacetanilide, 4-acetamidophenol, 4'-nitroacetanilide, and 6-amino-m-cresol. These unknown peaks have UV-Visible spectra similar to that of the dye, but these peaks were not identified at this time.

## 4.2 Quantification of products

### *4.2.1 Quantification of decolorization by UV-Vis spectrophotometric analysis*

Treatment of DY3 with *P. ostreatus* after 5 days caused 57 percent decolorization (Figure 4.4 and Table 4.2), which was indicated by calculation of the decrease in absorption at the wavelength maximum for this dye ($\lambda_{max}$=354 nm). There were no new absorbence peaks after biodegradation. Since the octanol-water partition coefficient ($K_{ow}$) of DY3 is $10^{2.9}$, which indicates DY3 is hydrophobic, its sorption by fungal cells could not be ignored. Sorption of DY3 on fungal biomass was determined by the method described in Chapter III. It was estimated that 11 percent of decolorization resulted from adsorption onto the biomass. Therefore, about 46 percent of the dye broke down during biodegradation.

### *4.2.2 Quantification of products by HPLC*

The kinetic profile of the degradation product, acetanilide, was determined by HPLC. The calibration curve was constructed by regressing the peak area against concentrations of the standard solutions in the range of 1-10 ppm. The concentration of products in the samples was calculated using linear regression equations from the calibration curves. HPLC quantification was carried out with the detection wavelength set at 254 nm. The calibration curve was linear ($r^2$

= 0.9999) over the investigated concentration range. The results for this product show that it is difficult to be further degraded in the biodegradation (Figure 4.5). The yield of acetanilide was determined by the ratio of the molar amount of product to molar amount of dye degradation (decolorization minus absorption) and was estimated to be about 25 percent.

### 4.3 Mechanism of degradation product formation

Spadaro and Renganathan (1994) suggested a peroxidase oxidation pathway for degradation of DY3 with purified lignin peroxidase, with acetanilide being the major product. Peroxidases oxidized DY3 by two electrons to produce a carbonium ion, followed by a nucleophilic reaction with water. An unstable tetrahedral intermediate (I) was generated and further transformed to 4-acetanidopheyldiazene (II) and a quinone. It is known that phenyldiazene is unstable and readily reacts with oxygen or peroxidase to produce a radical. This radical will then lose the azo group as nitrogen via homolytic bond cleavage. The generated phenyl radical easily abstracts a hydrogen from its surroundings to yield acetanilide (III) (Huang and Kosower, 1968, Spadaro and Renganathan, 1994). Laccase was also demonstrated to degrade phenolic azo dyes by a similar pathway (Chivukula and Renganathan 1995).

Formation of acetanilide in this study is consistent with the results of Spadaro and Renganathan (1994), which implicated LiP in the degradation of DY3 by *Pleurotus ostreatus*. Detection of veratryl alcochol by GC-MS and HPLC in the culture medium also supports the hypothesis of LiP involvement. Another major product suggested by Spadaro and Renganthan's pathway, 4-methyl-1,2-benzenequinone (IV), was not detected in our experiment. However, 4-methyl-1,2-benzenequinone (IV) is unstable in fungal culture and not commercially available. Only a trace of this product was detected in Spadaro and Renganathan's research (Spadaro and

Renganathan, 1994). The amount of acetanilide stayed constant in the later period of degradation (Figure 4.5), which indicated that it resisted further transformation or was degraded by fungi at a very low rate. The unidentified possible products might generate from further degradation of acetanilide or from biotransformation of DY3 by other enzymes of *P. ostreatus*. A possible brief scheme for formation of major products from DY3 is given in Figure 4.6.

**Table 4.1** TLC analysis of DY3 degradation samples

| SAMPLES | SAMPLE INFORMATION | $R_F$ VALUES OF SPOTS | COLOR OF SPOTS |
|---|---|---|---|
| Disperse Yellow 3 | Purified dye | 0.45 | Yellow |
| Disperse Yellow 3 | Control | 0.44 | Yellow |
| Degradation sample | 3 days degradation | 0.45<br>0.25 | Yellow<br>Colorless (UV) |

Mobile phase: ethyl acetate-n-hexane (4:1)
Plates were detected under daylight and UV 254 nm light after drying in air.

**Table 4.2** UV-Vis spectrophotometric analysis of DY3 in degradation

| DAY | ABSORBANCE DECREASE (@ $\lambda_{MAX}$) (%) |
|---|---|
| 0 | 0 |
| 1 | 26 |
| 2 | 32 |
| 3 | 44 |
| 4 | 50 |
| 5 | 57 |

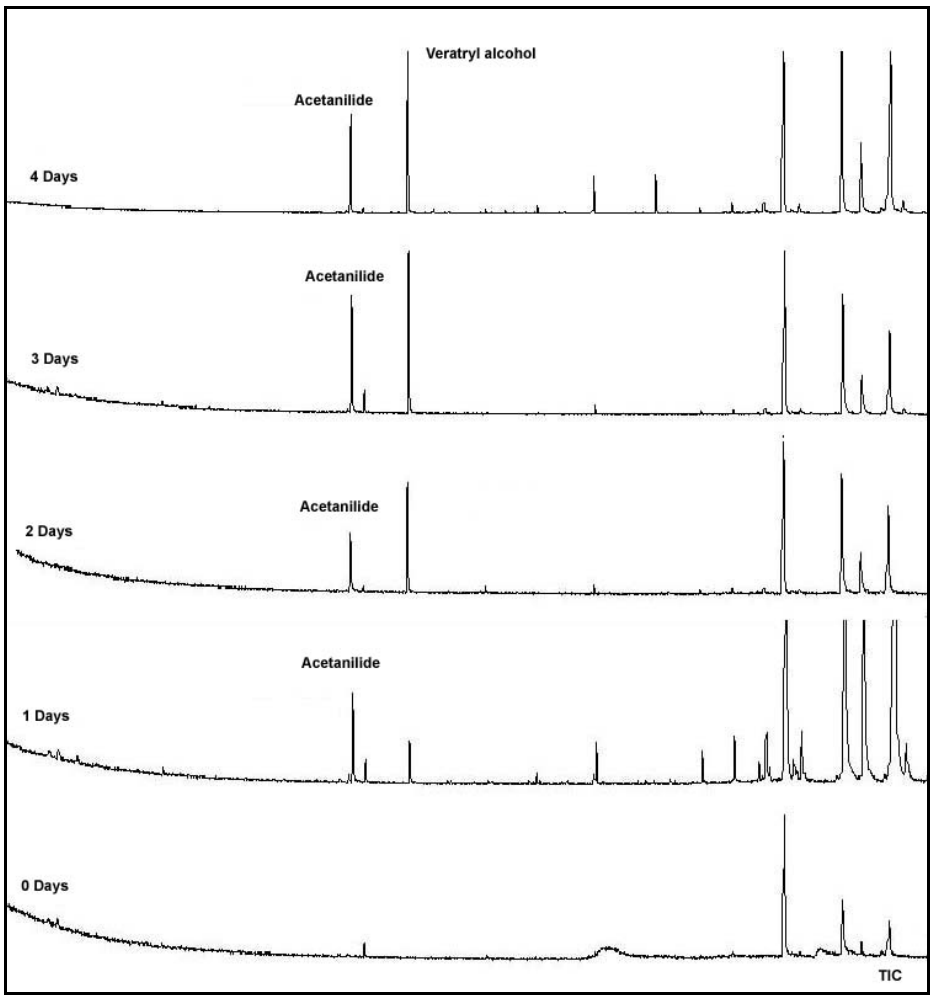


**Figure 4.1** Identification of acetanilide as the major degradation product from DY3 by *Pleurotus ostreatus* using GC-MS. Other major peaks are from background of fungal culture or impurities in the samples.

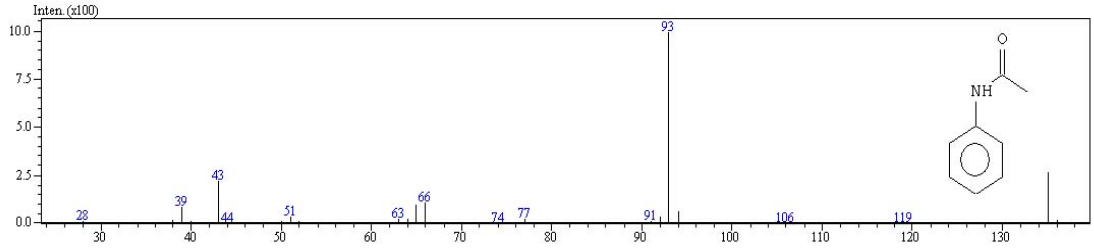


Mass spectrum of standard acetanilide

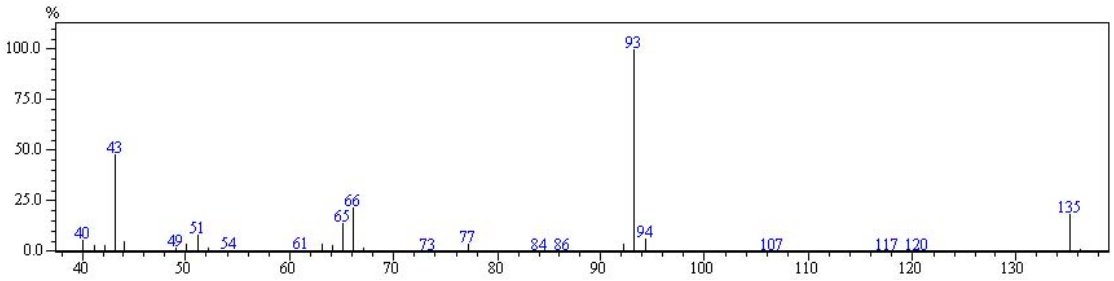


Mass spectrum of major product

**Figure 4.2** Mass spectra of major product (acetanilide) from DY3 by *Pleurotus ostreatus*

**(A)**

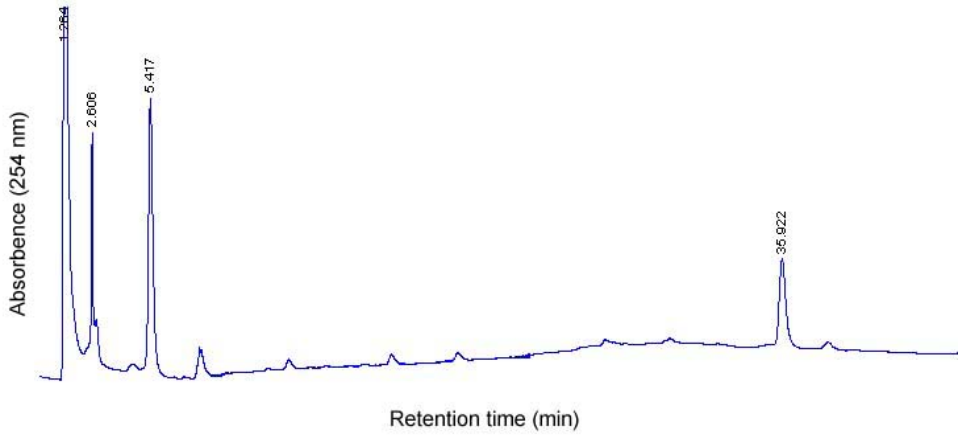


**(B)**

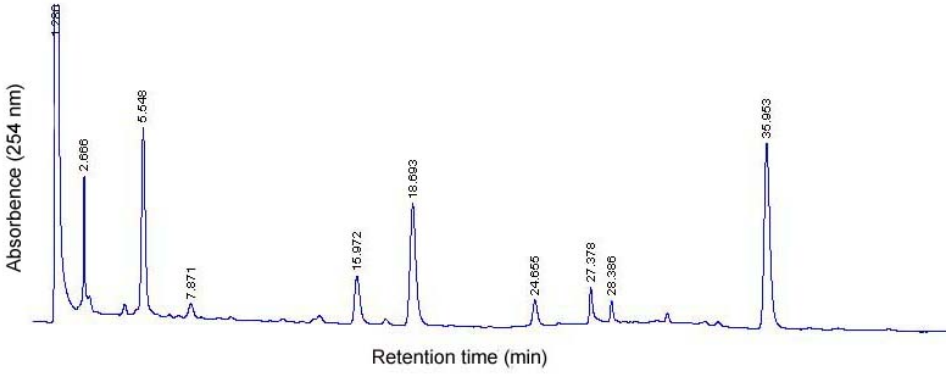


**Figure 4.3** HPLC chromatograms of fungal degradation samples from DY3.

**(A)** Days 0, Disperse Yellow 3 ($t_R$=35.922 min).

**(B)** Days 7, Veratryl alcohol ($t_R$=15.972 min), acetanilide ($t_R$=18.693 min), unknown metabolite 1 ($t_R$=24.655 min), unknown metabolite 2 ($t_R$=27.378 min), unknown metabolite 3 ($t_R$=28.386 min), Disperse Yellow 3 ($t_R$=35.953 min).

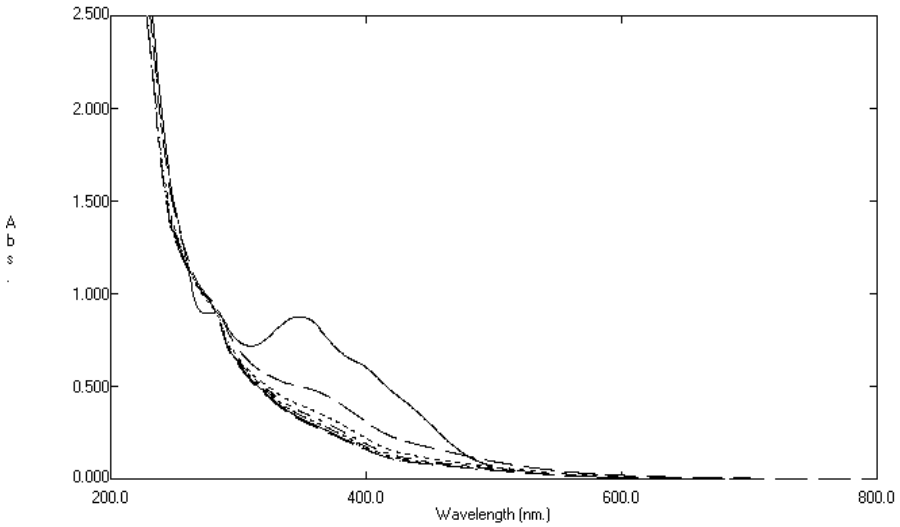


**Figure 4.4** UV-Vis spectra of DY3 during biodegradation by *P. ostreatus.* The curves represent 1 day intervals and absorbance at $\lambda_{max}$ (355nm) decrease continuously in the degradation.

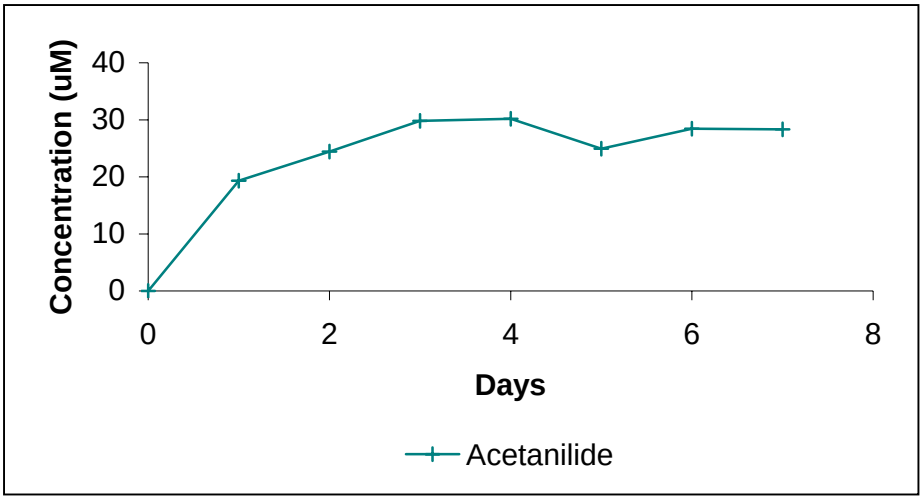


**Figure 4.5** Kinetic profile of acetanilide from DY3 by *Pleurotus ostreatus*

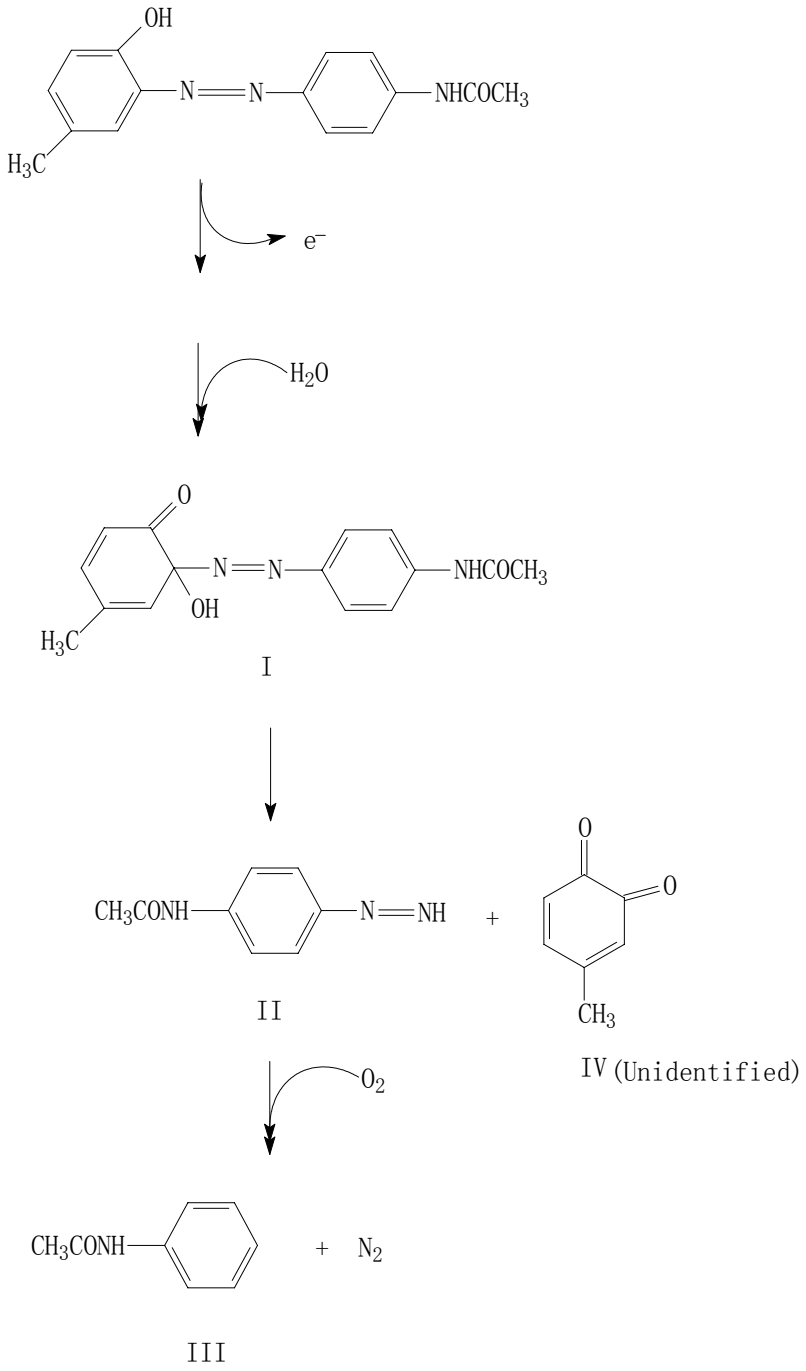


**Figure 4.6** Formation of acetanilide from DY3 degradation by *Pleurotus ostreatus* (Spadaro and Renganathan, 1994).

# CHAPTER 5

# IDENTIFICATION AND QUANTIFICATION OF PRODUCTS FROM MODEL IONIC DYES BY CAPILLARY ELECTROPHORESIS – MASS SPECTROMETRY AND HPLC

The identification of unknown degradation products of ionic model azo compounds in the complex fungal culture supernatant requires an effective analytical technique. The ideal technique should offer fast, high-resolution separation with sensitive, information-rich detection. Most ionic dyestuffs, such as sulfonated azo dyes, are nonvolatile and thermally unstable, and are thus not easily analyzed by gas chromatography (GC). On the other hand, the polar and ionic analytes, which are not GC amenable, are also problematic in usual HPLC separations. For the above reasons, capillary electrophoresis coupled with mass spectrometry (CE-MS) was chosen as the major analytical tool to separate and identify metabolites in the sample.

## 5.1 Setup of CE-MS method for identification of degradation products from ionic dyes

The combination of CE and MS is a relatively sophisticated analytical technique and a higher limit of detection compared to LC-MS is a drawback resulting from the employment of sheath liquid and a low injection volume. A robust interface is crucial for stable and sensitive CE-MS operation. Therefore, it is necessary to carefully optimize the parameters affecting the CE-MS performance to achieve the best sensitivity and stability.

### *5.1.1 Optimization of CE-ESI-MS interface with sheath liquid*

CE-MS interfacing is often achieved with a liquid sheath because of its versatility, which was first demonstrated by Smith and co-workers (1988). The interface is a tripletublar

configuration, with a separation capillary inside a coaxial liquid sheath tube, which is surrounded by a second coaxial tube supplying the nebulizing gas. The sheath liquid provides electrical contact for CE operation and a stable electrospray. However, achieving stable electrospray with a liquid sheath can be problematic and involves simultaneous balancing of multiple parameters such as capillary position, liquid sheath flow rate and composition, nebulizing gas flow, and ESI conditions (Kirby et al. 1996).

The mass spectra of the model azo dyes were obtained by direct infusion of the standard solution into ion trap MS. Base peaks for both azo compounds were the original compound sulfonated ions in solution, with m/z 277 for 4HABA (Figure 5.1) and m/z 327 for Orange II (Figure 5.2). Electrospray is a very soft ionization mode and molecular ions are usually the most abundant peak in the mass spectra. The dyes exist as sulfonated ions in the solution, thus readily forming gaseous ions during the ESI procedure. Optimization of the CE-MS interface conditions was made by monitoring the signal intensity of these sulfonated ions.

*5.1.1.1 Sheath liquid composition and flow rate*

Sheath liquid not only supplies the electric contact for the CE operation but also provides the necessary stable electrospray. Flow rate of sheath liquid should be small but still sufficient to give stable spray and electrical contact. Because 2-propanol is superior for the purpose of sheath liquid and best for ionization of negative sulfonate ions (Vuorensola et al. 2001), it was chosen for the organic solvent in the sheath liquid. The flow rate of sheath liquid was tested in a range of 2 µl/min to 4 µl/min, and the lower rate of 2 µl/min was suitable for CE-ESI-MS interfacing. The composition of sheath liquid was optimized with 2-propanol in water with a range of 50:50 – 100:0 v/v. The signal intensity increased considerably with the increasing proportion of organic solvent. A mixture of 80:20 v/v gave the most intense signals for both model azo compounds

(Figure 5.3). Furthermore, the electrospray was not stable with a very high percentage of organic solvent, for example more than 95 percent. Therefore, a 2-propanol to water mixture of 80:20 v/v was selected as the sheath liquid composition finally based on both the signal intensity and electrospray stability. Since the sulfonate ions are readily formed even before the ESI, there was no additive (e.g. ammonium hydroxide) used in the sheath liquid in order to keep the number of ionic compounds in the ESI to a minimum.

*5.1.1.2 Nebulizing gas*

The effect of nebulizing gas flow on the CE-MS was examined with the pressure raised in steps of 1 p.s.i. from 5 to 10 p.s.i. (1 p.s.i = 6894.76 Pa) while keeping the other parameters constant (Figure 5.4). The results showed that the influence from the nebulizing gas pressure on the sensitivity of ESI was not very significant from 5 p.s.i. to 10 p.s.i. for both azo compound ions. The signal-to-noise ratio of the 4HABA sulfonate ion increased from 5 p.s.i. to 6 p.s.i.. However, above 6 p.s.i., the signal-to-noise ratio did not increase anymore. For the Orange II molecular ion, an improvement of signal-to-noise ratio was not observed when nebulizing gas pressure changed. This observation probably indicated that the ion evaporation process was not improved by increasing the nebulizing gas pressure. On the other hand, it was found that increasing the gas pressure decreased the migration times and increased the apparent CE ion mobility of the analyte ions, an effect which decreased resolution. This effect was also observed by Huikko and co-workers (2002). This phenomenon resulted from the decrease of the pressure at the capillary tip when increasing nebulizing gas velocity, which brought about a hydrodynamic bulk flow inside the CE capillary (Huikko et al. 2002). Therefore, a low nebulizing gas pressure of 5 p.s.i. was chosen for this study.

*5.1.1.3 Drying gas flow and temperature*

Drying gas flow rate and temperature affects the intensity and stability of ESI signals (Huikko et al. 2002). The flow rate was changed from 3 to 5 l/min and its effect on ESI is shown in Figure 5.5. It was determined that 4 l/min was optimal for the ESI. The effect of drying gas temperature was also examined. The temperature was raised gradually from 150°C to 300°C. It was found that a high gas temperature did not enhance signal-to-noise ratio (Figure 5.6). Thus, 150°C was used in the interfacing.

*5.1.2 Optimization of CE operation*

Capillary positioning has a big influence on the stability of electrospray and the intensity of ion signals. The capillary tip was adjusted relative to the sprayer needle for best sensitivity. It was also found that the cross-sectional dimension of the capillary influenced the ESI significantly. A 360 μm O.D. capillary was found to give stable and sensitive ion signals.

The separation in CE was also optimized for satisfactory migration time and best sensitivity of MS signals. Because the length of capillary is 100 cm for the CE-MS coupling, a high separation voltage of positive 30 kV was applied to obtain a field strength of 300 V/cm. The concentration of carrying electrolyte (running buffer) of CE impacted the analyte ionization efficiency and MS signals. The range of 10 – 40 mM concentration of ammonium buffer was tested for their operation. When the concentration of ammonium acetate was more than 20 mM, the intensity of analyte ions was suppressed due to the ionization competition from acetate anion in ESI. A 10 mM running buffer was chosen because of the superior ionization efficiency of molecular ions of analytes at this concentration (Figure 5.7). The pH value of running buffer is critical to the electroosmotic flow velocity (EOF) and migration time of analytes. The EOF was strong enough to bring all ions from anode to cathode under a voltage of 30 kV in the neutral or

basic running buffer. The pH values in the range of 7.0 to 10.0 were tested, with pH 9.0 found suitable for both 4HABA and Orange II. The migration times for both model compounds were less than 15 min.

*5.1.3 Optimization of MS conditions*

The ESI voltage influenced the ionization efficiency and signal intensity. The voltage was optimized automatically in the range of 3.0 kV to 4.5 kV and 4.0 kV was chosen as the suitable parameter. The ESI voltage was thus + 4.0 kV, which was applied on the end plate of MS capillary instead of the sprayer needle. This design avoids introducing potential to the CE outlet.

## 5.2 Identification of degradation products from ionic azo compounds with CE-MS

The major degradation products in the *P. ostreatus* degradation flasks from both azo dyes were identified with the CE-ESI-MS method. The base peak electrophorogram (BPE) showed better peak shape and signal-to-noise ratio than the total ion electrophorogram (TIE) in the study. Thus, the possible products were determined by examining the BPE of samples during biodegradation and comparing with those of controls.

Before biodegradation of Orange II, a large electrophorogram peak having a base peak at m/z 327 was easily identified as the sulfonated anion of the dye itself (Figure 5.8). After incubation in *Pleurotus ostreatus* culture for two days, the dye peak totally disappeared from BPE with two potential new product peaks at migration times of 15 min and 17 min (Figure 5.9). Mass spectra of these CE peaks had their base peaks at m/z 156.9 (product 1) and 172.9 (product 2) respectively (Figure 5.10, Figure 5.11). Takeda (1999) reported the determination of products from wet oxidation of Orange II with solid catalysts by CE and CE-MS. In that case, Orange II was broken down into 4-hydroxy-benzenesulfonic acid (p-phenolsulfonate) and 1,2-

dihydroxynaphthalene. Thus, the product 2 with base peak at m/z 172.9 was inferred to be 4-hydroxy-bezenesulfonic acid. The identity of this product was confirmed by running the standard compound (Figure 5.12). Based on structure of the dye and molecular weight of the product, the peak with a base peak at m/z 156.9 was inferred to be benzenesulfonic acid. This product was also confirmed by running the reference compound (Figure 5.13).

In addition, HPLC was used for identification of nonionic or less polar products. Several possible products, including 2-naphthol, 1,2-naphthalenediol, 1,2-naphthoquinone, and 1-amino-2-naphthol, were examined based on analysis of the structure of the original azo dyes. Only 1,2-naphthoquinone was identified as a product from biodegradation by comparison of retention time and UV-Visible spectrum with the reference compound (Figure 5.14).

4HABA degradation by white rot fungas was studied using the same protocols as for the other dyes. Figure 5.15 shows the base peak electrophorogram of 4HABA before being subjected to fungal degradation. In comparison, Figure 5.16 shows the base peak electrophorogram of 4HABA after being subjected to degradation by *P. ostreatus*. A major peak in BPE having a base peak at m/z 156.9 was also found in the culture medium (Figure 5.17). By comparison with the reference compound, this product was also identified as benzenesulfonic acid. Because of the similarity of the structure of 4HABA with that of Orange II, 4-hydroxy-benzenesulfonic acid was also anticipated to be one of major products. Analysis of the extracted ion electrophorogram (EIE) of m/z 173 demonstrated that 4-hydroxy-benzenesulfonic acid was also a major product (Figure 5.18).

Therefore, benzenesulfonic acid salt and 4-hydroxy-benzenesulfonic acid salt were two major products from both model dyes, and 1,2-naphthoquinone was also a major product for Orange II.

### 5.3 Determination of biodegradation

Biodegradation of azo compounds is determined based on measurement of decolorization and sorption of dyes on biomass. Decolorization of both model ionic azo compounds with *Pleurotus ostreatus* was measured by UV-Visible spectrophotometer daily. It was found that decolorization was 75 percent and 98 percent for 4HABA and Orange II (Table 5.1), respectively, after 5 days. The sorption rates for the two ionic compounds on fungal biomass were 9 and 24 percent, respectively. Therefore, the actual biodegradation was estimated at 66 percent and 74 percent for 4HABA and Orange II, respectively, when adsorption was considered. The color of live cells in the biodegradation was lighter than that of dead cells, which were used in adsorption measurement. This observation indicated that dead cells absorbed more dyes than live cells, and adsorption in the biodegradation, therefore, should be less than the measured ones. A similar result was reported by Bakshi and co-workers (1999) in determination of biosorption of mixtures of textile dyes by *Phanerochaete chrysosporium* and reviewed by Baughman and Paris (1981).

### 5.4 Quantification of products

The running buffer of CE was optimized for quantification of target analytes, and pH 9.0 was finally chosen for giving best migration time and resolution in the electrophoresis.

Standards were prepared by dilution of stock solutions (1mg/ml) with fungal medium to give concentrations of benzenesulfonic acid ranging from 5 to 50 μg/ml and concentrations of 4-hydroxybenzenesulfonic acid ranging from 5 to 40 μg/ml. Quantification data were handled using the *QuantAnalysis*™ software of Bruker Daltonics. Calibration curves were obtained by regressing peak area of the extracted ion electrophorogram (EIE, m/z 157 for

benzenesulfonic acid salt and m/z 173 for 4-hydroxybenzenesulfonic acid salt) against concentrations of the standard solutions. Peak areas based on the EIE of each compound were used for determination. All calibration curves were linear ($r^2 > 0.99$) over the investigated concentration range (Table 5.2). The concentration of products in the samples was calculated using linear regression equations from the calibration curves. The LOD (Limit of detection) was calculated based on 3 times the noise level. The LOD was relatively high for CE-MS, i.e. 3 ppm for benzenesulfonic acid and 5 ppm for 4-hydroxybenzenesulfonic acid, due to dilution by sheath liquid in the ESI interface.

### 5.5 Biodegradation mechanism study

Quantification of products from both model azo dyes, i.e. benzenesulfonic acid and 4-hydroxybenzenesulfonic acid, and decrease of dyes, are shown in Figure 5.19 and Figure 5.20. The above mentioned products were found in the culture liquid of both model ionic dyes after 24 hour incubation. The highest level of 4-hydroxybenzenesulfonic acid was detected at the first day for Orange II and the second day for 4HABA. In this latter case, the product disappeared totally after 5 days. This observation led to the conclusion that 4-hydroxybenzenesulfonic acid was an intermediate in the fungal degradation and underwent further transformation. Thus, 4-hydroxybenzenesulfonic acid may not accumulate after degradation. On the other hand, a notable amount of benzenesulfonic acid in the culture liquid accumulated and stayed constant after several days' incubation, indicating that this product is not easily degraded further or degraded at very low rate. Accumulation of this compound is a potential source of secondary pollutants and should be further studied.

To determine if the products identified so far are responsible for most of biodegradation of dyes, a mass balance of degradation of model azo dyes and products was conducted (Table 5.1). The results of the mass balance calculation demonstrated that the yields of 4-hydroxybenzenesulfonic acid and benzenesulfonic acid accounted for 40 percent (for 4HABA) and 60 percent (for Orange II) of the total molar amount of the dyes. The comparison of the yield of products and extent of biodegradation of the dyes confirms that these compounds are major products in the fungal decolorization.

Because very little is known about how white rot fungi break down the azo compounds and the characteristics by which different enzymes act in the decolorization, it is only possible to assume that the known extracellur enzymes are responsible for the degradation and use this assumption to explain the results at this time. Fortunately, the mechanism of biodegradation of phenolic azo dyes by peroxidases and laccase from white rot fungi has been investigated before (Spadaro and Renganathan 1994, Chivukula and Renganathan 1995). Results with *Pleurotus ostreatus* suggest that peroxidases or laccase are (at least in part) responsible for the biodegradation of the model azo dyes because the degradation products from the fungal cultures in this study coincide well with the products expected for the peroxidase oxidation mechanism. A possible pathway, which illustrates the formation of identified products, is summarized in Figure 5.21 and Figure 5.22 for the dyes investigated. *Pleurotus ostreatus* probably adopts a pathway involving similar reactions as that of peroxidases. That is, the peroxidase substrate, ionic azo dyes, were metabolized to phenyldiazene intermediate and quinone in the degradation. Although 1,4-benzenequinone was not detected in the degradation of 4HABA, 1,2-naphthoquinone was identified in the degradation of Orange II to support this proposed pathway. The reason why 1.4-

benzenequinone was not detected in the culture medium could not be determined. Benzenesulfonic acid and 4-hydroxybenzenesulfonic acid were produced from phenyldiazene via radical reactions. It is expected to find some of same products generated from two model azo dyes with similar structures, and the results confirmed this proposition. This observation suggests that it is possible to predict products based on the structures of original dyes in biodegradation with more knowledge about fungal enzymes gained in the future.

**Table 5.1** Mass balance of products from model azo dyes degradation by *Pleurotus ostreatus*

| | 4HABA | ORANGE II |
|---|---|---|
| Decolorization rate (%) | 75 | 98 |
| Adsorption by biomass (%) | 9 | 24 |
| Biodegradation rate (%) | 66 | 74 |
| Yield of benzenesulfonic acid (%) | 30 | 39 |
| Yield of 4-hydroxybenzenesulfonic acid (%) | 10 | 20 |
| Unidentified (%) | 26 | 15 |

**Table 5.2** Calibration curves for products of ionic model azo compounds

| | EIE M/Z | CALIBRATION CURVE | $R^2$ | LOD (PPM) |
|---|---|---|---|---|
| Benzenesulfonic acid salt | 157 | 5-50 ppm | 0.9926 | 3 |
| 4-hydroxybenzenesulfonic acid salt | 173 | 5-40 ppm | 0.9918 | 5 |

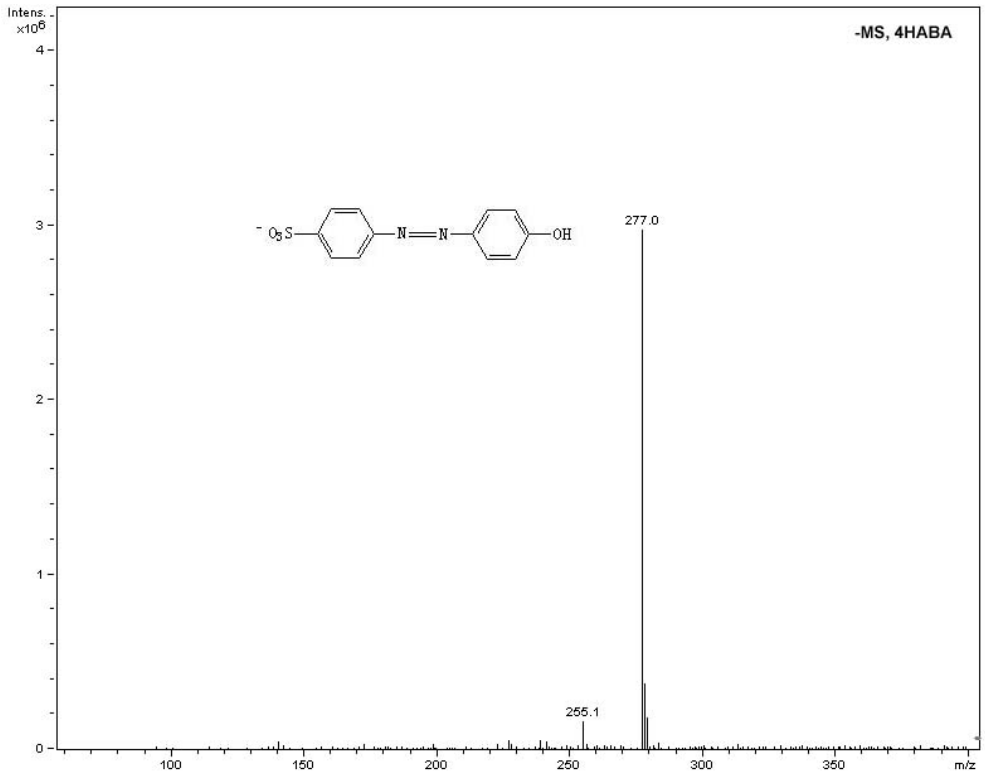


**Figure 5.1** Mass spectrum of 4HABA anion with CE-ESI-MS

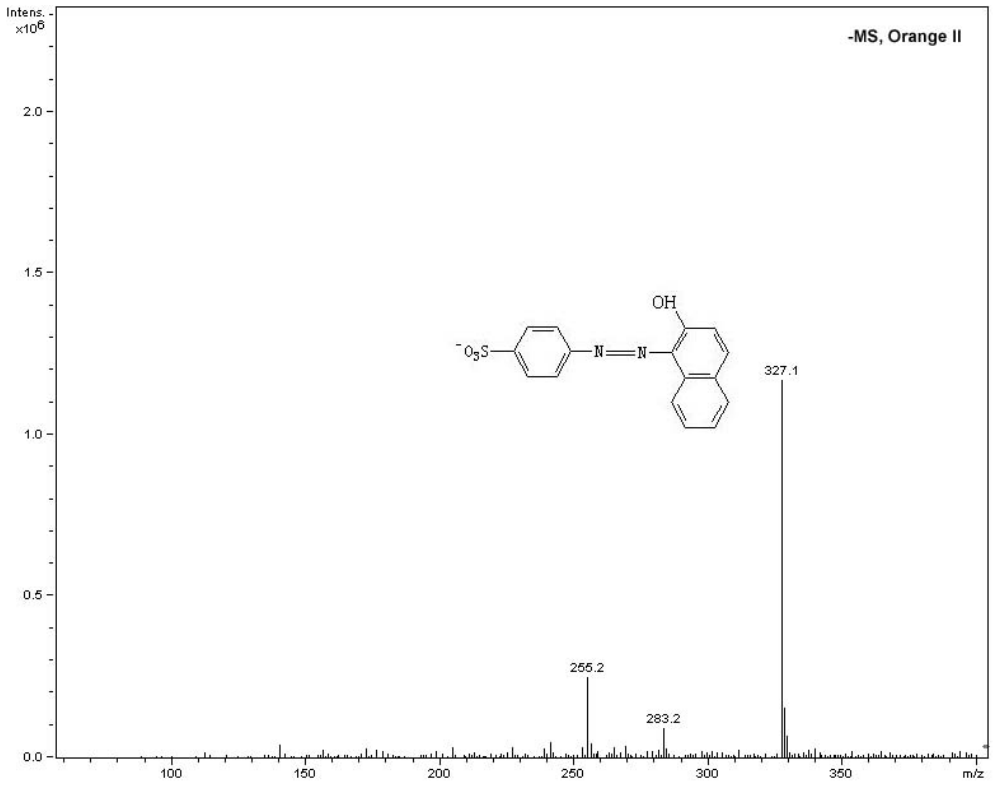


**Figure 5.2** Mass spectrum of Orange II anion with CE-ESI-MS

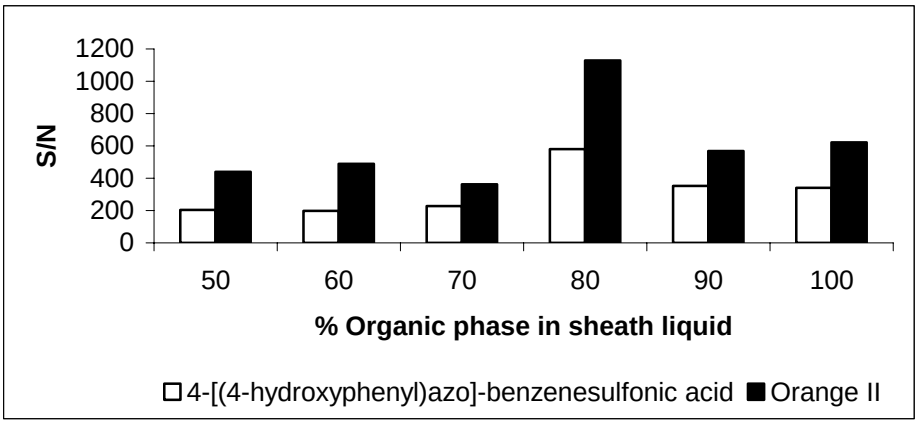


**Figure 5.3** Effect of the composition of sheath liquid on ion intensity with CE-MS

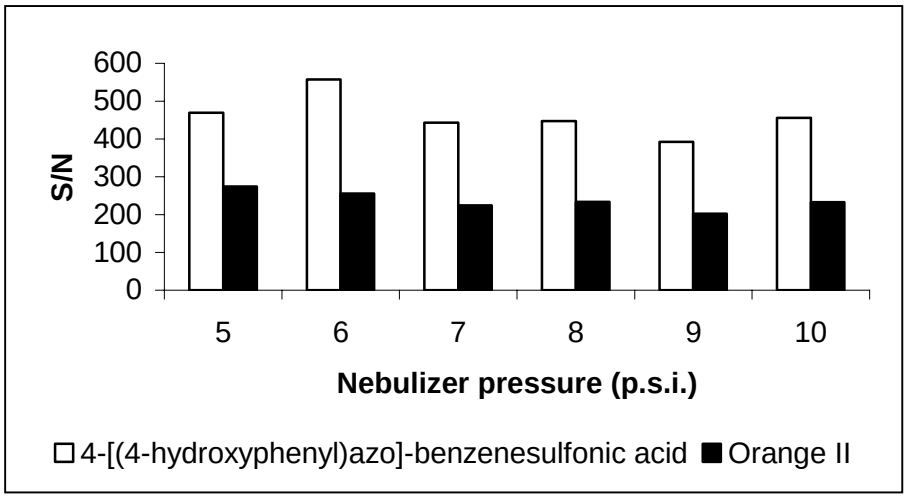


**Figure 5.4** Effect of the nebulizing gas flow on ion intensity with CE-MS

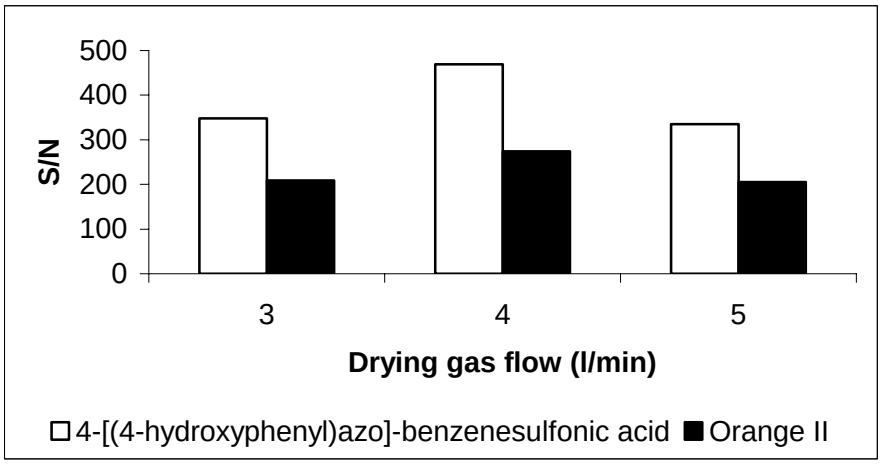


**Figure 5.5** Effect of the drying gas flow on ion intensity with CE-MS

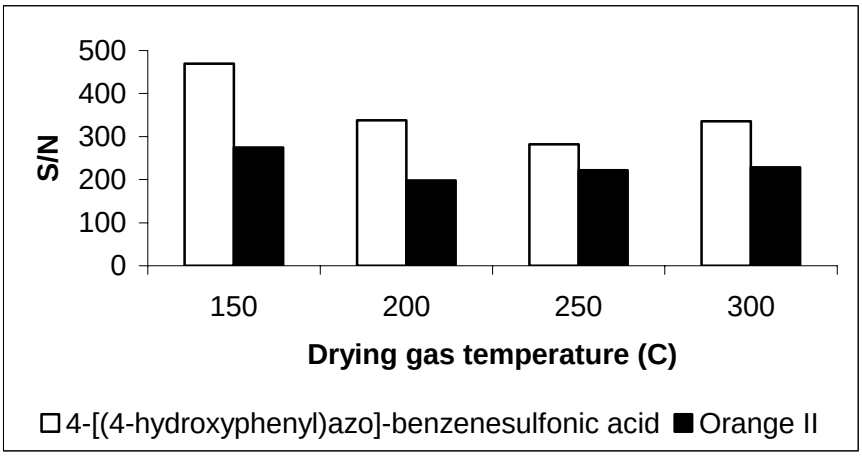


**Figure 5.6** Effect of the drying gas temperature on ion intensity with CE-MS

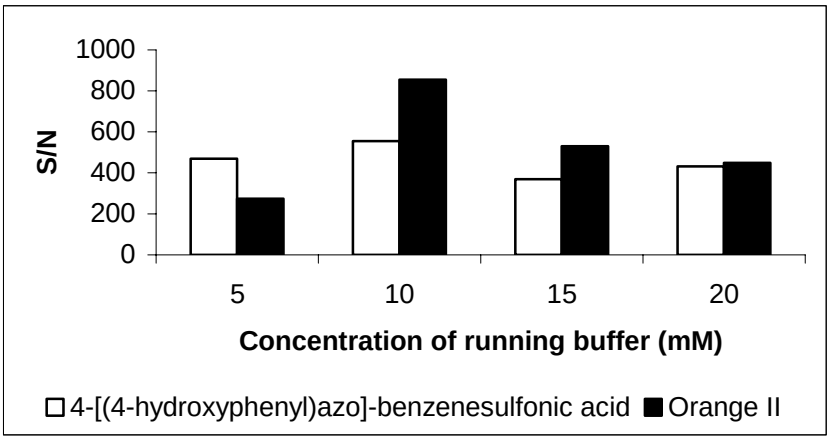


**Figure 5.7** Effect of concentration of running buffer on ion intensity with CE-MS

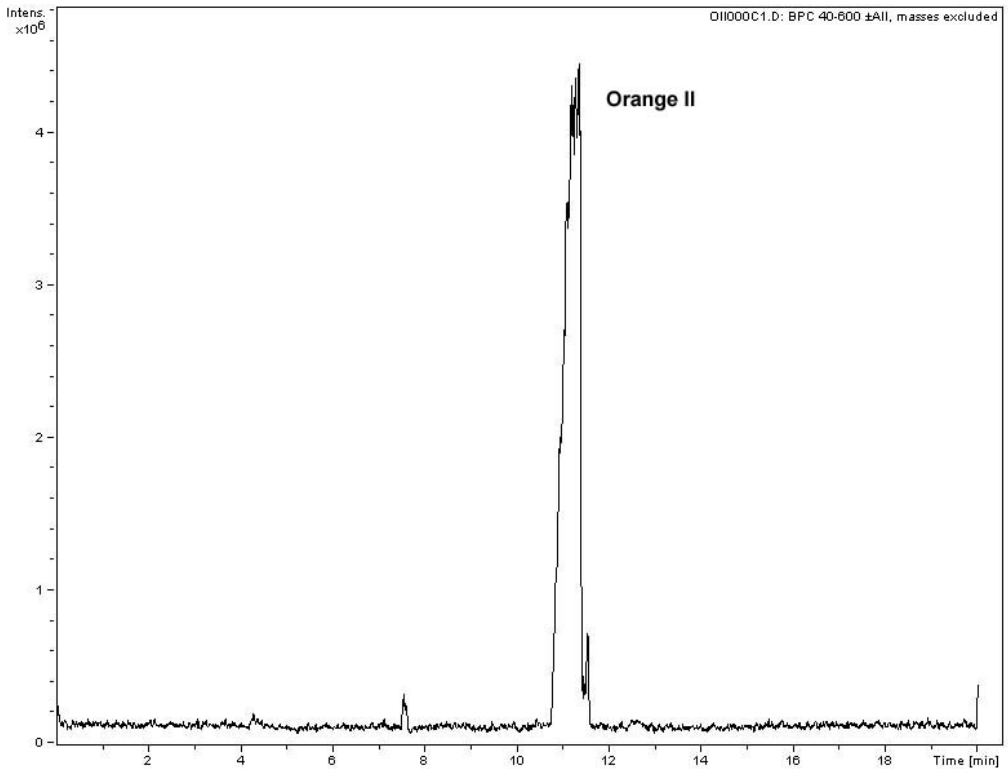


**Figure 5.8** CE-MS analysis of fungal degradation of Orange II: base peak electrophorogram before biodegradation

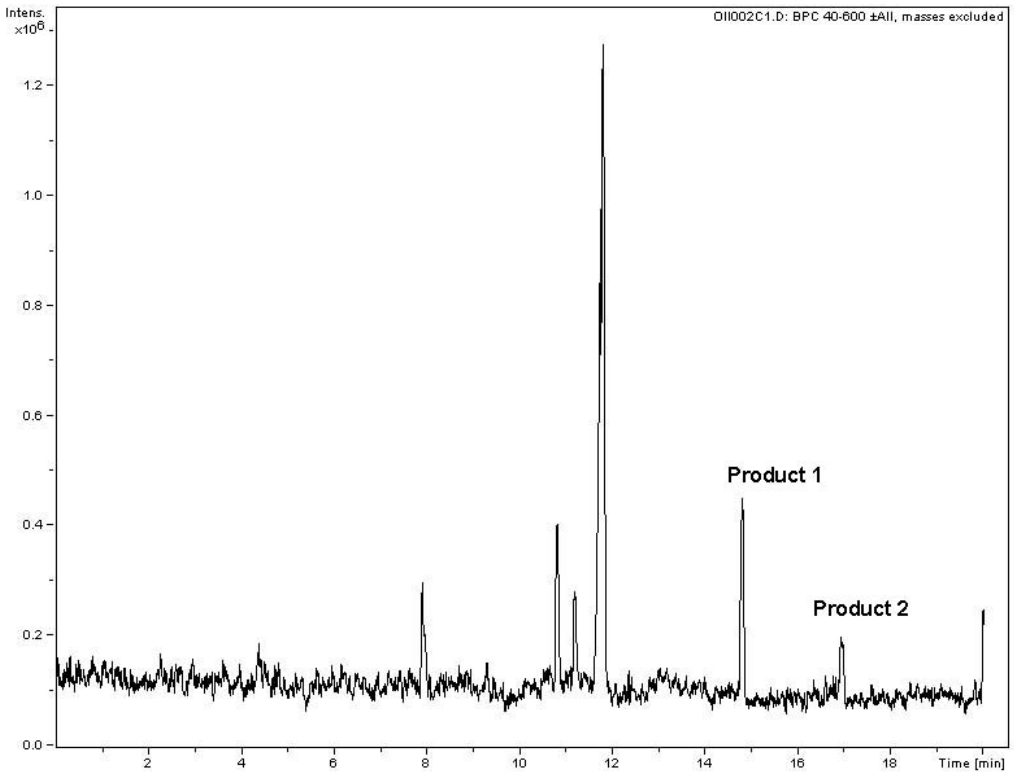


**Figure 5.9** CE-MS analysis of fungal degradation of Orange II: base peak electrophorogram after biodegradation (2 days). Product 1, benzenesulfonic acid; Product 2, 4-hydroxy-benzenesulfonic acid.

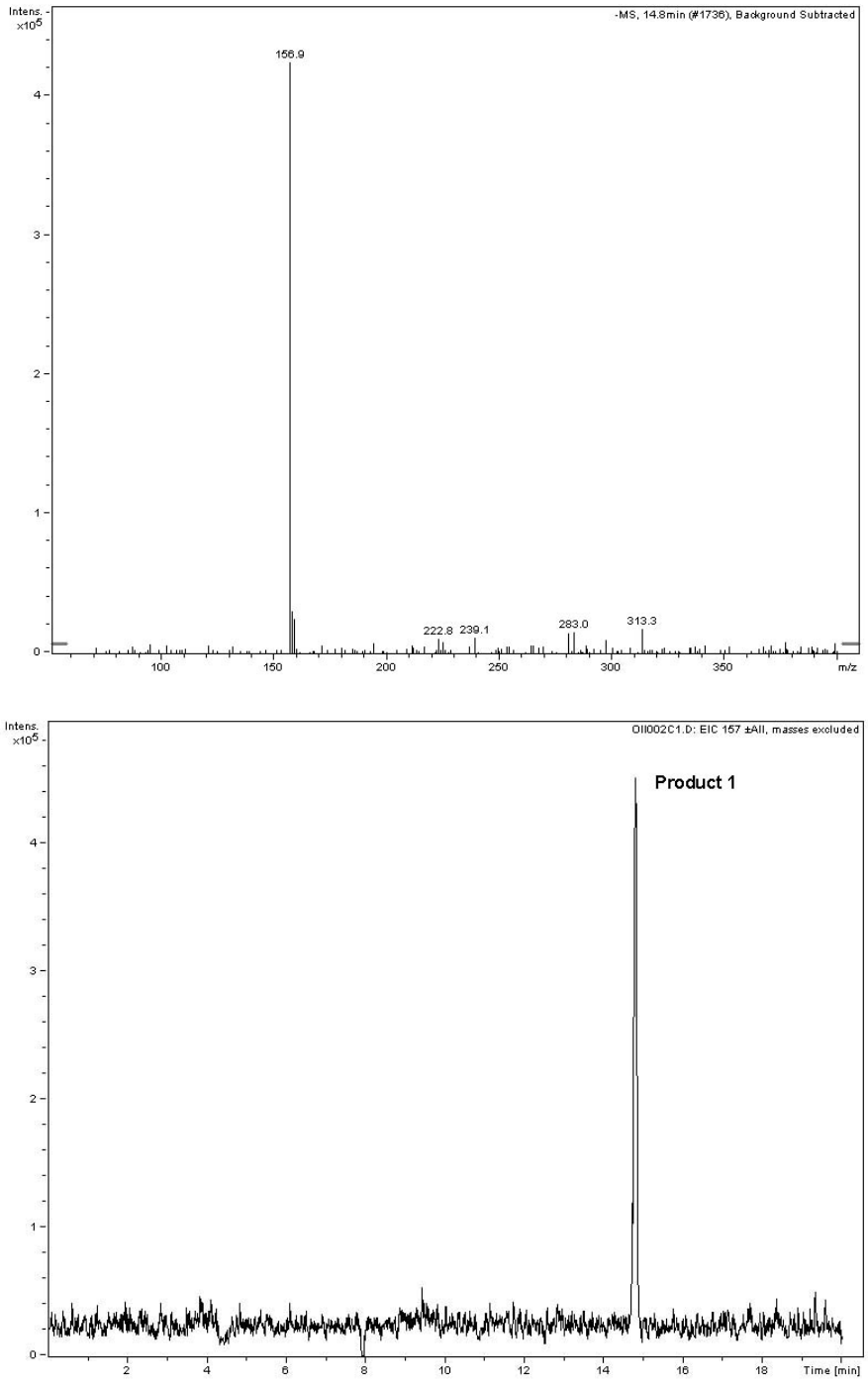


**Figure 5.10** CE-MS analysis of product 1, benesulfonic acid, from Orange II: mass spectrum and extracted ion electrophorogram (m/z 157).

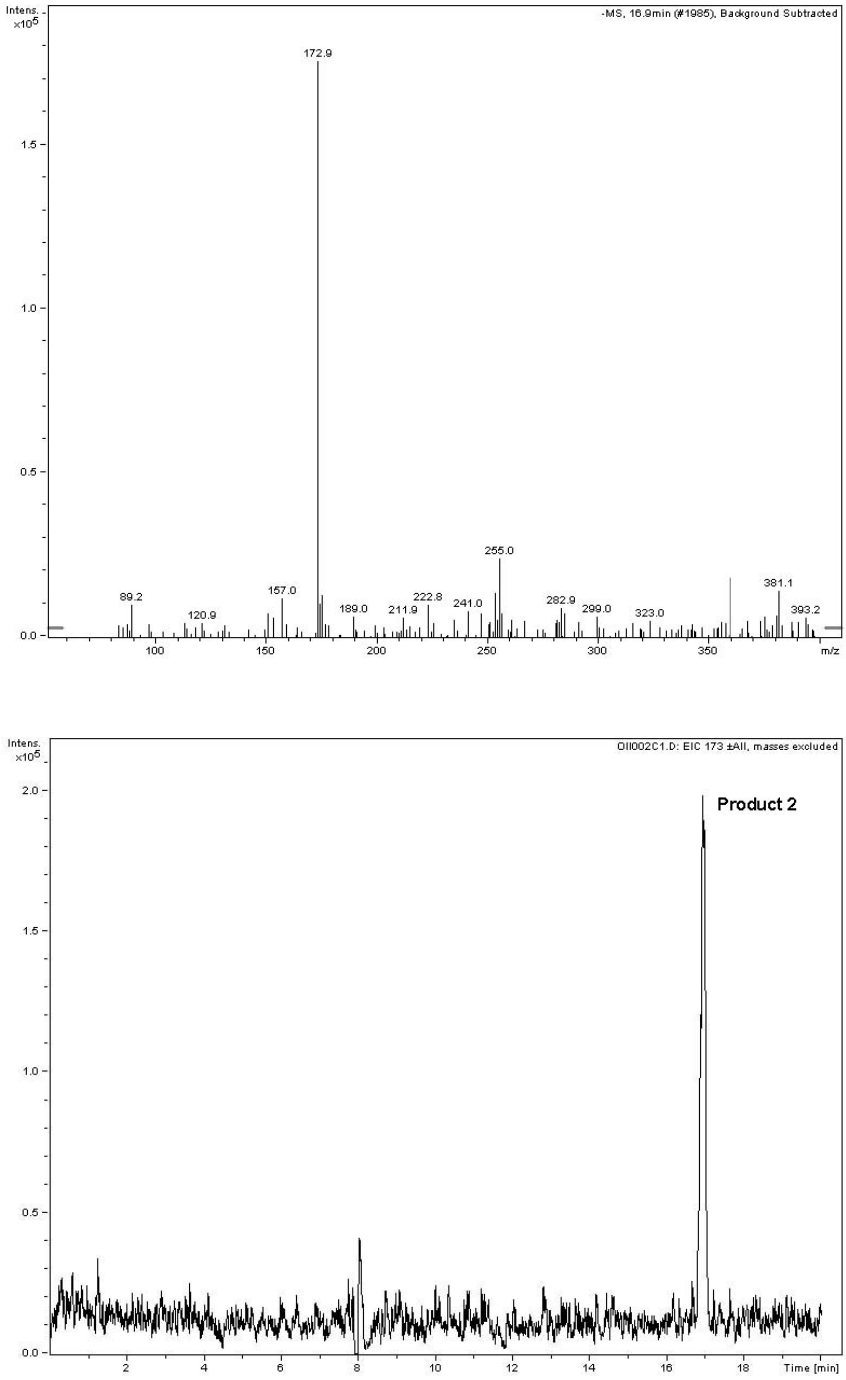


**Figure 5.11** CE-MS analysis of product 2, 4-hydroxy-benesulfonic acid, from Orange II: mass spectrum and extracted ion electrophorogram (m/z 173)

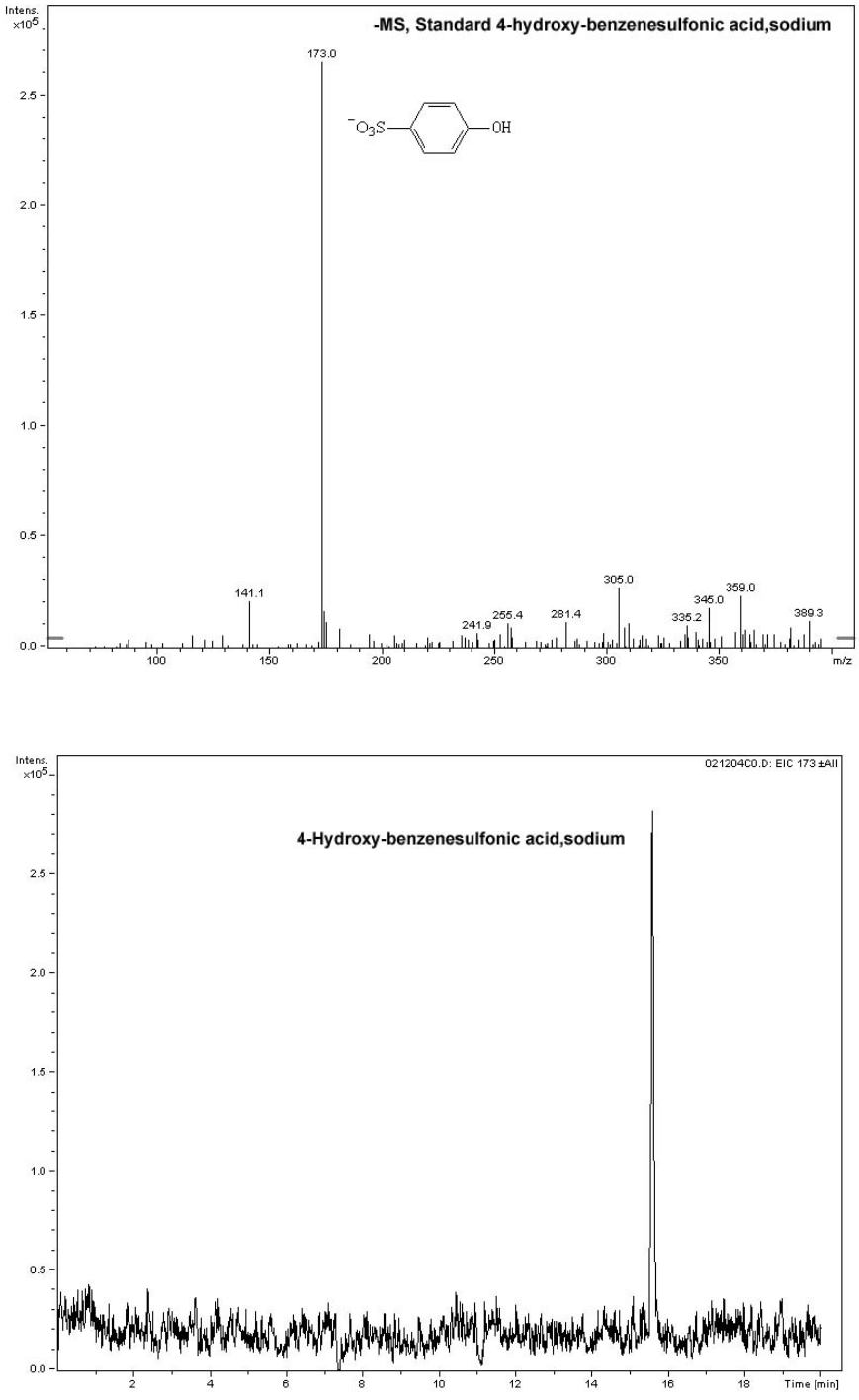


**Figure 5.12** CE-MS analysis of standard 4-hydroxy-benzenesulfonic acid, sodium salt: mass spectrum and extracted ion electrophorogram (m/z 173)

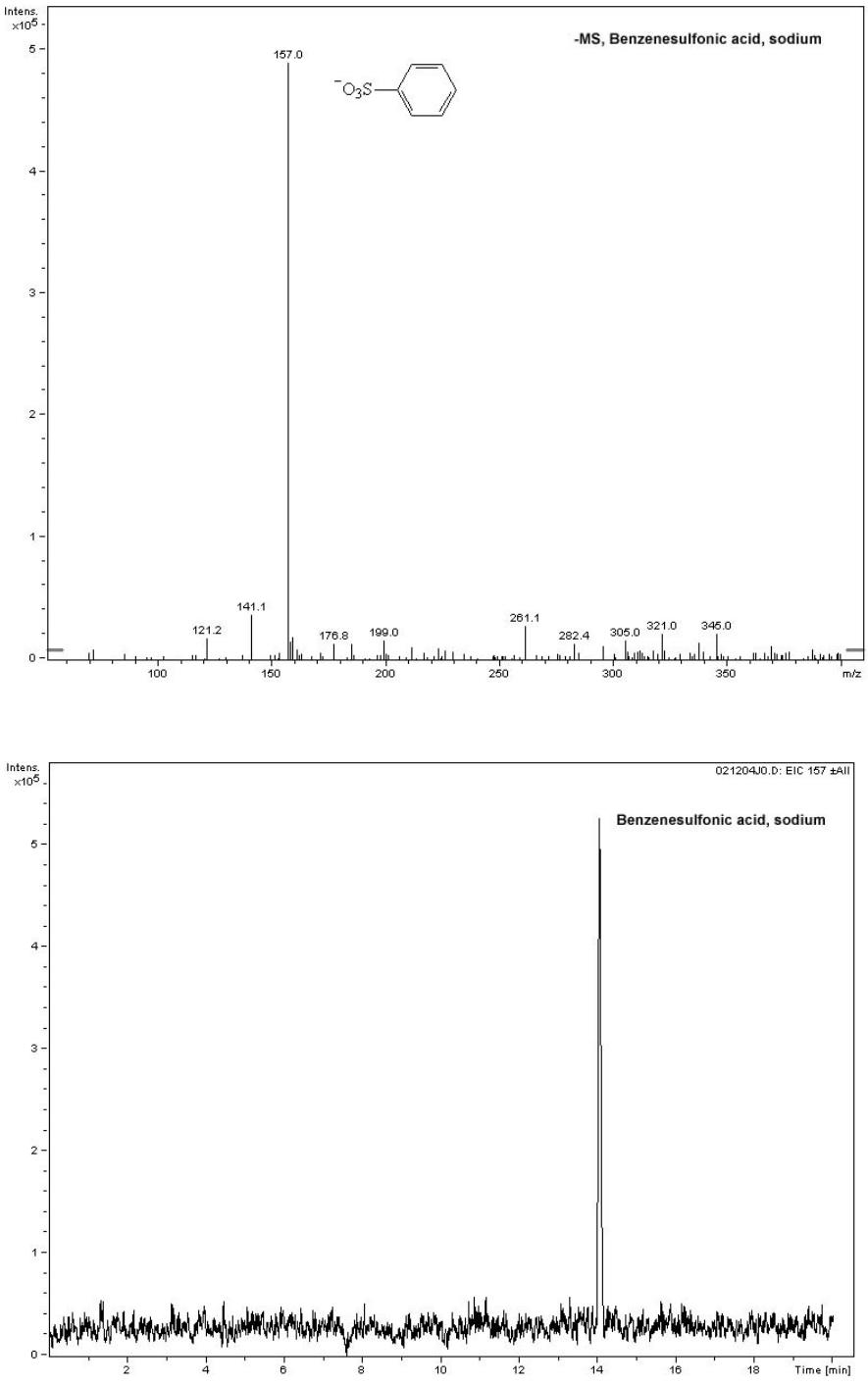


**Figure 5.13** CE-MS analysis of standard benzenesulfonic acid, sodium salt: mass spectrum and extracted ion electrophorogram (m/z 157)

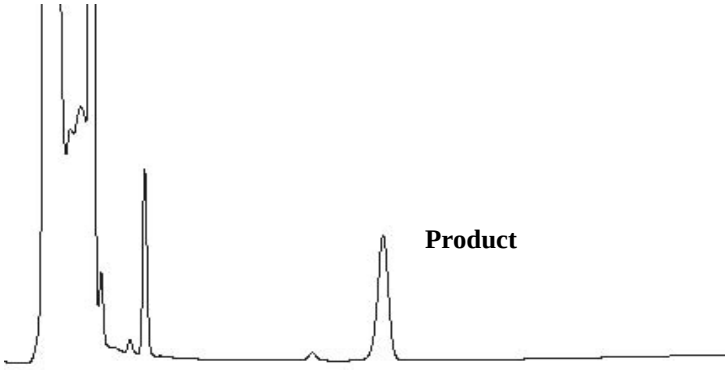


LC Chromatogram of degradation sample

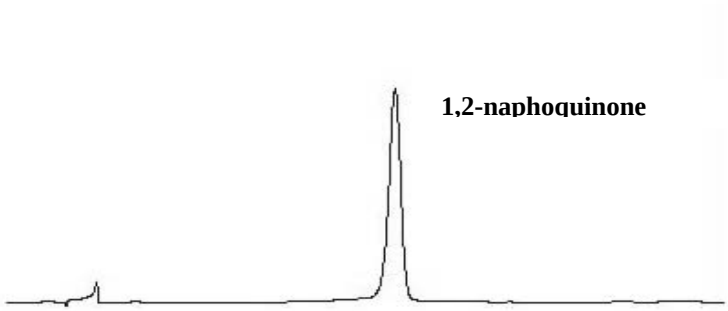


LC Chromatogram of standard1,2-naphthoqunione

**Figure 5.14a** HPLC analysis of fungal degradation of Orange II: identification of 1,2-naphthoquinone as a product

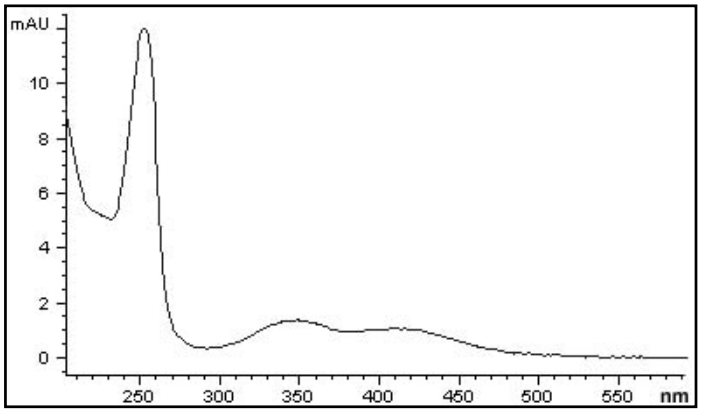


UV-Vis spectrum of product peak

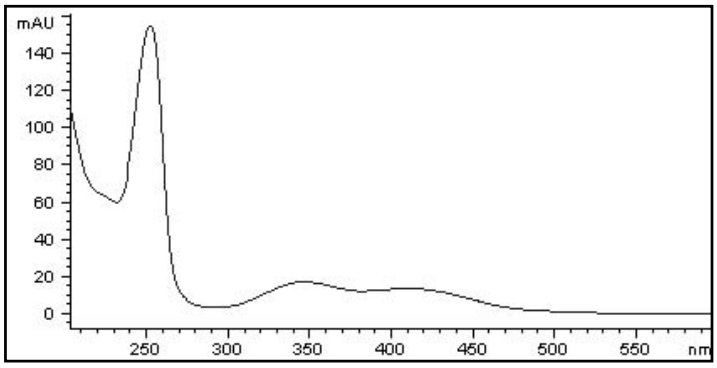


UV-Vis spectrum of standard 1,2-naphthoqunione

**Figure 5.14b** HPLC analysis of fungal degradation of Orange II: identification of 1,2-naphthoquinone as a product

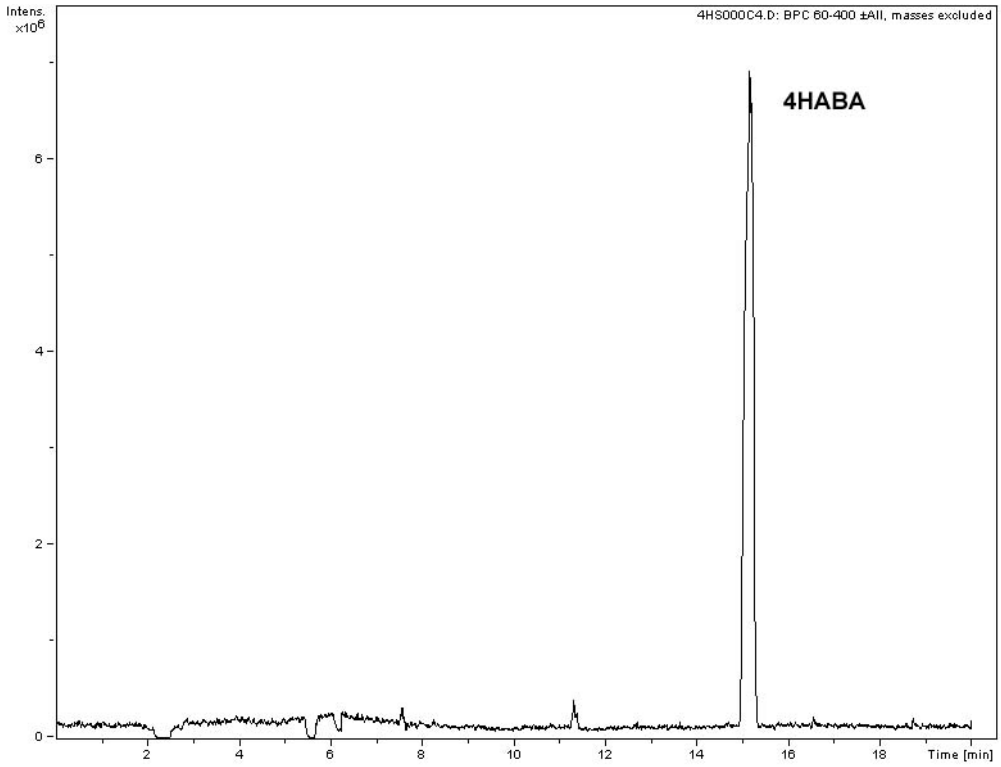


**Figure 5.15** CE-MS analysis of fungal degradation of 4HABA: Base peak electrophorogram before biodegradation

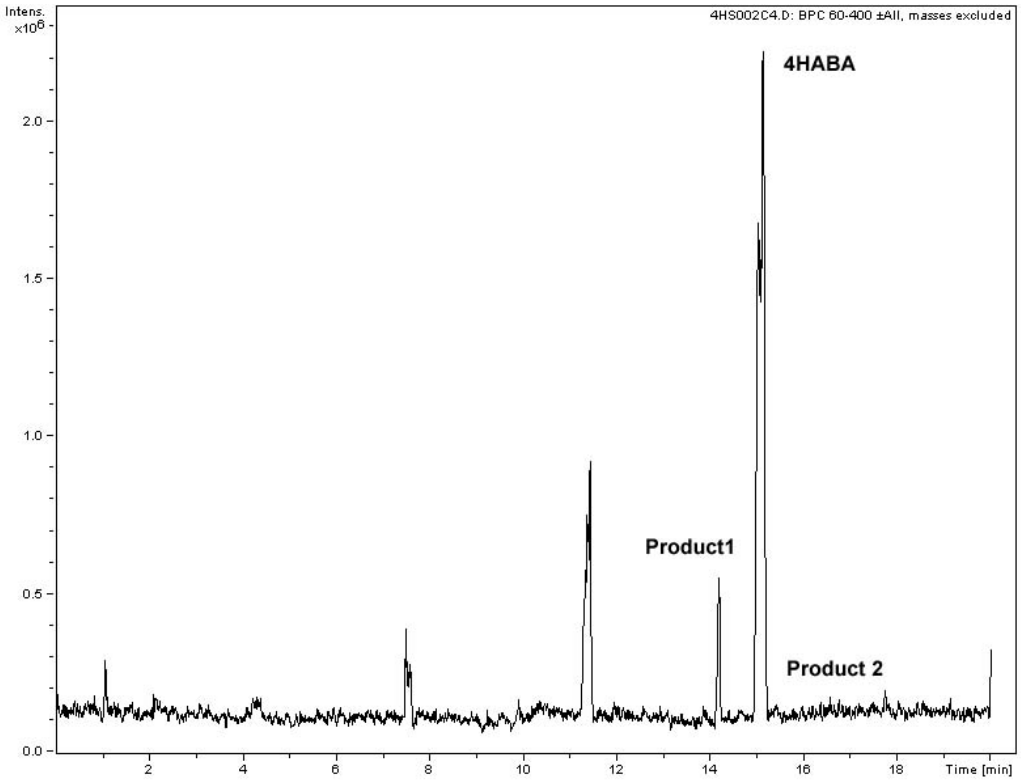


**Figure 5.16** CE-MS analysis of fungal degradation of 4HABA: Base peak electrophorogram after biodegradation (2 days). Product 1, benzenesulfonic acid; Product 2, 4-hydroxy-benzenesulfonic acid.

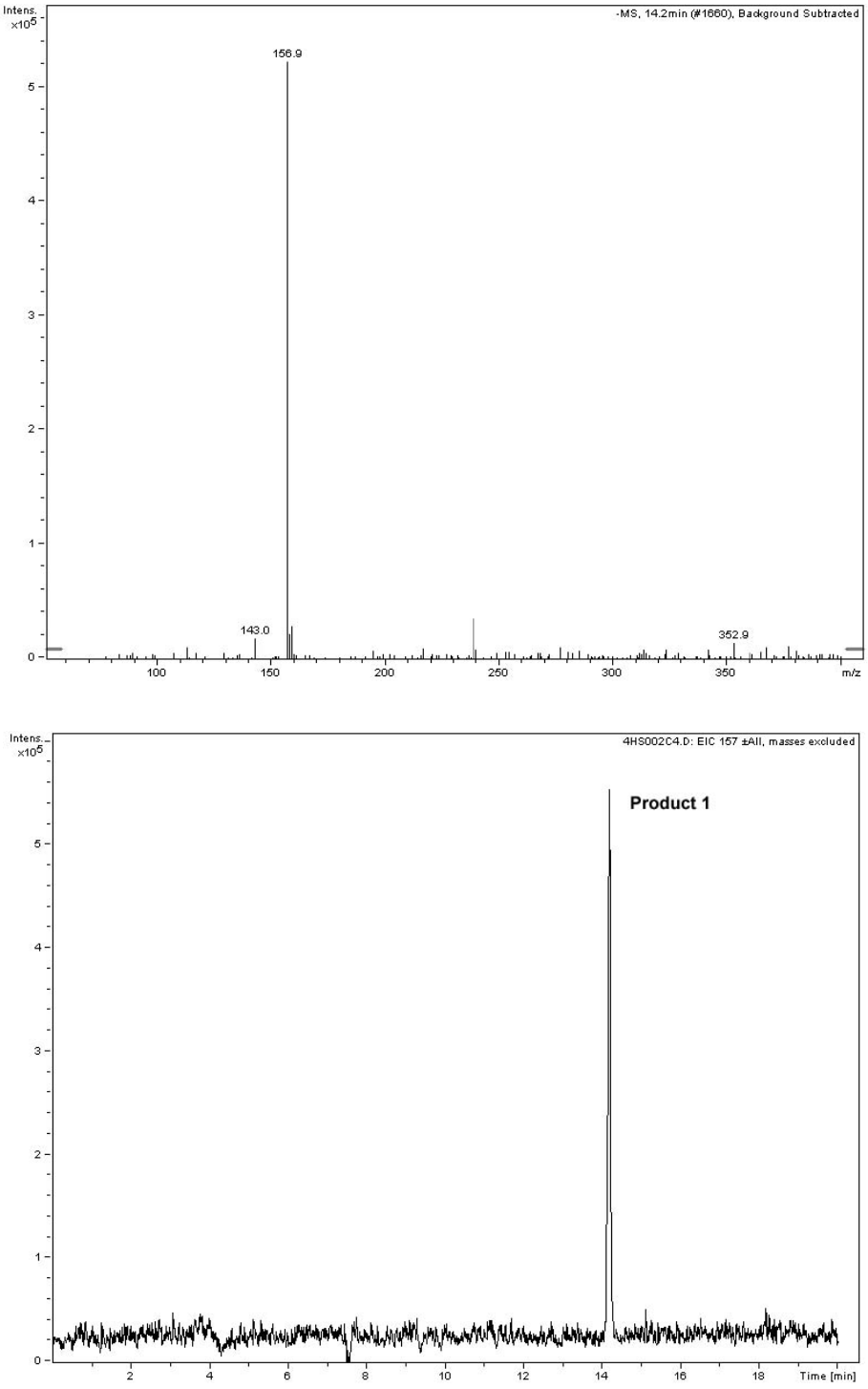


**Figure 5.17** CE-MS analysis of product 1, benzenesulfonic acid, from 4HABA: mass spectrum and extracted ion electrophorogram (m/z 157)

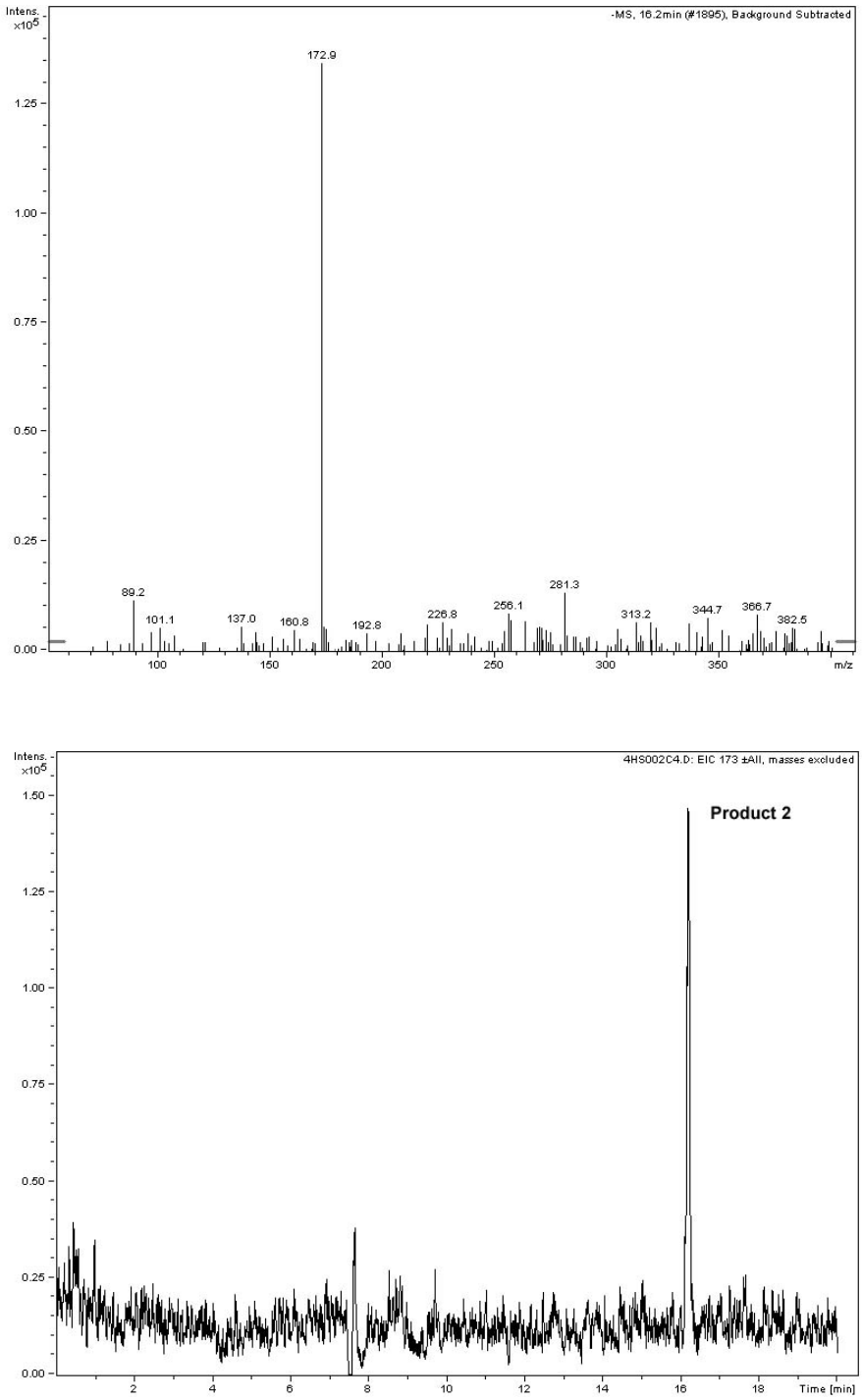


**Figure 5.18** CE-MS analysis of product 2, 4-hydroxy-benzenesulfonic acid, from 4HABA: mass spectrum and extracted ion electrophorogram (m/z 173)

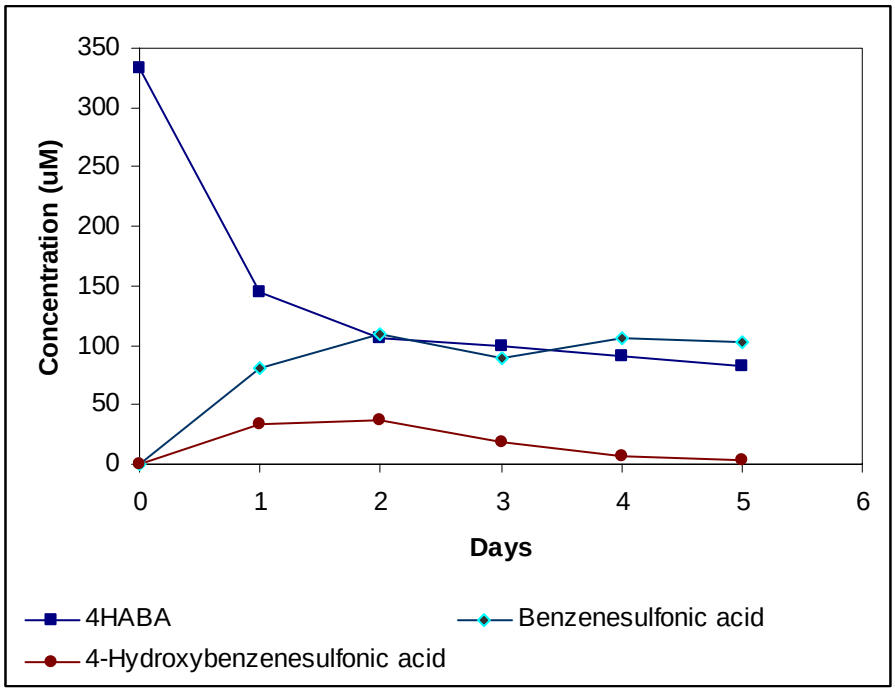


**Figure 5.19** Kinetic profiles of fungal degradation of 4HABA by *Pleurotus ostreatus*

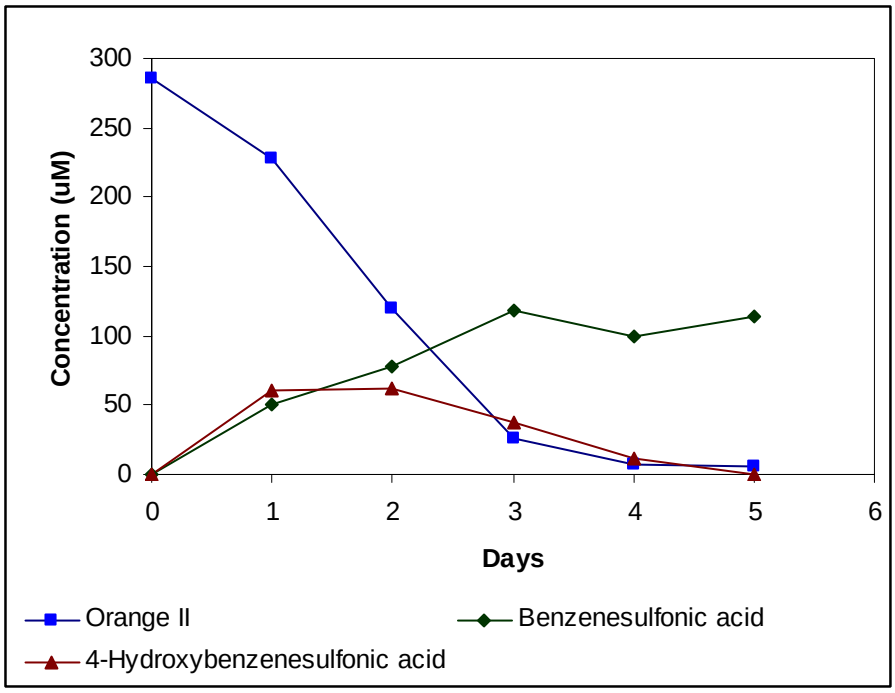


**Figure 5.20** Kinetic profiles of fungal degradation of Orange II by *Pleurotus ostreatus*

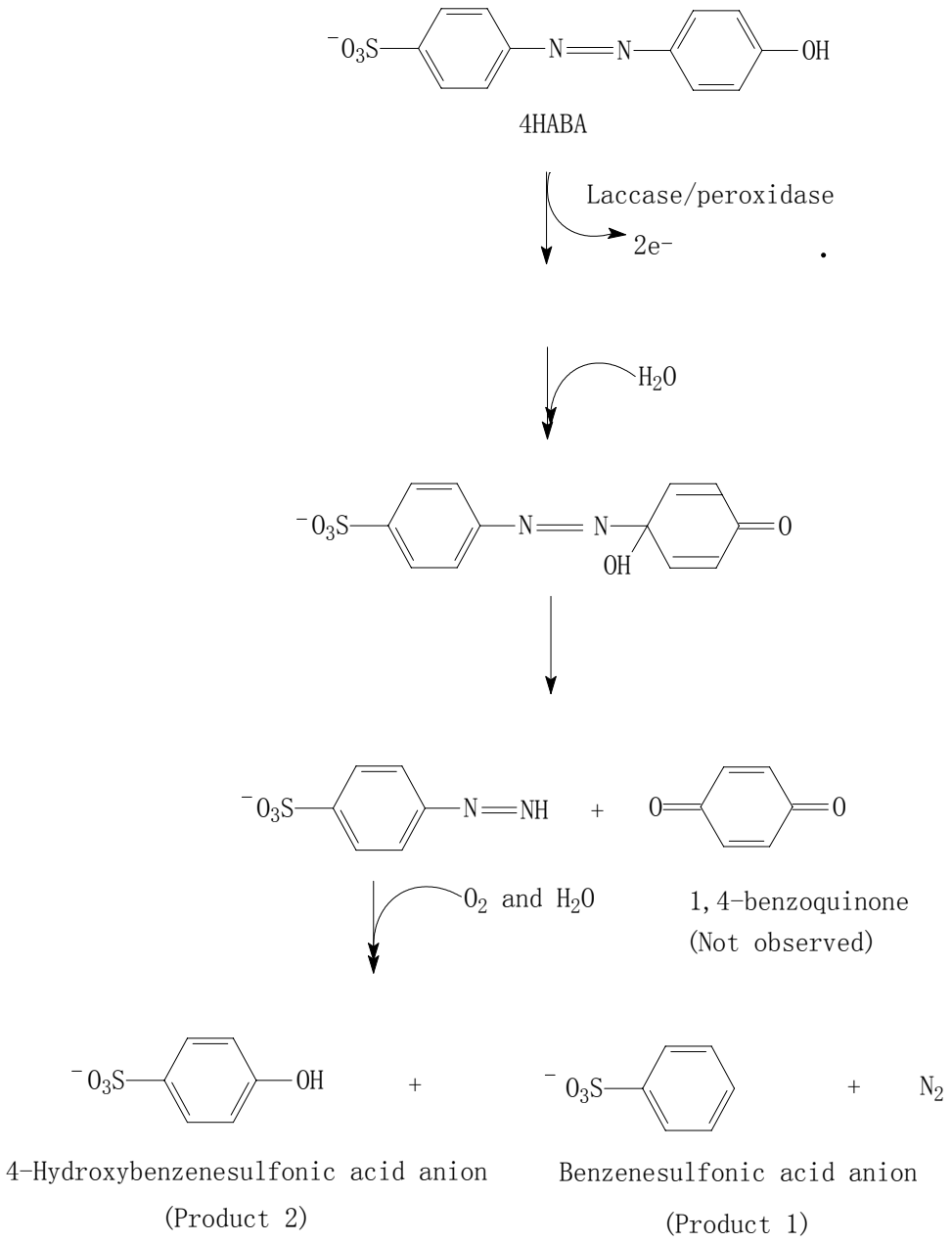


**Figure 5.21** Formation of degradation products of 4HABA by *Pleurotus ostreatus*

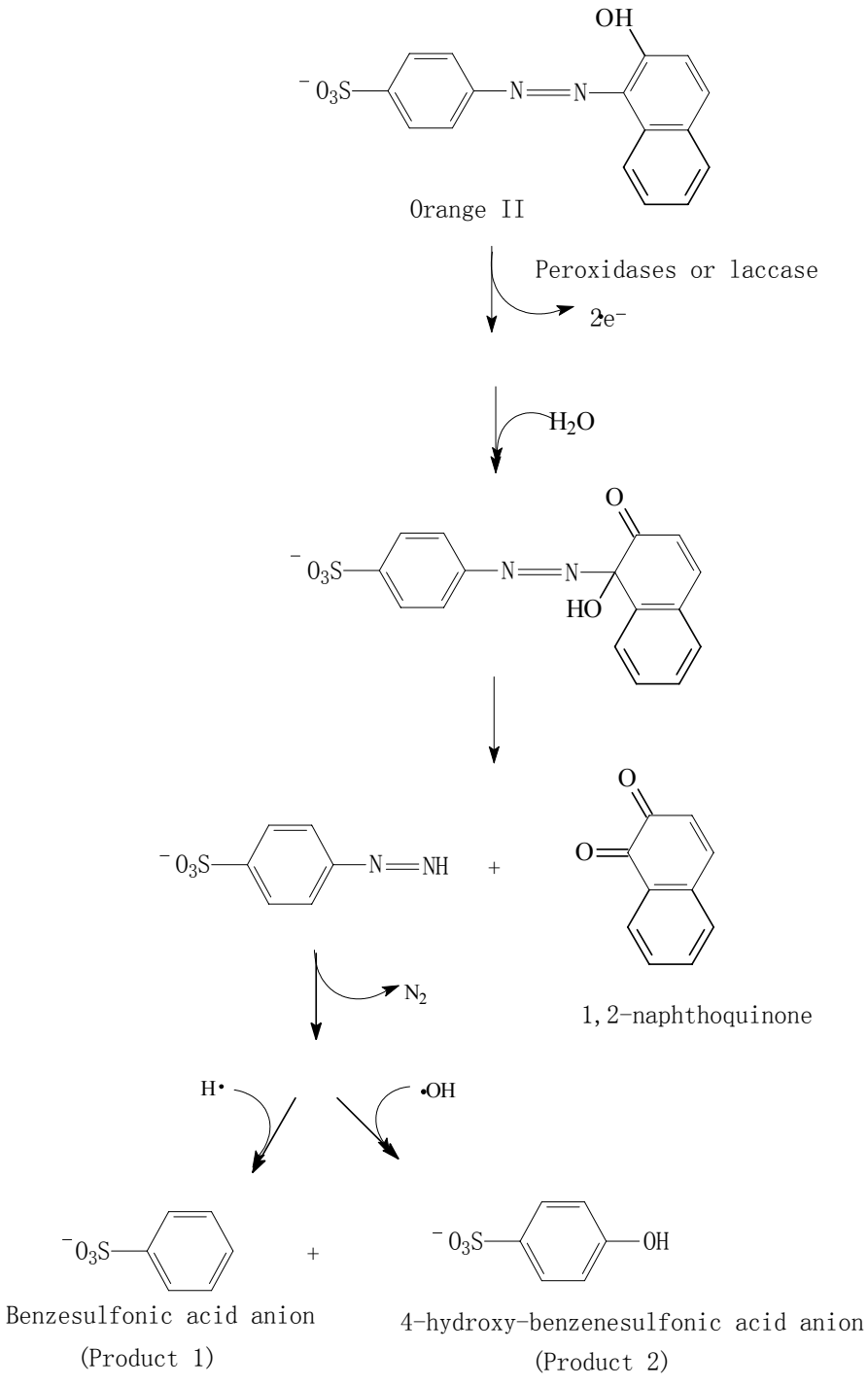


**Figure 5.22** Formation of degradation products of Orange II by *Pleurotus ostreatus*

# CHAPTER 6

# CONCLUSION AND FURTHER DISCUSSION

This study investigated the biodegradation of model nonionic and ionic azo dyes by a white rot fungus, *Pleurotus ostreatus*. The major products from the dyes during biodegradation have been identified and quantified. Possible pathways leading to formation of these products are discussed. The major findings are summarized as follows.

a. *Pleurotus ostreatus* is capable of degrading nonionic and anionic azo dyes. This white rot fungus is particularly efficient in degradation of anionic azo dyes with a phenolic structure or having hydroxyl groups on aromatic rings.
b. Biodegradation of different model azo dyes indicated that water-soluble anionic dyes were degraded more (up to 98 percent in 5 days) by *Pleurotus ostreatus* than water-insoluble nonionic dyes (up to 57 percent in 10 days).
c. Dyes with different structures, i.e. phenolic and nonphenolic dyes, showed that fungal biodegradation was influenced by the functional groups on the benzene ring. Azo dyes having a phenolic ring yield products expected from peroxidase oxidation; however, the model nonphenolic dye produced a range of compounds by an unidentified mechanism.
d. The model nonphenolic dye, DO3, produced 4-nitrophenol and 4-nitrobenzene in accordance with a peroxidase oxidation pathway, while production of 4-nitroaniline indicated that some new enzymatic systems may be involved.
e. Methylation of the hydroxyl group on 4-nitrophenol by *Pleurotus ostreatus* to produce 4-nitroanisole was confirmed by experiments with the reference compound. This finding

shows that methylation is a step in fungal degradation of aromatic compounds with hydroxyl groups.

f. DY3, 4HABA and Orange II all contain an aromatic hydroxy group and when degraded, they produce products indicative of peroxidase enzyme activity.

g. Veratryl alcohol, a redox mediator for LiP catalytic cycle, and its oxidant, veratraldehyde, were identified in the cultures of *Pleurotus ostreatus* in this study.

h. A quantification method for studying the biodegradation of nonionic azo dyes was established using HPLC and CE-MS was used for the quantitation of ionic azo dye products.

i. Kinetic studies of degradation products demonstrated that some primary products could be further transformed by *Pleurotus ostreatus*, while others did not because of a low degradation rate.

j. Possible pathways to form the identified products from model ionic and nonionic azo dyes with phenolic and nonphenolic structures were discussed and proposed (Chapter 3, 4, and 5).

It has been shown that the products from model azo dyes with a phenolic structure follow a proposed peroxidase or laccase oxidation pathway in the fungal degradation. This finding suggests that it is possible to predict the expected products based on the structure of azo dyes in the wastewater. However, analysis of model azo dyes with nonphenolic structures suggested that other mechanisms maybe involved in the fungal degradation. The analytical methods described herein can be used for the further study of dyes.

There is still some research needed to fully understand the biodegradation mechanism used by white rot fungi to degrade azo and other types of dyes. A series of experiments are recommended for the future study, specifically

a. Assessment of toxicity of organic pollutants after biodegradation

It has been demonstrated that some products accumulate after decolorization of azo dyes by white rot fungi. The biotransformation products that resist further degradation may be toxic or genotoxic. Thus, the toxicity of dyes after fungal degradation should be assayed. The relationship between the structures of parent pollutants and toxicity after treatment should be studied, and methods to detoxify the toxic products are needed.

b. Investigation of extracellular enzymes from white rot fungi

Nonspecific enzymes secreted from white rot fungi under food starvation are responsible for the biodegradation of lignin and structurally different organic compounds. To clarify how these enzymes respond to different dye structures is important to understanding of biodegradation by white rot fungi. This assessment could be done by:

- Measuring activities of major enzymes in white rot fungal culture, which are responsible for biodegradation;
- Comparing results of individual enzymes with those from fungal culture in biodegradation of azo dyes;
- Preparing and purifying crude enzymes from white rot fungal cultures and characterizing unknown enzymes contributing to the biodegradation;
- Examining other factors that may influence degradation, both enzymatic and non-enzymatic, such as mediators and the presence of small molecules;
- Setting up immobilization technology to reuse enzymes and fungi.

# REFERENCES


Adosinda, M.; Martins, M.; Ferreira, I.C.; Santos, I.M.; Wueiroz, M.J. and Lima, N. Biodegradation of bioaccessible textile azo dyes by *Phanerochaete chrysosporium.* Journal of Biotechnology, 89, 91-98, 2001.

Adosinda, M.; Martins, M.; Lima, N.; Silvestre, A.; Queiroz, M. Comparative studies of fungal degradation of single or mixed bioaccessible reactive azo dyes. Chemosphere, 52, 967, 2003.

Ansari, A. A.; Thakur, B. D. Extraction, characterisation and application of a natural dye: The eco-friendly textile colorant. Colourage, 47, 15-16, 18-20, 2000.

Aust, S.D. Mechanisms of degradation by white rot fungi. Environmental Health Perspectives, 103, 59-61, 1995

Baiocchi, C.; Brussino, M. C.; Pramauro, E.; Prevot, A. B.; Palmisano, L.; Marci, G. Characterization of methyl orange and its photocatalytic degradation products by HPLC/UV-VIS diode array and atmospheric pressure ionization quadrupole ion trap mass spectrometry. International Journal of Mass Spectrometry, 214, 247-256, 2002.

Bakshi, D. K., Gupta, K.G., and Sharma, P. Enhanced biodecolorization of synthetic textile dye effluent by *Phanerochaete chrysosporium* under improved culture conditions. World Journal of Microbiology and Biotechnology, 15, 507-509, 1999.

Banat, I.M., Nigam, P., Singh, D., and Marchant, R., Microbial decolorization of textile-dye-containing effluents: a review. Bioresource Technology, 58, 217-227, 1996.

Baughman, G. L. and Paris, D. F. Microbial bioconcentration of organic pollutants from aquatic systems – a critical review. CRC Critical Reviews in Microbiology, 7, 205-228,1981.

Benedek, K. and Guttman, A. High performance capillary electrophoresis: an overview. In HPLC: practical and industrial application. J. K. Swadesh, Ed., CRC press, Boca Raton, FL, 2001.

Bogan, B.W. and Lamar, R.T. One-electron oxidation in the degradation of creosote polycyclic aromatic hydrocarbons by *Phanerochaete chrysosporium*. Applied and Environmental Microbiology, 61, 2631-2635, 1995.

Bourbonnais, R., Paice, M.G., Freiermuth, B., Bodie, E., Bornemann, S. Reactivities of various mediators and laccases with kraft pulp and lignin model compounds. Applied and Environmental Microbiology, 63, 4627-4632, 1996.

Bras, R.; Ferra, M.; Isabel, M.; Pinheiro, H. M.; Goncalves, I. C. Batch tests for assessing decolorization of azo dyes by methanogenic and mixed cultures. Journal of Biotechnology, 89, 155-162, 2001.

Bumpus, J. Microbial Degradation of Azo Dyes. In Biotransformations: Microbial degradation of health-risk compounds. V. Singh, Ed., Elsevier, New York, 1995.

Cai, D. and Tien, M. Lignin-degrading peroxidases of *Phanerochaete chrysosporium*. Journal of Biotechnology, 30, 79-90, 1993.

Cai, D. and Tien, M. Kinetic studies on the formation and decomposition of compound II and III. Reactions of lignin peroxidase with $H_2O_2$. Journal of Biological Chemistry, 267, 11149-11155, 1992.

Call, H. P. and Mucke, I. Minireview: history, overview and applications of mediated ligninolytic systems, especially laccase-mediator-systems (Lignozym-Process). Journal of Biotechnology, 53, 163-202, 1997.

Cao, H. Decolorization of textile dyes by white rot fungi. Ph. D. dissertation, University of Georgia, Athens, GA, 2000

Chagas, E.P. and Durrant, L. R. Decolorization of azo dyes by *Phanerochaete chrysosporium* and *Pleurotus sajorcaju.* Enzyme and Microbial Technology, 29, 474-477, 2001.

Chivukula, M. and Renganathan, V. Phenolic azo dye oxidation by laccase from *Pyricularia oryzae*. Applied and Environmental Microbiology, 61, 4374-4377, 1995.

Chivukula, M.; Spadaro, J.T.; Renganathan, V. Lignin peroxidase-catalyzed oxidation of sulfonated azo dyes generates novel sulfophenyl hydroperoxides. Biochemistry, 34, 7765-7772, 1995.

Conneely, A.; Smyth, W. F.; McMullan, G. Metabolism of the phthalocyanine textile dye Remazol Turquoise Blue by *Phanerochaete chrysosporium*. FEMS Microbiology Letters, 179, 333-337, 1999.

Cripps, C.; Bumpus, J. and Aust, S. Biodegradation of azo and heterocyclic dyes by *Phanerochaete chrysosporium*. Applied and Environmental Microbiology, 56, 1114-1118, 1990.

Egli, T. W. General strategies in the biodegradation of pollutants. In Metal ions in biological systems. H. Sigel and A. Sigel, Eds., pp. 1-41, Marcel Dekker, New York, NY, 1992.

Faison, B.D. and Kirk, T.K. Factors involved in the regulation of ligninase activity in *Phanerochaete chrysosporium*. Applied and Environmental Microbiology, 49, 299-304, 1985.

Fenn, J. B.; Mann, M.; Meng, C.K.; Wong, S.F.; Whitehouse, G.M.; Electrospray Ionization for Mass Spectrometry of Large Biomolecules. Science, 246, 64-71,1989.

Fenn, P. and Kirk, T.K. Relationship of nitrogen to the onset and suppression of ligninolytic activity and secondary metabolism in *Phanerochaete chrysosporium*. Archives of Microbiology, 130, 59-65, 1981.

Glenn, J. K. and Gold, M. H. Purification and characterization of an extracellular Mn (II)-dependent peroxidase from the lignin-degrading basidiomycete, *Phanerochaete chrysosporium*. Archives of Biochemistry and Biophysics, 242, 329-341, 1985.

Glenn, J. K.; Alileswaran, L. and Gold, M. H. Mn(II) oxidation is the principal function of the extracellular Mn-peroxidase from *Phanerochaete chrysosporium*. Archives of Biochemistry and Biophysics, 251, 688-696, 1986.

Goodwin, D.C.; Aust, S.D. and Grover, T.A. Evidence for veratryl alcohol as a redox mediator in lignin peroxidase-catalysed oxidation. Biochemistry, 34, 5060-5065, 1995.

Goszczynski, S.; Paszczynski, A.; Pasti-Grigsby, M.B.; Crawford, R.L. New pathway for degradation of sulfonated azo dyes by microbial peroxidases of *Phanerochaete chrysosporium* and *Streptomyces chromofuscus.* Journal of Bacteriology, 176, 1339-1347,1994.

Hao, O. J., Kim, H., and Chiang, P. Decolorization of wastewater. Critical Reviews in Environmental Science and Technology, 30, 449-505, 2000.

Heinfling, A.; Bergbauer, M. and Szewzyk, U. Biodegradation of azo and phthalocyanine dyes by *Trametes versicolor* and *Bjerkandera adusta*. Applied Microbiology and Biotechnology, 48, 261-266, 1997.

Heinfling, A.; Ruiz-Duenas, F.J.; Martinez, F.J.; Bergbauer, M.; Szewzyk, U. and Martinez, A.T. A study on reducing substrates of manganese-oxidizing peroxidases from *Pleurotus eryngii*, and *Bjerkandera adusta*. FEBS Letters, 428, 141-146, 1998.

Hofrichter, M. Review: Lignin conversion by manganese peroxidase (MnP). Enzyme and Microbial Technology, 30, 454-466, 2002.

Hou, H.; Zhou, J.; Wang, J.; Du, C.; and Yan, B. Enhancement of laccase production by *Pleurotus ostreatus* and its use for the decolorization of anthraquinone dye. Process Biochemistry, 39, 1415-1419, 2003.

Huang, P.C. and Kosower, E. M. Diazenes. III. Properties of phenyldiazene. Journal of American Chemical Society, 90, 2367 – 2376, 1968.

Hublik, G. and Schinner, F. Characterization and immobilization of the laccase from *Pleurotus ostreatus* and its use for the continuous elimination of phenolic pollutants. Enzyme and Microbial Technology, 27, 330-336, 2000.

Huikko, K., Kotiaho, T., and Kostianinen, R. Effects of nebulizing and drying gas flow on capillary electrophoresis/mass spectrometry. Rapid Communications in mass spectrometry, 16, 1562-1568, 2002.

Jong, E. D.; Field, J.M. and De Bont, J.A.M. Aryl alcohols in the physiology of ligninolytic fungi. FEMS Microbiology Review, 13, 153-188, 1994.

Kang, S.O.; Shin, K.S.; Han, Y.H.; Youn, H.D. and Hah, Y.C. Purification and characterization of an extracellular peroxidase from white rot fungus *Pleurotus ostreatus*. Biochimica et Biophysica Acta, 1163, 158-164, 1993.

Kersten, P.J.; Tien, M.; Kalyanaraman, B. and Kirk, T.K. The ligninase of *Phanerochaete chrysosporium* generates cation radicals from methoxybenzenes. Journal of Biological Chemistry, 260, 2609-2612, 1985.

Kirby, D.P.; Thorne, J.M.; Gotzinger, W.K. and Karger, B.L. A CE/MS interface for stable, low-flow operation. Analytical Chemistry, 68, 4451-4457, 1996.

Kirk, T. K.; Schultz, E.; Cornors, W. J.; Lorenz, L. F.; and Zeikus, J. G. Influence of culture parameters on lignin metabolism by *Phanerochaete chrysosporium.* Archives of Microbiology, 117, 3144-3149, 1978.

Knapp, J.S.; Newby, P.S. and Reece, L.P. Decolorization of dyes by wood-rotting basidiomycete fungi. Enzyme and Microbiological Technology, 17, 664-668, 1995.

Kuan, I.C. and Tien, M. Stimulation of Mn peroxidase activity: A possible role for oxalate in lignin biodegradation. Proceeding of the National Academy of Sciences of the United States of America, 90, 1242-1246, 1993

Marshall, A. G. Milestones in Fourier transform ion cyclotron resonance mass spectrometry technique development. International Journal of Mass Spectrometry, 200, 331-356, 2000.

Martinez, A.T. Molecular biology and structure-function of lignin-degrading heme peroxidases. Enzyme and Microbial Technology, 30, 425-444, 2002.

McMullan, G.; Meehan, C.; Conneely, A.; Kirby, N.; Robinson, T. and Nigam, P. Mini-review: microbial decolourisation and degradation of textile dyes. Applied Microbiology and Biotechnology, 56, 81-87, 2001.

Mester, T. and Tien, M. Oxidation mechanism of ligninolytic enzymes involved in the degradation of environmental pollutants. International Biodeterioration & Biodegradation, 46, 51-59, 2000.

Milojkovic-Opsenica, D. M.; Lazarevic, K.; Ivackovic, V.; Tesic, Z. L. Reversed-phase thin-layer chromatography of some foodstuff dyes. Journal of Planar Chromatography—Modern TLC, 16, 276-279, 2003.

Morais, H.; Ramos, C., Forgacs, E.; Cserhati, T. and Oliviera, J. Using spectrophotometry and spectral mapping technique for the study of the production of manganese-dependent and manganese-independent peroxidases by *Pleurotus ostreatus*. Journal of Biochemical and Biophysical Methods, 50, 99-109, 2002.

Moreira, M.T.; Mielgo, I.; Feijoo, G. and Lema, J.M. Evaluation of different fungal strains in the decolorisation of synthetic dyes. Biotechnology letters, 22, 1499-1503, 2000.

Nachiyar, C. V.; Rajkumar, G. S. Degradation of a tannery and textile dye, Navitan Fast Blue S5R by *Pseudomonas aeruginosa*. World Journal of Microbiology & Biotechnology, 19, 609-614, 2003.

Novotny, C.; Rawal, B.; Bhatt, M.; Patel, M.; Sasek, V. and Molitoris, H.P. Capacity of *Irpex lacteus* and *Pleurotus ostreatus* for decolorization of chemically different dyes. Journal of Biotechnology, 89,113-122, 2001.

Olivares, J.A.; Nguyen, N.T.; Yonker, C. R. and Smith, R. D. On-line mass spectrometric detection for capillary zone electrophoresis. Analytical Chemistry, 59, 1230 – 1232, 1987.

Pasti-Grigsbty, M. B., Paszczynski, A., Gosczynski, S., Crawford, D. L., Crawford, R. L. Influence of aromatic substitution patterns on azo dye degradability by *Streptomyces chromofuscus* and *Phanerochaete chrysosporium.* Applied Environmental Microbiology, 58, 3605-3613, 1992.

Paszczynski, A. and Crawford, R.L. Degradation of azo compounds by ligninase from *Phanerochaete chrysosporium*: involvement of veratryl alcohol. Biochemical and Biophysical Research Communications, 178, 1056-1063, 1991.

Paszczynski, A; Pasti-Grigsby, M.B.; Goszczynski, S.; Crawford, R. L. and Crawford, D.L. Mineralization of sulfonated azo dyes and sulfanilic acid by *Phanerochaete chrysosporium* and *Streptomyces chromofuscus*. Applied and Environmental Microbiology, 58, 3598-3604, 1992.

Perkins, J. R.; Tomer, K. B. Capillary electrophoresis/electrospray mass spectrometry using a high-performance magnetic sector mass spectrometer. Analytical Chemistry, 66, 2835-40, 1994.

Pielesz, A.; Baranowska, I.; Rybak, A.; Wlochowicz, A. Detection and determination of aromatic amines as products of reductive splitting from selected azo dyes. Ecotoxicology and Environmental Safety, 53, 42-47, 2002.

Pinheiro, H.M., Touraud, E. and Thomas, O. Aromatic amines from azo dye reduction: status review with emphasis on direct UV spectrophotometric detection in textile industry wastewaters. Dyes and Pigments, 61, 121-139, 2004.

Plum, A.; Braun, G.; Rehorek, A. Process monitoring of anaerobic azo dye degradation by high-performance liquid chromatography-diode array detection continuously coupled to membrane filtration sampling modules. Journal of Chromatography, A, 987, 395-402, 2003.

Podgornik, H.; Grgic, I. and Perdih, A. Decolorization rate of dyes using lignin peroxidases of *Phanerochaete chrysosporium*. Chemosphere, 38, 1353-1359, 1999.

Poole, C. F. and Poole, S. K. Gas chromatography. In Chromatography, 5th edition, Fundamentals and applications of chromatography and related differential migration methods. E. Heftmann, Ed. Elsevier, New York, NY, 1992.

Razo-Flores, E.; Luijten, M.; Donlon, B.; Lettinga, G. and Field, J. Biodegradation of selected azo dyes under methanogenic conditions. Water Science and Technology, 36, 65-72, 1997.

Reichstein, T. Foreword. Chromatography, 5th edition, fundamentals and applications of chromatography and related differential migration methods. E. Heftmann, Ed. Elsevier, New York, NY, 1992.

Righetti, P. G. Electrophoresis. In Chromatography, 5th edition, Fundamentals and applications of chromatography and related differential migration methods. E. Heftmann, Ed. Elsevier, New York, NY, 1992.

Riu, J., Schonsee, I., Barcelo, D., Rafols, C., Determination of sulfonated azo dyes in water and wastewater. Trends in Analytical Chemistry, 16, 405-419, 1997.

Robinson, T., Chandran, B., and Nigam, P. Studies on the production of enzymes by white-rot fungi for the decolourisation of textile dyes. Enzyme and Microbial Technology, 29, 575-579, 2001.

Rodriguez, E.; Pickard, M.A. and Vazquez-Duhalt, R. Industrial dye decolorization by laccases from ligninolytic fungi. Current Microbiology, 38, 27-32, 1999.

Sarkar, S.; Martinez, A. T. and Martinez, M. J. Biochemical and molecular characterization of a manganese peroxidase isoenzyme from *Pleurotus ostreatus*. Biochimica et Biophysica Acta, 1339, 23-30, 1997.

Schmitt-Kopplin, P. and Frommberger, M., Capillary electrophoresis – mass spectrometry: 15 years of developments and applications. Electrophoresis, 24, 3837-3867, 2003.

Schoemaker, H.E.; Lundell, T.K.; Hatakka, A. and Piontek, K. The oxidation of veratryl alcohol, dimeric lignin model compounds and lignin peroxidase: the redox cycle revisited. FEMS Microbiology Review, 13, 321-332, 1994.

Selvam, K.; Swaminathan, K.; and Chae, K. S. Decolouriztion of azo dyes and a dye industry effluent by a white rot fungus *Thelephora sp*. Bioresource Technology, 88, 115-119, 2003.

Severs, J. C.; Hofstadler, S. A.; Zhao, Z.; Senh, R. T.; Smith, R. D. The interface of capillary electrophoresis with high performance Fourier transform ion cyclotron resonance mass spectrometry for biomolecule characterization. Electrophoresis, 17, 1808-1817, 1996.

Shaul, G.M.; Holdsworth, T.J.; Dempsey, C.R.; Dostall, K.A. Fate of water soluble azo dyes in the activated sludge process. Chemosphere, 22, 107-119, 1991.

Sherma, J. Planar chromatography. Analytical Chemistry, 72, 9-25, 2000.

Shin, K.S. and Kim, C.J. Decolorisation of artificial dyes by peroxidase from the white-rot fungus, *Pleurotus ostreatus*. Biotechnology letters, 20, 569-572, 1998.

Shin, K.S.; Oh, I. K. and Kim, C.J. Production and purification of Remazol Brilliant Blue R decolorizing peroxidase from the culture filtrate of *Pleurotus ostreatus*. Applied and Environmental Microbiology, 63, 1744-1748, 1997.

Shin, K.S.; Youn, H.D.; Han, Y.H.; Kang, S.O. and Hah, Y.C. Purification and characterization of D-glucose oxidase from white rot fungus *Pleurotus ostreatus*. European Journal of Biochemistry, 215, 747-752, 1993.

Smith, R. D.; Barinaga, C. J.; Udseth, H. R. Improved electrospray ionization interface for capillary zone electrophoresis-mass spectrometry. Analytical Chemistry, 60, 1948-1952, 1988.

Spadaro, J. T.; Gold, M. H. and Renganathan, V. Degradation of azo dyes by the lignin-degrading fungus *Phanerochaete chrysosporium.* Applied Environmental Microbiology, 58, 2397-2401, 1992.

Spadaro, J.T. and Renganathan, V. Peroxidase-catalyzed oxidation of azo dyes: mechanism of Disperse Yellow 3 degradation. Archives of Biochemistry and Biophysics. 312, 301-307, 1994.

Suguimoto, H. H.; Barbosa, A.M.; Dekker, R.F. and Castro-Gomez, R.J. Veratryl alcohol stimulates fruiting body formation in the oyster mushroom, *Pleurotus ostreatus.* FEMS Microbiology Letters 194, 235-238, 2001.

Takeda, S., Tanaka, Y., Nishimura, Y., Yamane, M., Siroma, Z., and Wakida, S., Analysis of dyestuff degradation products by capillary electrophoresis. Journal of Chromatography A, 853, 503-509, 1999.

Tien M. and Kirk, T.K. Lignin-degrading enzyme from *Phanerochaete chrysosporium*: purification, characterization, and catalytic properties of a unique $H_2O_2$ –requiring oxygenase. Proceeding of the National Academy of Sciences of the United States of America, 81, 2280-2284, 1984.

Tien, M. Properties of ligninase from *Phanerochaete chrysosporium* and their possible applications. CRC Critical Reviews in Microbiology, 15, 141-168, 1987.

Torres, E., Bustos-jaimes, I., and Borgne, S. L. Potential use of oxidative enzymes for the detoxification of organic pollutants. Applied Catalysis B: Environmental, 46, 1-15, 2003.

Valli, K. and Gold, M. Degradation of 2,4-dichlorophenol by the lignin-degrading fungus *Phanerochaete chrysosporium*. Journal of Bacteriology, 173, 345-352, 1991.

Valli, K., Brock, B., Joshi, D., and Gold, M. Degradation of 2,4-dinitrotoluene by the lignin-degrading fungus *Phanerochaete chrysosporium*. Applied and Environmental Microbiology, 58, 221-228, 1992.

Verhaert, P.; Uttenweiler-Joseph, S.; Vries, M.; Loboda, A.; Ens, W.; Standing, K. G. Matrix-assisted laser desorption/ionization quadrupole time-of-flight mass spectrometry: an elegant tool for peptidomics. Proteomics, 1, 118-131, 2001.

Vinodgopal, K.; Peller, J. Hydroxyl radical-mediated advanced oxidation processes for textile dyes: A comparison of the radiolytic and sonolytic degradation of the monoazo dye Acid Orange 7. Research on Chemical Intermediates, 29, 307-316, 2003.

Vuorensola, K.; Kollonen, J.; Siren, H.; Ketola, R. Optimization of capillary electrophoretic-electrospray ionization-mass spectrometric analysis of catecholamines. Electrophoresis, 22, 4347-4354, 2001.

Wang, L. and Tsai, S. Simultaneous determination of oxidative hair dye p-phenylenediamine and its metabolites in human and rabbit biological fluids. Analytical Biochemistry, 312, 201-207, 2003.

Wariishi, H.; Akileswaran, L. and Gold, M.H. Manganese peroxidase from the basidiomycete *Phanerochaete chrysosporium*: spectral characterization of the oxidized states and the catalytic cycle. Biochemistry, 27, 5365-5370, 1988.

Wariishi, H.; Valli, K. and Gold, M.H. Manganese(II) oxidation by manganese peroxidase from the basidiomycete *Phanerochaete chrysosporium.* Journal of Biological Chemistry, 267, 23688-23695, 1992.

Wesenberg, D.; Kyriakides, I.; and Agathos, S.N. White-rot fungi and their enzymes for the treatment of industrial dye effluents. Biotechnology Advances, 22, 161-187, 2003.

Wey, A.B. and Thormann, W., Capillary electrophoresis and capillary electrophoresis – ion trap multiple stage mass spectrometry for the differentiation and identification of oxycodone and its major metabolites in human urine. Journal of Chromatography B, 770, 191-205, 2002.

Zapanta, L.S. and Tien, M. The roles of veratryl alcohol and oxalate in fungal lignin degradation. Journal of Biotechnology, 53, 93-102, 1997.

Zheng, Z and Obbard, J.P. Oxidation of polycyclic aromatic hydrocarbons (PAH) by the white rot fungus, *Phanerochaete chrysosporium*. Enzyme and Microbial Technology, 31, 3-9, 2002.